



www.offalmoloji.org

E-ISSN: 2149-8709

TURKISH JOURNAL OF OPHTHALMOLOGY

TURKISH JOURNAL OF OPHTHALMOLOGY

TJO

Original Articles

Research Articles

The Role of Optical Coherence Tomography Signal Strength in the Diagnosis and Follow-up of Patients with Posterior Capsular Opacification Treated with Nd:YAG Laser Capsulotomy

Mustafa Vatanserver et al.; Mersin, Turkey

Evaluation of Peripheral Retinal Changes on Ultra-Widefield Fundus Autofluorescence Images of Patients with Age-Related Macular Degeneration

Kübra Küçükiba et al.; Eskişehir, Turkey

Stereoacuity, Fusional Vergence Amplitudes, and Refractive Errors Prior to Treatment in Patients with Attention-Deficit Hyperactivity Disorder

Irmak Karaca et al.; Izmir, Turkey

The Effect of Topical Cyclopentolate on Anterior Segment Parameters in Patients with Keratoconus

Ahmet Kırgız et al.; Istanbul, Turkey

The Diagnostic Ability of Ganglion Cell Complex Thickness-to-Total Retinal Thickness Ratio in Glaucoma in a Caucasian Population

Almila Sarıgül Sezenöz et al.; Ankara, Turkey

Iris Cysts: Clinical Features, Imaging Findings, and Treatment Results

Helin Ceren Köse et al.; Ankara, Türkiye

Review

Artificial Intelligence and Ophthalmology

Kadircan Keskinbora and Fatih Güven; Istanbul, Turkey

Case Reports

Efficacy of Topical Brinzolamide Treatment in Posterior Microphthalmos-Related Macular Cystoid Lesions: A Case Series

Ceren Durmaz Engin et al.; Zonguldak, Manisa, Izmir, Turkey

Sarcoid-like Granulomatous Intraocular Inflammation Caused by Vemurafenib Treatment for Metastatic Melanoma

Hilal Eser Öztürk and Yüksel Süllü; Samsun, Turkey

Extranodal Ocular Adnexal Marginal Zone Lymphoma in a Ten-Year-Old Child

Nazan Çetingül et al.; Izmir, Turkey

An Unusual Case: Self-separation of an Idiopathic Epiretinal Membrane

Jale Menteş and Serhad Nalçacı; Izmir, Turkey

TURKISH JOURNAL OF OPHTHALMOLOGY



www.ofthalmoloji.org

TJO

Editor-in-Chief

Murat İRKEÇ, MD

Hacettepe University Faculty of Medicine, Department of Ophthalmology, Ankara, Turkey

Areas of Interest: Cornea and Ocular Surface Disease, Glaucoma, Allergy and Immunology

E-mail: mirkec@hacettepe.edu.tr

ORCID ID: orcid.org/0000-0001-8892-4811

Associate Editors

Tomris ŞENGÖR, MD

İstanbul Bilim University Faculty of Medicine, Department of Ophthalmology, İstanbul, Turkey

Areas of Interest: Cornea and Ocular Surface Disease, Contact Lens

E-mail: tomris.sengor@gmail.com

ORCID ID: orcid.org/0000-0002-9436-5582

Sait EĞRİLMEZ, MD

Ege University Faculty of Medicine, Department of Ophthalmology, İzmir, Turkey

Areas of Interest: Cornea and Ocular Surface Disease, Contact Lens, Refraction, Cataract and Refractive Surgery

E-mail: saitegrilmez@gmail.com

ORCID ID: orcid.org/0000-0002-6971-527X

Özlem YILDIRIM, MD

Mersin University Faculty of Medicine, Department of Ophthalmology, Mersin, Turkey

Areas of Interest: Uveitis, Medical Retina, Glaucoma

E-mail: dryildirimoz@hotmail.com

ORCID ID: orcid.org/0000-0002-3773-2497

Banu BOZKURT, MD, FEBO

Selçuk University Faculty of Medicine, Department of Ophthalmology, Konya, Turkey

Areas of Interest: Cornea and Ocular Surface Disease, Glaucoma, Allergy and Immunology

E-mail: drbanubozkurt@yahoo.com

ORCID ID: orcid.org/0000-0002-9847-3521

Statistical Board

Ahmet DİRİCAN

İstanbul University İstanbul Faculty of Medicine, Department of Biostatistics and Medical Informatics, İstanbul, Turkey

English Language Editor

Jacqueline Renee GUTENKUNST, Maryland, USA

Publishing House

Molla Gürani Mah. Kaçamak Sokak No: 21,
34093 Fındıkzade-İstanbul-Turkey

Publisher Certificate Number: 14521

Phone: +90 212 621 99 25 Fax: +90 212 621 99 27

E-mail: info@galenos.com.tr

Online Publishing Date: February 2020

International scientific journal published bimonthly.

E-ISSN: 2149-8709



Advisory Board

Yonca AYDIN AKOVA,

Bayındır Kavaklıdere Hospital, Ophthalmology Clinic, Ankara, Turkey

Mustafa Kemal ARICI,

Bezmialem Vakıf University Faculty of Medicine, Department of Ophthalmology, İstanbul, Turkey

Atila BAYER,

Ophthalmology, Dünyagöz Hospital, Ankara, Turkey

Kamil BİLGİHAN,

Gazi University Faculty of Medicine, Department of Ophthalmology, Ankara, Turkey

İzzet CAN,

Ophthalmology, Independent Practitioner, Ankara, Turkey

Jose M. BENİTEZ-del-CASTILLO,

Universidad Complutense de Madrid, Hospital Clinico San Carlos, Department of Ophthalmology, Madrid, Spain

Murat DOĞRU,

Keio University Faculty of Medicine, Department of Ophthalmology, Tokyo, Japan

Şansal GEDİK,

Selçuk University Faculty of Medicine, Department of Ophthalmology, Konya, Turkey

Ömür UÇAKHAN GÜNDÜZ,

Ankara University Faculty of Medicine, Department of Ophthalmology, Ankara, Turkey

Banu Melek HOŞAL,

Ankara University Faculty of Medicine, Department of Ophthalmology, Ankara, Turkey

Sibel ÇALIŞKAN KADAYIFÇILAR,

Hacettepe University Faculty of Medicine, Department of Ophthalmology, Ankara, Turkey

Murat KARAÇORLU,

İstanbul Retina Institute, Ophthalmology Clinic, İstanbul, Turkey

Sarper KARAKÜÇÜK,

Anadolu Medical Center, Ophthalmology Clinic, Kocaeli, Turkey

Tero KİVELÄ,

University of Helsinki, Helsinki University Hospital, Department of Ophthalmology, Helsinki, Finland

Hayyam KIRATLI,

Hacettepe University Faculty of Medicine, Department of Ophthalmology, Ankara, Turkey

Anastasio G.P. KONSTAS,

Aristotle University of Thessaloniki, Department of Ophthalmology, Thessaloniki, Greece

Anat LOEWENSTEIN,

Tel Aviv University Sackler Faculty of Medicine, Department of Ophthalmology, Tel Aviv, Israel

Mehmet Cem MOCAN,

University of Illinois at Chicago, Department of Ophthalmology and Visual Sciences, Chicago

Pınar AYDIN O'DWYER,

Ophthalmology, Independent Practitioner, Ankara, Turkey

Şengül ÖZDEK,

Gazi University Faculty of Medicine, Department of Ophthalmology, Ankara, Turkey

Hakan ÖZDEMİR,

Bezmialem Vakıf University Faculty of Medicine, Department of Ophthalmology, İstanbul, Turkey

Banu TURGUT ÖZTÜRK,

Selçuk University Faculty of Medicine, Department of Ophthalmology, Konya, Turkey

Seyhan Bahar ÖZKAN,

Adnan Menderes University Faculty of Medicine, Department of Ophthalmology, Aydın, Turkey

Afsun ŞAHİN,

Koç University Faculty of Medicine, Department of Ophthalmology, İstanbul, Turkey

H. Nida ŞEN,

George Washington University, National Eye Institute, Department of Ophthalmology, Washington, USA

İlknur TUĞAL-TUTKUN,

İstanbul University İstanbul Faculty of Medicine, Department of Ophthalmology, İstanbul, Turkey

Nilgün YILDIRIM,

Eskişehir Osmangazi University Faculty of Medicine, Department of Ophthalmology, Eskişehir, Turkey

Nurşen YÜKSEL,

Kocaeli University Faculty of Medicine, Department of Ophthalmology, Kocaeli, Turkey

The Turkish Journal of Ophthalmology is an official journal of the Turkish Ophthalmological Association.

On Behalf of Turkish Ophthalmological Association Owner

Osman Şevki ARSLAN,

İstanbul University Cerrahpaşa Faculty of Medicine, Department of Ophthalmology, İstanbul, Turkey

TURKISH JOURNAL OF OPHTHALMOLOGY



www.ofthalmoloji.org

TJO

ABOUT US

The Turkish Journal of Ophthalmology (TJO) is the only scientific periodical publication of the Turkish Ophthalmological Association and has been published since January 1929. In its early years, the journal was published in Turkish and French. Although there were temporary interruptions in the publication of the journal due to various challenges, the Turkish Journal of Ophthalmology has been published continually from 1971 to the present.

The Turkish Journal of Ophthalmology is currently published in Turkish and English languages. TJO is an independent international periodical journal based on single-blind peer-review principle. TJO is regularly published six times a year and special issues are occasionally released. The aim of TJO is to publish original research papers of the highest scientific and clinical value at an international level. Furthermore, review articles, case reports, editorial comments, letters to the editor, educational contributions and congress/meeting announcements are released.

The target audience includes specialists and physicians in training in ophthalmology in all relevant disciplines.

The editorial policies are based on the "Recommendations for the Conduct, Reporting, Editing, and Publication of Scholarly Work in Medical Journals (ICMJE Recommendations)" by the International Committee of Medical Journal Editors (2013, archived at <http://www.icmje.org/>) rules.

The Turkish Journal of Ophthalmology is indexed in the **PubMed/MEDLINE, PubMed Central (PMC), Web of Science-Emerging Sources Citation Index (ESCI), Scopus, TUBITAK/ULAKBIM, Directory of Open Access Journals (DOAJ), EBSCO Database, CINAHL, Proquest, Embase, British Library, Index Copernicus, J-Gate, ROOT INDEXING, IdealOnline, Turk Medline, Hinari, GOALI, ARDI, OARE** and **Turkish Citation Index**.

Open Access Policy

This journal provides immediate open access to its content on the principle that making research freely available to the public supports a greater global exchange of knowledge.

Open Access Policy is based on the rules of the Budapest Open Access Initiative (BOAI) <http://www.budapestopenaccessinitiative.org/>. By "open access" to peer-reviewed research literature, we mean its free availability on the public internet, permitting any users to read, download, copy, distribute, print, search, or link to the full texts of these articles, crawl them for indexing, pass them as data to software, or use them for any other lawful purpose, without financial, legal, or technical barriers other than those inseparable from gaining access to the internet itself. The only constraint on reproduction and distribution, and the only role for copyright in this domain, should be to give authors control over the integrity of their work and the right to be properly acknowledged and cited.

Subscription Information

TJO is sent free of charge to subscribers. Address changes should be immediately reported to the affiliates and to the managing editor. Subscribers who do not receive the journal in the relevant time period should contact the managing editor. All published volumes in full text can be reached free of charge through the website www.ofthalmoloji.org. Requests for subscription should be addressed to the Turkish Ophthalmological Association.

Manuscripts can only be submitted electronically through the Journal Agent website (<http://journalagent.com/tjo/>) after creating an account. This system allows online submission and review.

Membership Procedures

Turkish Ophthalmological Association

Bank Account: Yapı Kredi Bankası, Şehremini Şubesi 65774842

IBAN: TR10 0006 7010 0000 0065 7748 42

Annual Subscription: Domestic: 100.-TL (Tax Incl)

Abroad: 100 USD (Tax Incl.)

Correspondence Address

Editor-in-Chief, Murat İrkeç, MD, Professor in Ophthalmology
Hacettepe University Faculty of Medicine, Department of Ophthalmology
06100 Sıhhiye-Ankara-Turkey

Phone: +90 212 801 44 36/37 Fax: +90 212 801 44 39

E-mail: mirkec@hacettepe.edu.tr

Secretary, Selvinaz Arslan

E-mail: dergi@ofthalmoloji.org - sekreter@ofthalmoloji.org

Address: Avrupa Konutları Kale, Maltepe Mah. Yedikule Çırpıcı Yolu Sk.

9. Blok No: 2 Kat:1 Ofis:1 Zeytinburnu-Istanbul-Turkey

Phone: +90 536 656 87 26 Fax: +90 212 801 44 39

Web Page: www.ofthalmoloji.org

Permissions

Requests for permission to reproduce published material should be sent to the editorial office.

Editor-in-Chief: Murat İrkeç, MD, Professor in Ophthalmology

Address: Avrupa Konutları Kale, Maltepe Mah. Yedikule Çırpıcı Yolu Sk.

9. Blok No: 2 Kat:1 Ofis:1 Zeytinburnu-Istanbul-Turkey

Phone: +90 212 801 44 36/37 Fax: +90 212 801 44 39

Web Page: www.ofthalmoloji.org

E-mail: dergi@ofthalmoloji.org - sekreter@ofthalmoloji.org

Advertisement

Applications for advertisement should be addressed to the editorial office.

Address: Avrupa Konutları Kale, Maltepe Mah. Yedikule Çırpıcı Yolu Sk.

9. Blok No: 2 Kat:1 Ofis:1 Zeytinburnu-Istanbul-Turkey

Phone: +90 212 801 44 36/37 Fax: +90 212 801 44 39

Web Page: www.ofthalmoloji.org

E-mail: dergi@ofthalmoloji.org - sekreter@ofthalmoloji.org

Publisher Corresponding Address

Publisher: Erkan Mor

Galenos Yayınevi Tic. Ltd. Şti.

Address: Molla Gürani Mah. Kaçamak Sk. No: 21, 34093

Fındıkzade-Istanbul-Turkey

Phone: +90 212 621 99 25 Fax: +90 212 621 99 27

E-mail: info@galenos.com.tr

Instructions for Authors

Instructions for authors are published in the journal and on the website www.ofthalmoloji.org

Material Disclaimer

The author(s) is (are) responsible for the articles published in the Turkish Journal of Ophthalmology.

The editor, editorial board and publisher do not accept any responsibility for the articles.

The journal is printed on acid-free paper.

This work is licensed under a Creative Commons Attribution-Non Commercial-No Derivatives 4.0 International License.

INSTRUCTIONS TO AUTHORS

The Turkish Journal of Ophthalmology is an official peer-reviewed publication of the Turkish Ophthalmological Association. Accepted manuscripts are printed in Turkish and published online in both Turkish and English languages. Manuscripts written in Turkish should be in accordance with the Turkish Dictionary and Writing Guide ("Türkçe Sözlüğü ve Yazım Kılavuzu") of the Turkish Language Association. Turkish forms of ophthalmology-related terms should be checked in the TODNET Dictionary ("TODNET Sözlüğü" <http://www.todnet.org/sozlu/>) and used accordingly.

The Turkish Journal of Ophthalmology does not charge any article submission or processing charges.

A manuscript will be considered only with the understanding that it is an original contribution that has not been published elsewhere.

Reviewed and accepted manuscripts are translated either from Turkish to English or from English to Turkish by the Journal through a professional translation service. Prior to publishing, the translations are submitted to the authors for approval or correction requests, to be returned within 7 days. If no response is received from the corresponding author within this period, the translation is checked and approved by the editorial board.

The abbreviation of the Turkish Journal of Ophthalmology is TJO, however, it should be denoted as Turk J Ophthalmol when referenced. In the international index and database, the name of the journal has been registered as Turkish Journal of Ophthalmology and abbreviated as Turk J Ophthalmol.

The scientific and ethical liability of the manuscripts belongs to the authors and the copyright of the manuscripts belongs to the Turkish Journal of Ophthalmology. Authors are responsible for the contents of the manuscript and accuracy of the references. All manuscripts submitted for publication must be accompanied by the Copyright Transfer Form. Once this form, signed by all the authors, has been submitted, it is understood that neither the manuscript nor the data it contains have been submitted elsewhere or previously published and authors declare the statement of scientific contributions and responsibilities of all authors.

All manuscripts submitted to the Turkish Journal of Ophthalmology are screened for plagiarism using the 'iThenticate' software. Results indicating plagiarism may result in manuscripts being returned or rejected.

Experimental, clinical and drug studies requiring approval by an ethics committee must be submitted to the Turkish Journal of Ophthalmology with an ethics committee approval report confirming that the study was conducted in accordance with international agreements and the Declaration of Helsinki (revised 2013) (<https://www.wma.net/policies-post/wma-declaration-of-helsinki-ethical-principles-for-medical-research-involving-human-subjects/>). The approval of the ethics committee and the fact that informed consent was given by the patients should be indicated in the Materials and Methods section. In experimental animal studies, the authors should indicate that the procedures followed were in accordance with animal rights as per the Guide for the Care and Use of Laboratory Animals (<http://oacu.od.nih.gov/regs/guide/guide.pdf>) and they should obtain animal ethics committee approval.

Authors must provide disclosure/acknowledgment of financial or material support, if any was received, for the current study.

If the article includes any direct or indirect commercial links or if any institution provided material support to the study, authors must state in the cover letter that they have no relationship with the commercial product, drug, pharmaceutical company, etc. concerned; or specify the type of relationship (consultant, other agreements), if any.

Authors must provide a statement on the absence of conflicts of interest among the authors and provide authorship contributions.

The Turkish Journal of Ophthalmology is an independent international journal based on single-blind peer-review principles. The manuscript is assigned to the Editor-in-Chief, who reviews the manuscript and makes an initial decision based on manuscript quality and editorial priorities. Manuscripts that pass initial evaluation are sent for external peer review, and the Editor-in-Chief assigns an Associate Editor. The Associate Editor sends the manuscript to three reviewers (internal and/or external reviewers). The reviewers must review the manuscript within 21 days. The Associate Editor recommends a decision based on the reviewers' recommendations and returns the manuscript to the Editor-in-Chief. The Editor-in-Chief makes a final decision based on editorial priorities, manuscript quality, and reviewer recommendations. If there are any conflicting recommendations from reviewers, the Editor-in-Chief can assign a new reviewer.

The scientific board guiding the selection of the papers to be published in the Journal consists of elected experts of the Journal and if necessary, selected from national and international authorities. The Editor-in-Chief, Associate Editors, biostatistics expert and English language consultant may make minor corrections to accepted manuscripts that do not change the main text of the paper.

In case of any suspicion or claim regarding scientific shortcomings or ethical infringement, the Journal reserves the right to submit the manuscript to the supporting institutions or other authorities for investigation. The Journal accepts the responsibility of initiating action but does not undertake any responsibility for an actual investigation or any power of decision.

The Editorial Policies and General Guidelines for manuscript preparation specified below are based on "Recommendations for the Conduct, Reporting, Editing, and Publication of Scholarly Work in Medical Journals (ICMJE Recommendations)" by the International Committee of Medical Journal Editors (2013, archived at <http://www.icmje.org/>).

Preparation of research articles, systematic reviews and meta-analyses must comply with study design guidelines: CONSORT statement for randomized controlled trials (Moher D, Schultz KF, Altman D, for the CONSORT Group. The CONSORT statement revised recommendations for improving the quality of reports of parallel group randomized trials. JAMA 2001; 285: 1987-91) (<http://www.consort-statement.org/>);

PRISMA statement of preferred reporting items for systematic reviews and meta-analyses (Moher D, Liberati A, Tetzlaff J, Altman DG, The PRISMA Group. Preferred Reporting Items

for Systematic Reviews and Meta-Analyses: The PRISMA Statement. PLoS Med 2009; 6(7): e1000097.) (<http://www.prisma-statement.org/>);

STARD checklist for the reporting of studies of diagnostic accuracy (Bossuyt PM, Reitsma JB, Bruns DE, Gatsonis CA, Glasziou PP, Irwig LM, et al., for the STARD Group. Towards complete and accurate reporting of studies of diagnostic accuracy: the STARD initiative. Ann Intern Med 2003; 138:40-4.) (<http://www.stard-statement.org/>);

STROBE statement, a checklist of items that should be included in reports of observational studies (<http://www.strobe-statement.org/>);

MOOSE guidelines for meta-analysis and systemic reviews of observational studies (Stroup DF, Berlin JA, Morton SC, et al. Meta-analysis of observational studies in epidemiology: a proposal for reporting Meta-analysis of observational Studies in Epidemiology (MOOSE) group. JAMA 2000; 283: 2008-12).

GENERAL GUIDELINES

Manuscripts can only be submitted electronically through the Journal Agent website (<http://journalagent.com/tjo/>) after creating an account. This system allows online submission and review.

The manuscripts are archived according to ICMJE, Index Medicus (Medline/PubMed) and Ulakbim-Turkish Medicine Index Rules.

Format: Manuscripts should be prepared using Microsoft Word, size A4 with 2.5 cm margins on all sides, 12 pt Arial font and 1.5 line spacing.

Abbreviations: Abbreviations should be defined at first mention and used consistently thereafter. Internationally accepted abbreviations should be used; refer to scientific writing guides as necessary.

Cover letter: The cover letter should include statements about manuscript type, single-journal submission affirmation, conflict of interest statement, sources of outside funding, equipment (if applicable), approval of language for articles in English and approval of statistical analysis for original research articles.

REFERENCES

Authors are solely responsible for the accuracy of all references.

In-text citations: References should be indicated as a superscript immediately after the period/full stop of the relevant sentence. If the author(s) of a reference is/are indicated at the beginning of the sentence, this reference should be written as a superscript immediately after the author's name. If relevant research has been conducted in Turkey or by Turkish investigators, these studies should be given priority while citing the literature.

Presentations presented in congresses, unpublished manuscripts, theses, Internet addresses, and personal interviews or experiences should not be indicated as references. If such references are used, they should be indicated in parentheses at the end of the relevant sentence in the text, without reference number and written in full, in order to clarify their nature.

References section: References should be numbered consecutively in the order in which they are first mentioned in the text. All authors should be listed regardless of number.

INSTRUCTIONS TO AUTHORS

The titles of journals should be abbreviated according to the style used in the Index Medicus.

Reference Format

Journal: Last name(s) of the author(s) and initials, article title, publication title and its original abbreviation, publication date, volume, the inclusive page numbers. Example: Collin JR, Rathbun JE. Involitional entropion: a review with evaluation of a procedure. Arch Ophthalmol. 1978;96:1058-1064.

Book: Last name(s) of the author(s) and initials, chapter title, book editors, book title, edition, place of publication, date of publication and inclusive page numbers of the extract cited. Example: Herbert L. The Infectious Diseases (1st ed). Philadelphia; Mosby Harcourt; 1999:11;1-8.

Book Chapter: Last name(s) of the author(s) and initials, chapter title, book editors, book title, edition, place of publication, date of publication and inclusive page numbers of the cited piece.

Example: O'Brien TP, Green WR. Periocular Infections. In: Feigin RD, Cherry JD, eds. Textbook of Pediatric Infectious Diseases (4th ed). Philadelphia; W.B. Saunders Company; 1998:1273-1278.

Books in which the editor and author are the same person: Last name(s) of the author(s) and initials, chapter title, book editors, book title, edition, place of publication, date of publication and inclusive page numbers of the cited piece. Example: Solcia E, Capella C, Kloppel G. Tumors of the exocrine pancreas. In: Solcia E, Capella C, Kloppel G, eds. Tumors of the Pancreas. 2nd ed. Washington: Armed Forces Institute of Pathology; 1997:145-210.

TABLES, GRAPHICS, FIGURES, AND IMAGES

All visual materials together with their legends should be located on separate pages that follow the main text.

Images: Images (pictures) should be numbered and include a brief title. Permission to reproduce pictures that were published elsewhere must be included. All pictures should be of the highest quality possible, in JPEG format, and at a minimum resolution of 300 dpi.

Tables, Graphics, Figures: All tables, graphics or figures should be enumerated according to their sequence within the text and a brief descriptive caption should be written. Any abbreviations used should be defined in the accompanying legend. Tables in particular should be explanatory and facilitate readers' understanding of the manuscript, and should not repeat data presented in the main text.

BIOSTATISTICS

To ensure controllability of the research findings, the study design, study sample, and the methodological approaches and applications should be explained and their sources should be presented.

The "P" value defined as the limit of significance along with appropriate indicators of measurement error and uncertainty (confidence interval, etc.) should be specified. Statistical terms, abbreviations and symbols used in the article should be described and the software used should be defined. Statistical terminology (random, significant, correlation, etc.) should not be used in non-statistical contexts.

All results of data and analysis should be presented in the Results section as tables, figures and graphics; biostatistical methods used and application details should be presented

in the Materials and Methods section or under a separate title.

MANUSCRIPT TYPES

Original Articles

Clinical research should comprise clinical observation, new techniques or laboratories studies. Original research articles should include title, structured abstract, key words relevant to the content of the article, introduction, materials and methods, results, discussion, study limitations, conclusion references, tables/figures/images and acknowledgement sections. Title, abstract and key words should be written in both Turkish and English. The manuscript should be formatted in accordance with the above-mentioned guidelines and should not exceed sixteen A4 pages.

Title Page: This page should include the title of the manuscript, short title, name(s) of the authors and author information. The following descriptions should be stated in the given order:

1. Title of the manuscript (Turkish and English), as concise and explanatory as possible, including no abbreviations, up to 135 characters
2. Short title (Turkish and English), up to 60 characters
3. Name(s) and surname(s) of the author(s) (without abbreviations and academic titles) and affiliations
4. Name, address, e-mail, phone and fax number of the corresponding author
5. The place and date of scientific meeting in which the manuscript was presented and its abstract published in the abstract book, if applicable

Abstract: A summary of the manuscript should be written in both Turkish and English. References should not be cited in the abstract. Use of abbreviations should be avoided as much as possible; if any abbreviations are used, they must be taken into consideration independently of the abbreviations used in the text. For original articles, the structured abstract should include the following sub-headings:

Objectives: The aim of the study should be clearly stated.

Materials and Methods: The study and standard criteria used should be defined; it should also be indicated whether the study is randomized or not, whether it is retrospective or prospective, and the statistical methods applied should be indicated, if applicable.

Results: The detailed results of the study should be given and the statistical significance level should be indicated.

Conclusion: Should summarize the results of the study, the clinical applicability of the results should be defined, and the favorable and unfavorable aspects should be declared.

Keywords: A list of minimum 3, but no more than 5 key words must follow the abstract. Key words in English should be consistent with "Medical Subject Headings (MESH)" (www.nlm.nih.gov/mesh/MBrowser.html). Turkish key words should be direct translations of the terms in MESH.

Original research articles should have the following sections: **Introduction:** Should consist of a brief explanation of the topic and indicate the objective of the study, supported by information from the literature.

Materials and Methods: The study plan should be clearly described, indicating whether the study is randomized or not, whether it is retrospective or prospective, the number of trials, the characteristics, and the statistical methods used.

Results: The results of the study should be stated, with tables/figures given in numerical order; the results should

be evaluated according to the statistical analysis methods applied. See General Guidelines for details about the preparation of visual material.

Discussion: The study results should be discussed in terms of their favorable and unfavorable aspects and they should be compared with the literature. The conclusion of the study should be highlighted.

Study Limitations: Limitations of the study should be discussed. In addition, an evaluation of the implications of the obtained findings/results for future research should be outlined.

Conclusion: The conclusion of the study should be highlighted.

Acknowledgements: Any technical or financial support or editorial contributions (statistical analysis, English/Turkish evaluation) towards the study should appear at the end of the article.

References: Authors are responsible for the accuracy of the references. See General Guidelines for details about the usage and formatting required.

Case Reports

Case reports should present cases which are rarely seen, feature novelty in diagnosis and treatment, and contribute to our current knowledge. The first page should include the title in Turkish and English, an unstructured summary not exceeding 150 words, and key words. The main text should consist of introduction, case report, discussion and references. The entire text should not exceed 5 pages (A4, formatted as specified above).

Review Articles

Review articles can address any aspect of clinical or laboratory ophthalmology. Review articles must provide critical analyses of contemporary evidence and provide directions of current or future research. Most review articles are commissioned, but other review submissions are also welcome. Before sending a review, discussion with the editor is recommended.

Reviews articles analyze topics in depth, independently and objectively. The first chapter should include the title in Turkish and English, an unstructured summary and key words. Source of all citations should be indicated. The entire text should not exceed 25 pages (A4, formatted as specified above).

Letters to the Editor

Letters to the Editor should be short commentaries related to current developments in ophthalmology and their scientific and social aspects, or may be submitted to ask questions or offer further contributions in response to work that has been published in the Journal. Letters do not include a title or an abstract; they should not exceed 1,000 words and can have up to 5 references.

CORRESPONDENCE

All correspondence should be directed to the TJO editorial board:

Post: Turkish Ophthalmological Association
Avrupa Konutları Kale, Maltepe Mah. Yedikule Çırpıcı Yolu
Sk. 9. Blok No: 2 Kat:1 Ofis:1 Zeytinburnu-Istanbul-Turkey
Phone: +90 212 801 44 36/37 Fax: +90 212 801 44 39
Web Page: www.ofthalmoloji.org
E-mail: dergi@ofthalmoloji.org / sekreter@ofthalmoloji.org

CONTENTS

Research Articles

- 1 The Role of Optical Coherence Tomography Signal Strength in the Diagnosis and Follow-up of Patients with Posterior Capsular Opacification Treated with Nd:YAG Laser Capsulotomy
Mustafa Vatanserver, Erdem Dinç, Özer Dursun, Ufuk Adıgüzel, Ayça Yılmaz, Gülhan Ö. Temel; Mersin, Turkey
- 6 Evaluation of Peripheral Retinal Changes on Ultra-Widefield Fundus Autofluorescence Images of Patients with Age-Related Macular Degeneration
Kübra Küçükba, Nazmiye Erol, Muzaffer Bilgin; Eskişehir, Turkey
- 15 Stereoacuity, Fusional Vergence Amplitudes, and Refractive Errors Prior to Treatment in Patients with Attention-Deficit Hyperactivity Disorder
Irmak Karaca, Elif Demirkılıç Biler, Melis Palamar, Burcu Özbaran, Önder Üretmen; İzmir, Turkey
- 20 The Effect of Topical Cyclopentolate on Anterior Segment Parameters in Patients with Keratoconus
Ahmet Kırgız, Sevil Karaman Erdur, Semih Çakmak, Funda Dikkaya, Rukiye Aydın; İstanbul, Turkey
- 26 The Diagnostic Ability of Ganglion Cell Complex Thickness-to-Total Retinal Thickness Ratio in Glaucoma in a Caucasian Population
Almila Sarıgül Sezenöz, Sirel Gür Güngör, Ahmet Akman, Caner Öztürk, Şefik Cezairlioğlu, Mustafa Aksoy, Meriç Çolak; Ankara, Turkey
- 31 Iris Cysts: Clinical Features, Imaging Findings, and Treatment Results
Helin Ceren Köse, Kaan Gündüz, Melek Banu Hoşal; Ankara, Türkiye

Review

- 37 Artificial Intelligence and Ophthalmology
Kadircan Keskinbora, Fatih Güven; İstanbul, Turkey

Case Reports

- 44 Efficacy of Topical Brinzolamide Treatment in Posterior Microphthalmos-related Macular Cystoid Lesions: A Case Series
Ceren Durmaz Engin, Umut Baran Ekinci, Alper Selver, Ali Osman Saatci; Zonguldak, Manisa, İzmir, Turkey
- 50 Sarcoid-like Granulomatous Intraocular Inflammation Caused by Vemurafenib Treatment for Metastatic Melanoma
Hilal Eser Öztürk, Yüksel Süllü; Samsun, Turkey
- 53 Extranodal Ocular Adnexal Marginal Zone Lymphoma in a Ten-Year-Old Child
Nazan Çetingül, Melis Palamar, Şükriye Hacıkara, Serra Kamer, Hamiyet Hekimci Özdemir, Eda Ataseven, Özlem Barut Selver, Mine Hekimgil; İzmir, Turkey
- 56 An Unusual Case: Self-separation of an Idiopathic Epiretinal Membrane
Jale Menteş, Serhad Nalçacı; İzmir, Turkey

EDITORIAL

2020 Issue 1 at a Glance:

This issue of our journal features six original articles, one review, and four case reports that we hope you will find interesting and informative.

Posterior capsule opacification (PCO) is a clinical condition that develops after cataract surgery and leads to reductions in visual acuity and contrast sensitivity. The gold standard treatment for PCO is neodymium-doped yttrium aluminum garnet (Nd:YAG) laser. PCO is one of the main factors that can affect signal strength (SS) in optical coherence tomography (OCT). Vatansever et al. used Nd:YAG laser to treat 41 eyes of 35 patients who developed PCO after uncomplicated cataract surgery and had a PCO score of 3 or higher. The authors compared OCT data obtained before and 1 month after laser treatment and showed that postoperative best corrected visual acuity, SS, and central retinal thickness were significantly increased and SS was correlated with visual acuity in patients with PCO. They emphasized that PCO may affect the accuracy of objective data acquired with OCT (See pages 1-5).

Küçükiba et al. conducted a study to determine the prevalence of peripheral retinal changes in patients with age-related macular degeneration (AMD). They evaluated color and autofluorescence fundus images obtained in that order from 550 eyes of 277 AMD patients and 90 eyes of 45 healthy individuals in the control group using an ultra-wide-angle imaging system. They determined that peripheral retinal changes were more prevalent in AMD patients compared to healthy controls and concluded that AMD is not just a macular disease, but can affect the entire retina (See pages 6-14).

In their study evaluating pre-treatment stereopsis and fusional vergence amplitudes in children diagnosed with attention deficit and hyperactivity disorder (ADHD) compared to a control group, Karaca et al. retrospectively analyzed the detailed ophthalmologic examination with stereopsis and fusional vergence amplitudes of 23 newly diagnosed and untreated ADHD patients and 48 control subjects. They found that mean pretreatment stereopsis was significantly lower in children with ADHD while fusional vergence amplitudes did not differ significantly (See pages 15-19).

Kirgiz et al. conducted a prospective study using corneal topography to evaluate the effect of cycloplegia on the anterior

segment structures of patients with keratoconus and form fruste keratoconus. Their study included single eyes of 40 patients with keratoconus (group 1), 40 patients with form fruste keratoconus (group 2), and 40 healthy individuals (group 3), and showed that cycloplegia caused corneal steepening only in patients with manifest keratoconus but caused an increase in anterior chamber depth in all groups. This result highlights the importance of considering these effects of cycloplegia when conducting refraction examination, monitoring progression, and using contact lenses and phakic intraocular lenses in cases of keratoconus.

Sezenöz et al., analyzed macular ganglion cell complex (GCC) thickness, total retinal thickness, retinal nerve fiber layer thickness, and ganglion cell complex/total retinal thickness (G/T) ratio data from 9 healthy patients, 18 ocular hypertension patients, 28 preperimetric glaucoma patients, and 31 early glaucoma patients. They concluded that G/T ratio did not contribute significantly to the differentiation of ocular hypertension, preperimetric, and early glaucoma patients from the healthy population and had lower diagnostic value than the other examined parameters (See pages 26-30).

Köse et al. conducted a retrospective study evaluating the demographic, clinical, and imaging characteristics, treatment, and follow-up results of patients with iris cysts. In their study, 37 patients followed and treated for iris cysts were examined using ultrasound biomicroscopy (UBM), swept source OCT (SS-OCT), and SS-OCT angiography (SS-OCTA). The authors reported that most of the cysts were of primary etiology, originated from the pigment epithelium, and were located peripherally; that pigment epithelial cysts do not require any treatment, while stromal cysts usually require treatment; that UBM is superior to anterior segment OCT for imaging iris lesions and differentiating cystic and solid lesions; and that the development of anterior segment OCTA techniques has enabled the acquisition of information about the internal vascular structure of these tumors by non-invasive means (See pages 31-36).

Artificial intelligence is the ability of a computer to mimic the intellectual intelligence unique to humans. This intelligence framework may include qualities such as the ability to identify causation, make generalizations, and learn from experience. Artificial intelligence is developing rapidly and making its way into all areas of our lives, and in this issue's review, Keskinbora and Güven discuss advances and potential applications of

TURKISH JOURNAL OF OPHTHALMOLOGY



www.ofthalmoloji.org

TJO

EDITORIAL

artificial intelligence both in ophthalmology and within the framework of medical ethics. They share with readers that several artificial intelligence algorithms, some of which have been approved by the US Food and Drug Administration, have found their place in the field of ophthalmology, especially in studies focused on diagnosis, and that several studies have been developed that demonstrate the utility of artificial intelligence algorithms in the specific areas of diabetic retinopathy, AMD, and retinopathy of prematurity (See pages 37-43).

Posterior microphthalmia (PM) is a type of microphthalmia characterized by hyperopia, short axial length, posterior segment foreshortening, and normal or nearly normal anterior segment dimensions. Prominent posterior segment changes in PM include retinal folds, macular schisis, cystoid lesions, reduction or absence of the foveal avascular zone, pseudopapilledema, and uveal effusion. Engin et al. evaluated treatment response in 4 patients (8 eyes) diagnosed with PM and treated with topical 1% brinzolamide (AzoptTM; Alcon Inc., Belgium) for at least 6 months. They reported that during follow up, central macular thickness and cystoid lesion area decreased bilaterally in 3 patients and increased bilaterally in the other patient, while visual acuity remained stable in 5 eyes and improved in 3 eyes. Their study draws attention to the potential effectiveness of topical brinzolamide in the treatment of macular cystoid lesions in selected patients (See pages 44-49).

Öztürk and Süllü describe a 56-year-old male patient who presented with complaints of new-onset conjunctival hyperemia and blurred vision in both eyes. The patient reported having used 960 mg vemurafenib twice a day for the last 9 months due to cutaneous melanoma. Slit-lamp examination revealed bilateral keratic precipitates, +4 cells in the anterior chamber, and a pupillary membrane, while optic disc staining was observed on fluorescein angiography (FA). Etiological studies indicated no additional pathology, and the uveitis was attributed to vemurafenib. Due to the life-threatening nature of cutaneous melanoma, it was decided to continue treatment and initiate topical corticosteroid and cycloplegics. During follow-up, the uveitis assumed a granulomatous character and the patient's serum angiotensin converting enzyme (ACE) level increased. The authors emphasize with this case report that ocular sarcoidosis must be considered in patients with vemurafenib-associated uveitis (See pages 50-52).

Ocular adnexal lymphomas (OALs) usually arise from B cell proliferation and can develop in the conjunctiva, eyelid,

lacrimal glands, and orbit. The most common form of OAL is extranodal marginal zone B cell lymphoma (MZL), a very rare subtype of childhood non-Hodgkin lymphoma (NHL). Although most NHLs have an aggressive course in children, this rare type tends to have a slow course. In a case report by Çetingül et al., a 10-year-old girl presented with a rapidly growing salmon-colored mass protruding from the medial right lower eyelid that was noticed about 1 month earlier. The lesion was imaged using magnetic resonance imaging (MRI) and removed by mass excisional biopsy. Histopathological examination revealed B cell MZL. No involvement other than the lesion in the right eye was detected, and the patient was treated with external radiotherapy at a total dose of 36 Gy divided into fractions of 1.8 Gy/day for 17 days. The authors point out that although rare, ocular adnexal MZL can also be seen in children and that, just as with adult patients, conducting a biopsy is necessary in suspicious cases for definitive diagnosis and performing systemic evaluation for involvement of other areas is important (See pages 53-55).

Menteş and Nalçacı used clinical examination and spectral domain OCT to diagnose idiopathic epiretinal membrane (ERM) and stage 3 posterior vitreous detachment (PVD) in a 54-year-old woman presenting with complaints of floaters in her right eye, and they decided to follow-up with observation. Four months later, the patient presented with metamorphosis, and examination showed that she had decreased visual acuity but nearly no change in ERM findings. The patient presented again 1 week later due to the sudden resolution of her metamorphosis, and examination showed that her visual acuity had increased to 20/20, the ERM had spontaneously separated from the retinal surface in the form of a flap and was floating in the vitreous, and the foveal contour had normalized. The etiological mechanism was shown to be the stronger contraction forces within the immature ERM relative to the adhesive forces of the membrane to the retina (See pages 56-58).

We hope that the articles featured in the first issue of this year will be interesting to you and guide you in your professional practice.

**Respectfully on behalf of the Editorial Board,
Özlem Yıldırım, MD**



The Role of Optical Coherence Tomography Signal Strength in the Diagnosis and Follow-up of Patients with Posterior Capsular Opacification Treated with Nd:YAG Laser Capsulotomy

Mustafa Vatansever*, Erdem Dinç**, Özer Dursun**, Ufuk Adıgüzel**, Ayça Yılmaz**,
Gülhan Ö. Temel***

*Toros State Hospital, Clinic of Ophthalmology, Mersin, Turkey

**Mersin University Faculty of Medicine, Department of Ophthalmology, Mersin, Turkey

***Mersin University Faculty of Medicine, Department of Biostatistics and Medical Informatics, Mersin, Turkey

Abstract

Objectives: To investigate the relationship between optical coherence tomography (OCT) signal strength (SS) and visual acuity in patients with posterior capsule opacification (PCO) and evaluate the effect of PCO on retinal thickness measurements.

Materials and Methods: Forty-one eyes of 35 patients who were diagnosed with PCO were included in the study. Patients with any anterior or posterior segment pathology other than PCO were excluded. After ophthalmologic examination, pupil dilation was induced using 0.5% tropicamide and OCT images were acquired. The assessment was repeated 1 month after Nd:YAG laser capsulotomy and postoperative values were compared with baseline values.

Results: The patients' mean best corrected visual acuity (BCVA) was 0.28 ± 0.13 preoperatively and 0.78 ± 0.09 postoperatively ($p < 0.0001$). Strong positive correlations were observed between BCVA and SS both pre- and postoperatively ($p < 0.0001$ and $p = 0.01$, respectively). Central retinal thickness (CRT) and SS increased significantly postoperatively ($p < 0.0001$ for both). OCT SS and CRT were strongly correlated preoperatively ($p = 0.001$) but not postoperatively ($p = 0.46$).

Conclusion: OCT SS correlates with visual acuity in patients with PCO, and PCO can affect the accuracy of objective data obtained with OCT.

Keywords: Optical coherence tomography, posterior capsular opacification, signal strength, visual acuity

Introduction

Optical coherence tomography (OCT), introduced into use in 1990, is a low-coherence interferometry instrument that enables non-contact measurement of posterior segment structures.¹ OCT is widely used because it is a convenient, non-invasive, and

sensitive method, and has an important place in the diagnosis and follow-up of many macular diseases.^{1,2} The first OCT devices used in the clinic were time domain OCT (TD-OCT); these were followed by spectral domain OCT (SD-OCT) instruments, which feature faster data acquisition and provide higher resolution images compared to TD-OCT.^{3,4,5}

Address for Correspondence: Mustafa Vatansever MD, Toros State Hospital, Clinic of Ophthalmology, Mersin, Turkey
Phone: +90 507 340 89 58 E-mail: vatansevermustafa@hotmail.com **ORCID-ID:** orcid.org/0000-0003-2020-4417

Received: 15.05.2019 **Accepted:** 08.08.2019

Cite this article as: Vatansever M, Dinç E, Dursun Ö, Adıgüzel U, Yılmaz A, Temel GÖ. The Role of Optical Coherence Tomography Signal Strength in the Diagnosis and Follow-up of Patients with Posterior Capsular Opacification Treated with Nd:YAG Laser Capsulotomy. Turk J Ophthalmol. 2020;50:1-5

While signal-to-noise ratio was used to express image quality in early devices, this was replaced by signal strength (SS) in later models. With each scan, the instrument displays the SS to the operator, with higher SS corresponding to better image quality. SS may be affected by operator technique, eye and head movements during scan acquisition, and anterior or posterior segment opacities in the eye.⁶

Posterior capsule opacification (PCO) is one of the main factors that can affect SS. PCO is a clinical condition which develops after cataract surgery and results in reduced visual acuity and contrast sensitivity. The gold standard treatment for PCO is neodymium-doped yttrium aluminum garnet (Nd:YAG) laser application.^{7,8,9} The aim of the present study was to investigate the relationship between OCT SS and visual acuity in patients with PCO and evaluate the effect of Nd:YAG laser treatment on OCT measurements in these patients.

Materials and Methods

The medical records of patients who had Nd:YAG laser capsulotomy to treat PCO were reviewed retrospectively. Nd:YAG laser capsulotomy was performed at Mersin Toros State Hospital in Mersin, Turkey between July 2016 and July 2017. All procedures involving human subjects were performed according to the tenets of the Declaration of Helsinki. Informed consent forms were signed by the patients before enrollment. Forty-one eyes of 35 patients who presented with complaints of low vision after undergoing uncomplicated cataract surgery and were diagnosed with PCO were included in the study. Patients with any anterior or posterior segment pathology other than PCO were excluded. Patients with postoperative macular edema were also excluded from the study. Best corrected visual acuity (BCVA) was evaluated by Snellen chart. After a complete ophthalmologic examination, mydriasis was induced with 0.5% tropicamide.

PCO scoring was performed clinically by two blinded specialists using the biomicroscope. Nd:YAG laser capsulotomy was planned for patients with PCO scores of 3 or over. Cross-sectional images were acquired using the macular program in the OCT instrument (Nidek RS 3000; Nidek Co. Ltd., Aichi, Japan). All patients in the study underwent uncomplicated Nd:YAG laser capsulotomy (1.5-2.5 mJ; central opening of 3-4 mm) performed by the same surgeon. All patients received topical prednisolone acetate 4 times a day for 1 week after the procedure. At postoperative 1 month, BCVA was reassessed and postoperative OCT images were acquired after pupil dilation as before. The same experienced operator conducted all OCT scans, and repeated scans in cases with movement-related artifacts. We statistically analyzed the relationship between pre- and postoperative values and OCT SS, and the effect of laser capsulotomy on OCT measurements.

Statistical Analysis

SPSS version 11.5 software was used for statistical analysis. Each parameter was assessed for normal data distribution using the Shapiro-Wilk test. Pre- and postoperative values were compared using Wilcoxon test. Mean and standard deviation were calculated for each parameter. Spearman's correlation coefficient was calculated for the relationships between parameters. P values <0.05 were accepted as statistically significant.

Results

The mean age of the study patients (17 women, 18 men) was 62.37±7.2 years. Mean BCVA of the study group was 0.55±0.88 logMAR before Nd:YAG laser surgery and 0.10±1.04 logMAR postoperatively (p<0.0001) (Table 1). Significant positive correlations were observed between BCVA and OCT SS both pre- and postoperatively (p<0.0001 and p=0.01, respectively) (Table 2). Preoperative and postoperative central retinal thickness (CRT)

Table 1. Best corrected visual acuity, signal strength, central retinal thickness, and intraocular pressure values before and after Nd:YAG laser treatment

	Before Nd:YAG (n=41)	After Nd:YAG (n=41)	p
Best corrected visual acuity	0.28±0.13	0.78±0.09	<0.0001
Signal strength	2.98±1.38	7.29±1.27	<0.0001
Central retinal thickness (µm)	124.49±109.43	239.78±57.66	<0.0001
Intraocular pressure (mmHg)	13±2.41	12.93±2.25	0.81

Table 2. Comparison of best corrected visual acuity, signal strength, central retinal thickness, and intraocular pressure values before and after Nd:YAG laser treatment

		Correlation coefficient	p
Preoperative SS	BCVA	0.7	<0.0001
	CRT	0.51	0.001
	IOP	-0.07	0.96
Postoperative SS	BCVA	0.5	0.001
	CRT	-0.11	0.46
	IOP	0.12	0.45

SS: Signal strength, BCVA: Best corrected visual acuity, CRT: Central retinal thickness, IOP: Intraocular pressure

values were 124.49 ± 109.43 and $239.78 \pm 57.66 \mu\text{m}$ ($p < 0.0001$). The mean preoperative SS was 2.98 ± 1.38 and SS increased to 7.29 ± 1.27 postoperatively ($p < 0.0001$) (Table 1). There was also a significant positive correlation between preoperative OCT SS and CRT ($p = 0.001$) (Table 2) (Figure 1 and 2). However, CRT was not correlated with OCT SS after Nd:YAG laser treatment ($p = 0.46$) (Table 2). There was no significant change in intraocular pressure between measurements taken before and after the procedure ($p = 0.81$) (Table 1).

Discussion

OCT has become an indispensable tool in both the diagnosis and follow-up of macular diseases, glaucoma, and even anterior segment pathologies. However, with the increasing clinical use of OCT instruments, certain technical details involved in data acquisition have gained attention. The most important of these details is the SS obtained during acquisition, which is closely related to the image quality of the scanned sections. Previous studies have shown that OCT measurements can be affected

by factors such as age, race, and ocular pathologies, as well as SS.^{10,11,12,13,14,15,16,17}

PCO is the most common long-term complication of cataract surgery with intraocular lens implantation, and its prevalence is higher among pediatric patients and patients with trauma, uveitis, and diabetes mellitus.^{18,19,20,21} In a meta-analysis published by Schaumberg et al.,²² the incidence of PCO was reported to be 11.8% at postoperative 1 year, 20.7% at 3 years, and 28.4% at 5 years. PCO occurs when epithelial cells remaining in the capsular bag undergo fibrous metaplasia, proliferation, and migration. However, the cause of this process is not fully understood. The postoperative inflammatory response is thought to increase lens epithelial cell proliferation.^{23,24}

Hougaard et al.²⁵ suggested that PCO obscures retinal details by reducing signal quality, but reported no significant change between macular thickness measurements taken before and after laser treatment. In another study, it was observed that SS and visual acuity were correlated in PCO patients prior to Nd:YAG laser treatment, but PCO did not have an effect on macular measurements.²⁶ Considering both of these studies,

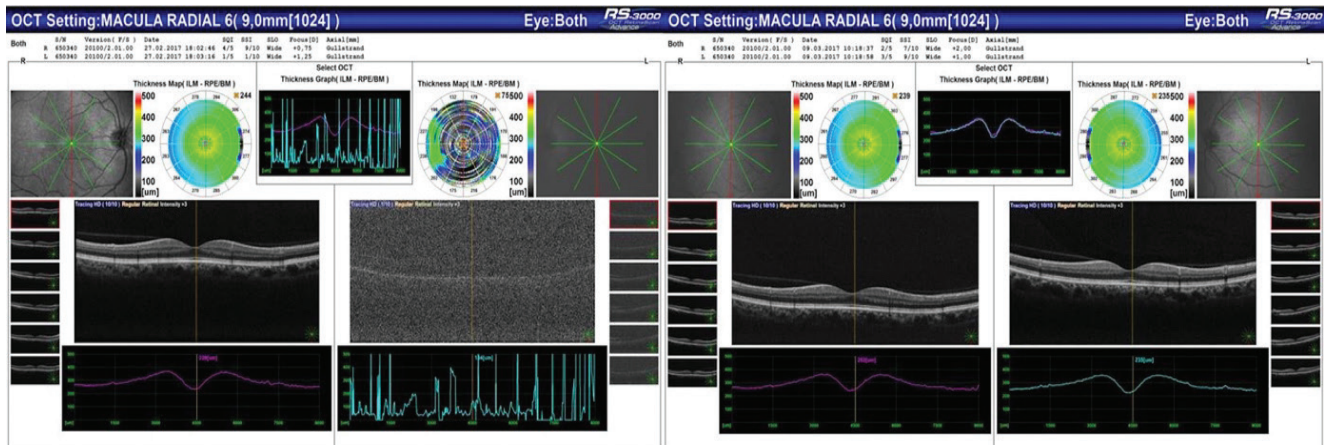


Figure 1. Macular OCT sections before and after Nd:YAG laser treatment of the left eye

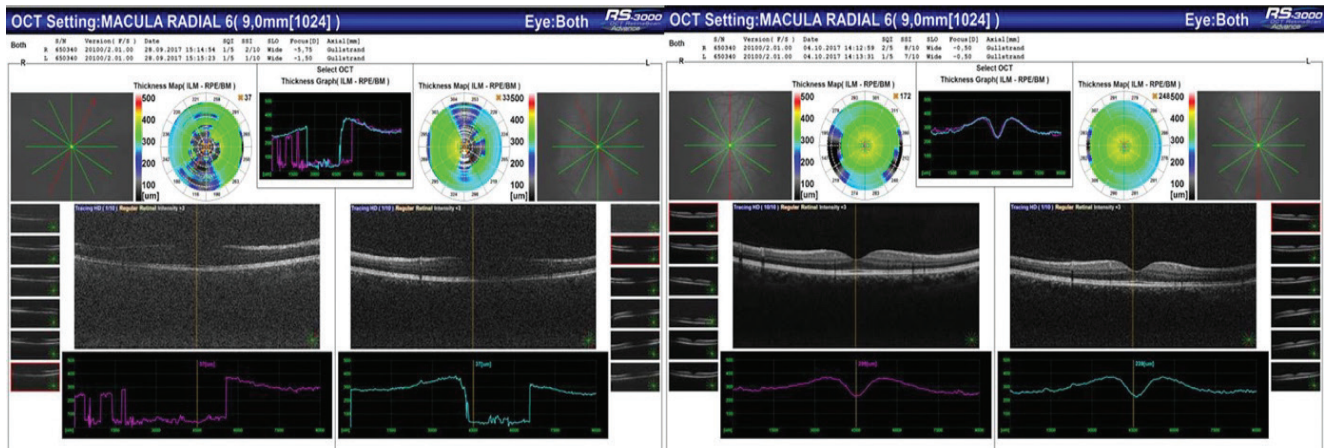


Figure 2. Macular OCT sections before and after Nd:YAG laser treatment of a patient treated in both eyes

it should be noted that Hougaard et al.²⁵ had a small sample number, while the postoperative SS in the other study was low (6.3). Another study by Kara et al.²⁷ reported that retinal nerve fiber layer thickness measurements significantly increased in patients with dense PCO following laser treatment. However, the same study reported no such relationship in cases without dense PCO. Cagini et al.²⁸ evaluated the quality and accuracy of measurements taken with both TD-OCT and SD-OCT devices in patients with PCO. The authors stated that PCO lowered the quality of measurements taken using TD-OCT, while the same effect was not observed in SD-OCT. They also observed that measurements taken with TD-OCT were lower than those taken with SD-OCT. Taken collectively, these studies lead to the conclusion that measurements can be affected in patients with dense PCO. In the present study, measurements were taken using SD-OCT in patients with PCO score of 3 or greater. Our results showed that despite taking measurements with SD-OCT, the presence of dense PCO could affect the values obtained, and that signal power was correlated with visual acuity and measured values. This finding demonstrates that the accuracy of measured values is affected as PCO increases in severity.

OCT SS was 6 or less before the Nd:YAG laser treatment and increased after laser treatment in all patients. These findings indicate that OCT SS can provide objective data when determining the Nd:YAG laser indications in patients with PCO. The increase in OCT SS after Nd:YAG laser capsulotomy may provide an objective measure of whether laser treatment was completed successfully.

Conclusion

In conclusion, OCT SS can provide information about opacity density in addition to that gained through biomicroscopic evaluation. It can also provide more objective data compared to subjective examination findings and help prevent unnecessary procedures. Considering that OCT is a non-invasive, easy, and rapid imaging technique, adding OCT SS as a parameter in the evaluation of patients with PCO may be beneficial.

Ethics

Ethics Committee Approval: (Local Ethics Committee of Mersin University-357)

Informed Consent: Consent was obtained from the patients.

Authorship Contributions

Surgical and Medical Practices: M.V., E.D., Ö.D., U.A., A.Y., G.Ö.T., Concept: M.V., E.D., Ö.D., U.A., A.Y., G.Ö.T., Design: M.V., E.D., Ö.D., U.A., A.Y., G.Ö.T., Data Collection or Processing: M.V., E.D., Ö.D., U.A., A.Y., G.Ö.T., Analysis or Interpretation: M.V., E.D., Ö.D., U.A., A.Y., G.Ö.T., Literature Search: M.V., E.D., Ö.D., U.A., A.Y., G.Ö.T., Writing: M.V., E.D., Ö.D., U.A., A.Y., G.Ö.T.

Conflict of Interest: No conflict of interest was declared by the authors.

Financial Disclosure: The authors declared that this study received no financial support.

References

- Huang D, Swanson EA, Lin CP, Schuman JS, Stinson WG, Chang W, Hee MR, Flotte T, Gregory K, Puliafito CA, Fujimoto JG. Optical coherence tomography. *Science* 1991;254:1178-1181.
- Puliafito C, Hee M, Schuman J. *Optical coherence tomography of ocular diseases*. Thorofare, NJ: Slack Inc; 1996.
- Sehi M, Grewal DS, Sheets CW, Greenfield DS. Diagnostic ability of fourier-domain vs time domain optical coherence tomography for glaucoma detection. *Am J Ophthalmol*. 2009;148:597-605.
- Chang RT, Knight OJ, Feuer WJ, Budenz DL. Sensitivity and specificity of time-domain versus spectral-domain optical coherence tomography in diagnosing early to moderate glaucoma. *Ophthalmology*. 2009;116:2294-2299.
- Leitgeb R, Hitzenberger C, Fercher A. Performance of fourier domain ve time domain optical coherence tomography. *Opt Express*. 2003;11:889-894.
- Zhang X, Iverson SM, Tan O, Huang D. Effect of signal intensity on measurement of ganglion cell complex and retinal nerve fiber layer scans in fourier domain optical coherence tomography. *Transl Vis Sci Technol*. 2015;4:7.
- MacEwen CJ, Dutton GN. Neodymium-YAG Laser in the management of posterior capsular opacification: complications and current trends. *Trans Ophthalmol Soc U K* 1986;105:337-344.
- Wormstone IM, Wang L, Liu CS. Posterior capsule opacification. *Exp Eye Res*. 2008;88:257-269.
- Hu CY, Woung LC, Wang MC. Change in the area of laser posterior capsulotomy: 3 month follow-up. *J Cataract Refract Surg*. 2001;27:538-542.
- Kim NR, Lee H, Lee ES, Kim JH, Hong S, Je Seong G, Kim CY. Influence of cataract on time domain and spectral domain optical tomography retinal nerve fiber layer measurements. *J Glaucoma*. 20012;21:116-122.
- Cheung CY, Leung CK, Lin D, Pang CP, Lam DS. Relationship between retinal nerve fiber layer measurement and signal strength in optical coherence tomography. *Ophthalmology*. 2008;115:1347-1351.
- Samarawickrama C, Pai A, Huynh SC, Burlutsky G, Wong TY, Mitchell P. Influence of OCT signal strength on macular, optic nerve head, and retinal nerve fiber layer parameters. *Invest Ophthalmol Vis Sci*. 2010;51:4471-4475.
- Wu Z, Huang J, Dustin L, Sadda SR. Signal strength is an important determinant of accuracy of nerve fiber layer thickness measurement by optical coherence tomography. *J Glaucoma*. 2009;18:213-216.
- Huang J, Liu X, Wu Z, Sadda S. Image quality affects macular and retinal nerve fiber layer thickness measurements on fourier-domain optical coherence tomography. *Ophthalmic Surg Laser Imaging*. 2011;42:216-221.
- Vizzeri G, Bowd C, Medeiros FA, Weinreb RN, Zangwill LM. Effect of signal strength and improper alignment on the variability of stratus optical coherence tomography retinal nerve fiber layer thickness measurements. *Am J Ophthalmol*. 2009;148:249-255.
- Knight OJ, Girkin CA, Budenz DL, Durbin MK, Feuer WJ; Cirrus OCT Normative Database Study Group. Effect of race, age, and axial length on optic nerve head parameters and retinal nerve fiber layer thickness measured by Cirrus HD-OCT. *Arch Ophthalmol*. 2012;130:312-318.
- Hirasawa K, Shoji N. Association between ganglion cell complex and axial length. *Jpn J Ophthalmol*. 2013;57:429-34.
- Apple DJ, Peng Q, Visessook N, Werner L, Pandey SK, Escobar-Gomez M, Ram J, Auffarth GU. Eradication of posterior capsule opacification: documentation of a marked decrease in Nd:YAG laser posterior capsulotomy rates noted in an analysis of 5416 pseudophakic human eyes obtained postmortem. *Ophthalmology*. 2001;108:505-518.
- Pollack A, Leiba H, Bukelman A, Oliver M. Cystoid macular oedema following cataract extraction in patients with diabetes. *Br J Ophthalmol*. 1992;76:221-224.

20. Hooper PL, Rao NA, Smith RE. Cataract extraction in uveitis patients. *Surv Ophthalmol.* 1990;35:120-144.
21. Ionides A, Dowler JG, Hykin PG, Rosen PH, Hamilton AM. Posterior capsule opacification following diabetic extracapsular cataract extraction. *Eye (Lond).* 1994;8:535-537.
22. Schaumberg DA, Dana MR, Christen WG, Glynn RJ. A systematic overview of the incidence of posterior capsule opacification. *Ophthalmology.* 1998;105:1213-1221.
23. Miyake K, Asakura M, Kobayashi H. Effect of intraocular lens fixation on the blood-aqueous barrier. *Am J Ophthalmol.* 1984;98:451-455.
24. Apple DJ, Mamalis N, Brady SE, Lofthfield K, Kavka-Van Norman D, Olson RJ. Biocompatibility of implant materials: a review and scanning electron microscopic study. *J Am Intraocul Implant Soc* 1984;10:53-66.
25. Hougaard JL, Wang M, Sander B, Larsen M. Effects of pseudophakic lens capsule opacification on optical coherence tomography of the macula. *Curr Eye Res.* 2001;23:415-421.
26. Gonzalez-Ocampo-Dorta S, Garcia-Medina JJ, Feliciano-Sanchez A, Scalerandi G. Effect of posterior capsular opacification removal on macular optical coherence tomography. *Eur J Ophthalmol.* 2008;18:435-441.
27. Kara N, Altinkaynak H, Yuksel K, Kurt T, Demirok A. Effects of posterior capsular opacification on the evaluation of retinal nerve fiber layer as measured by Stratus optical coherence tomography. *Can J Ophthalmol.* 2012;47:176-180.
28. Cagini C, Pietrolucci F, Lupidi M, Messina M, Piccinelli F, Fiore T. Influence of pseudophakic lens capsule opacification on spectral domain and time domain optical coherence tomography image quality. *Curr Eye Res.* 2015;40:579-584.



Evaluation of Peripheral Retinal Changes on Ultra-Widefield Fundus Autofluorescence Images of Patients with Age-Related Macular Degeneration

© Kübra Küçükiba, © Nazmiye Erol, © Muzaffer Bilgin

Eskişehir Osmangazi University Hospital, Clinic of Ophthalmology, Eskişehir, Turkey

Abstract

Objectives: Age-related macular degeneration (AMD) is the most common cause of central vision loss in individuals aged 65 years and older in developed countries. Earlier imaging systems did not enable visualization of the peripheral retina in diseases affecting the macula. With the introduction of new-generation devices, the peripheral retina is easily visualized. In our study, we aimed to evaluate the incidence of peripheral retinal changes in the color and autofluorescence fundus images of patients with AMD.

Materials and Methods: In the study group, 550 eyes of 277 patients who were diagnosed with AMD and 90 eyes of 45 healthy patients in the control group were evaluated. An ultra-wide-angle imaging device was used to record standard 200° color and autofluorescence fovea-centered fundus images followed by superior and inferior fundus images obtained using the device's fixation light. The fundus images were examined in 3 sections: zone 1, zone 2, and zone 3.

Results: Evaluation of color fundus images revealed peripheral retinal changes in 67.8% of the 550 AMD eyes and 47.8% of the healthy eyes. Drusen was the most common peripheral retinal change. Evaluation of autofluorescence images revealed peripheral autofluorescence changes in 39.6% of the AMD eyes and 28.9% of the healthy eyes. Hypoautofluorescence was the most common autofluorescence change.

Conclusion: Peripheral retinal changes were more common in AMD patients than the control group, indicating that AMD is not only a macular disease, but can affect the entire retina. Future prospective studies will elucidate the relationship between these peripheral retinal changes and patients' genetic features and their importance in prognosis, diagnosis, and treatment.

Keywords: Age-related macular degeneration, autofluorescence, peripheral abnormalities, ultrawide-field imaging

Introduction

Age-related macular degeneration (AMD) is the most common cause of central vision loss among individuals aged 65 years and older in developed countries.¹ While hyperpigmentation of the retinal pigment epithelium (RPE) and lipofuscin deposition in the macula are the earliest signs of the disease, there are studies demonstrating that findings such as drusen and pigmentary changes in the retina are present not only in the macula but also in the peripheral retina.^{2,3,4,5}

Thanks to advances in imaging methods, high-resolution images of the central and peripheral retina have been acquired since the 2000s using ultra-wide-angle imaging systems that can capture a 200° section of retina. With peripheral retinal imaging, color and autofluorescence images revealed that peripheral retinal changes occurred in extramacular areas in AMD patients. Color and autofluorescence images demonstrated that more peripheral retinal changes take place in patients with AMD compared to healthy individuals.^{4,5}

Address for Correspondence: Kübra Küçükiba MD, Eskişehir Osmangazi University Hospital, Clinic of Ophthalmology, Eskişehir, Turkey
Phone: +90 553 272 11 61 E-mail: duygululukubra@hotmail.com **ORCID-ID:** orcid.org/0000-0002-2290-8138

Received: 24.04.2019 **Accepted:** 03.12.2019

Cite this article as: Küçükiba K, Erol N, Bilgin M. Evaluation of Peripheral Retinal Changes on Ultra-Widefield Fundus Autofluorescence Images of Patients with Age-Related Macular Degeneration. Turk J Ophthalmol. 2020;50:6-14

©Copyright 2020 by Turkish Ophthalmological Association
Turkish Journal of Ophthalmology, published by Galenos Publishing House.

The aim of the present study was to determine and compare the prevalence of peripheral retinal changes in color and autofluorescence images in healthy individuals and AMD patients.

Materials and Methods

This prospective analysis included 550 eyes of 277 patients who presented to the Ophthalmology Department of the Eskişehir Osmangazi University Medical Faculty Hospital between June 2016 and July 2017 and were diagnosed with AMD, as well as 90 eyes of 45 patients with healthy retinas. Ethics committee approval was obtained before the study (number 980558721/137, dated May 30, 2016).

The 277 patients in the AMD group were selected from patients who were over 55 years of age, had no more than 6 diopters of refractive error, had not undergone retinal surgery or laser photocoagulation, and had no history of retinal disease other than AMD. AMD was diagnosed by evaluating the patients' fundus examinations and optical coherence tomography (OCT) images.

The 45 healthy individuals in the control group were over 55 years of age, had no more than 6 diopters of refractive error, had not undergone retinal surgery or laser photocoagulation, and had no history of any retinal disease.

After being informed about the study, all patients signed written consent forms. The age and gender of the patients in the AMD and control groups were recorded. All patients' pupils were dilated by instilling 2.5% phenylephrine and 1% tropicamide drops into both eyes. OCT images were acquired after dilation. An ultra-wide-angle Optos 200 Tx device was used to take 200° standard fovea-centered color images of both eyes, followed by superior and inferior fundus images obtained using the device's fixation light. Fundus autofluorescence images were acquired and recorded following the same protocol.

Image Evaluation

The obtained images were viewed using the Optos V2 Vantage Pro Review software. Fovea-centered, superior, and inferior color and autofluorescence images were acquired, for a total of 6 different images for each eye. All images were evaluated together with an experienced retina specialist. Evaluation began with fovea-centered images. Color fundus images were evaluated in 3 sections (zone 1, zone 2, and zone 3), as described in previous studies (Figure 1).^{4,5,6}

Zone 1 was defined as the area within a 5.4 mm diameter centered on the fovea and including the nasal edge of the optic disc and the temporal macula. It corresponds to approximately 3 optic disc diameters (DD). For AMD patients, zone 1 images were evaluated together with OCT images AMD grading was done according to AREDS Research Group criteria.⁷ AMD was graded as early in the presence of drusen smaller than 125 μm , intermediate if drusen were larger than 125 μm , and late in the presence of findings characteristic of geographic atrophy or neovascular AMD. Patients with late AMD were further divided into neovascular and geographical atrophy subgroups.

Zone 2 was defined as the area within a 16.2 mm circle, equivalent to 9 DD. Its inner boundary starts from zone 1 and its outer boundary coincides with the vortex veins. Changes observed in zone 2 color fundus images were recorded as drusen (Figure 2), RPE hypopigmentation (Figure 3), RPE hyperpigmentation (Figure 4), and reticular changes (Figure 5). Changes observed in zone 2 FAF images were recorded as hyperautofluorescence (Figure 6), hypoautofluorescence (Figure 7), and a halo (a lesion with a hypoautofluorescent center surrounded by hyperautofluorescence) (Figure 8).

Zone 3 was defined as the peripheral retina beyond zone 2 and was divided into 180° sections. Superior images obtained with upward gaze fixation were used to evaluate the upper half and inferior images obtained with downward gaze fixation were used to evaluate the lower half. Drusen, RPE hypopigmentation, RPE hyperpigmentation, reticular changes, cobblestone degeneration

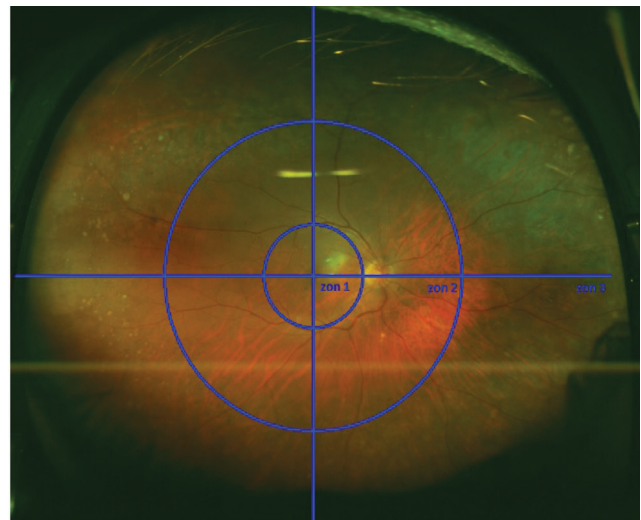


Figure 1. Zones 1, 2, and 3 on the fovea-centered image



Figure 2. Color fundus image acquired with upward gaze fixation showing peripheral drusen (arrow)

(Figure 9), and other changes observed in zone 3 color images were recorded. The area covered by the lesion was expressed in degrees by dividing the retina into clock hours (Figure 10). In eyes with multiple lesions, the largest was recorded as the primary lesion. Changes in zone 3 FAF images were recorded as hyperautofluorescence, hypoautofluorescence, halo, nummular (small, round hypoautofluorescent lesion with smooth border) (Figure 11), and cobblestone (multiple medium to large round hyperautofluorescent lesions with smooth borders) (Figure 12). Similar to the protocol used for color images, the area covered by the lesions was recorded in degree according to clock hour and the largest of multiple lesions was recorded as primary.

After zones 1 and 2 were evaluated based on fovea-centered images as shown in Figure 1, zone 3 was evaluated based on upward and downward gaze images.

An image was considered acceptable for analysis if the entirety of zone 1 and zone 2 and more than 50% of zone 3 were visible. Other images were excluded from the study.

Statistical Analysis

All data were entered into Microsoft Office 2013 Excel software. Continuous data were expressed as mean \pm standard deviation. Categorical data were expressed as percentage (%). The Shapiro-Wilk test was used to determine whether the data were normally distributed. When comparing groups with normal distribution, independent samples t-test was used in comparisons of 2 groups and one-way analysis of variance (ANOVA) was used for 3 or more groups. Pearson's chi-square and Fisher's exact tests were used to analyze the resulting contingency tables. IBM SPSS Statistics 21.0 software was used to perform the analyses. A p value <0.05 was accepted as the criterion for statistical significance.



Figure 3. Color fundus image acquired with upward gaze fixation showing peripheral RPE hypopigmentation (arrow)



Figure 5. Color fundus image acquired with upward gaze fixation showing reticular changes (arrow)

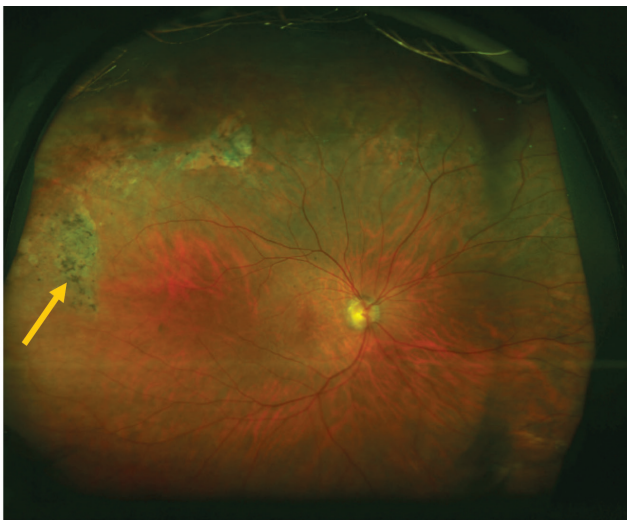


Figure 4. Fovea-centered color fundus image showing RPE hyperpigmentation (arrow)

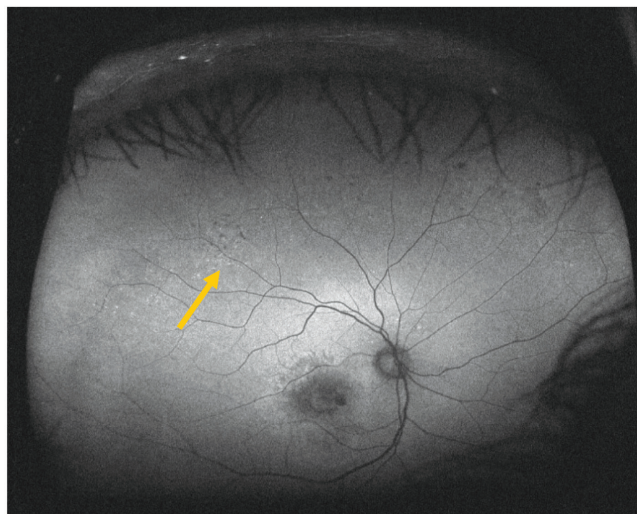


Figure 6. Fundus autofluorescence image acquired during upward gaze fixation showing hyperautofluorescence (arrow)

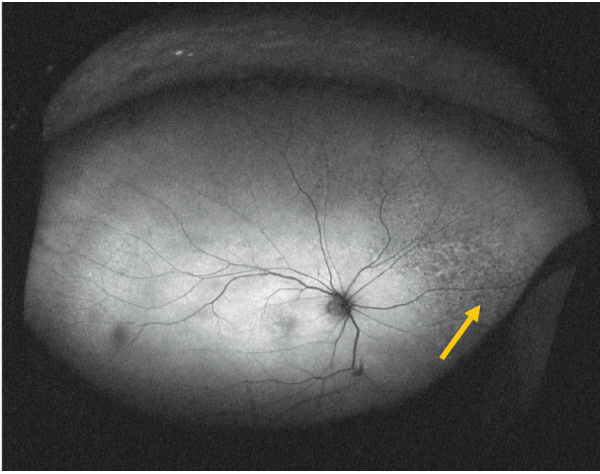


Figure 7. Fundus autofluorescence image acquired during upward gaze fixation showing hypoautofluorescence (arrow)

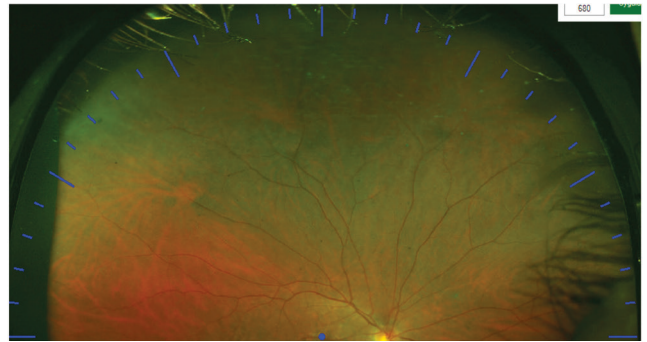


Figure 10. Clock-hour division of the retina in images acquired with upward gaze fixation

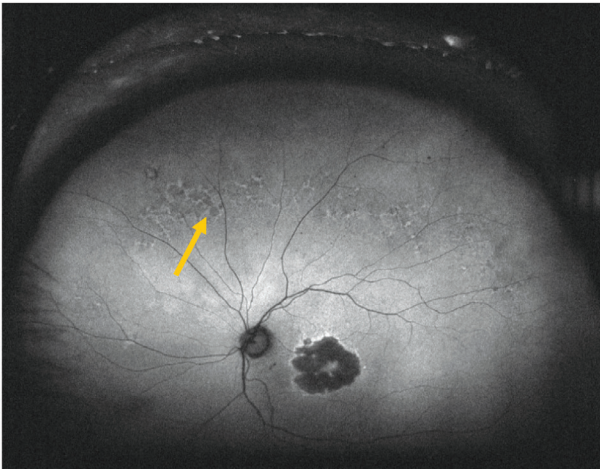


Figure 8. Fundus autofluorescence image acquired with upward gaze fixation showing a halo (lesion with hyperautofluorescent ring surrounding a hypoautofluorescent center) (arrow)

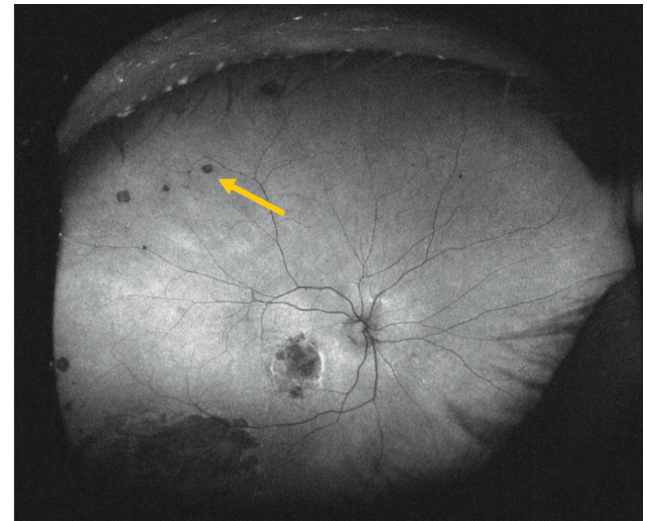


Figure 11. Fundus autofluorescence image acquired with downward gaze fixation showing a nummular lesion (arrow)

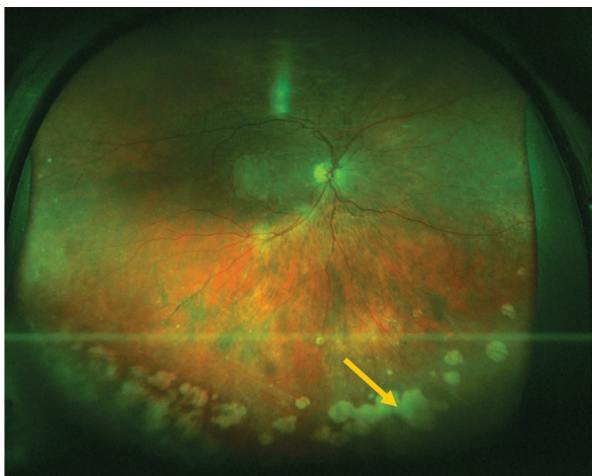


Figure 9. Color fundus image acquired with downward gaze fixation showing cobblestone degeneration (arrow)

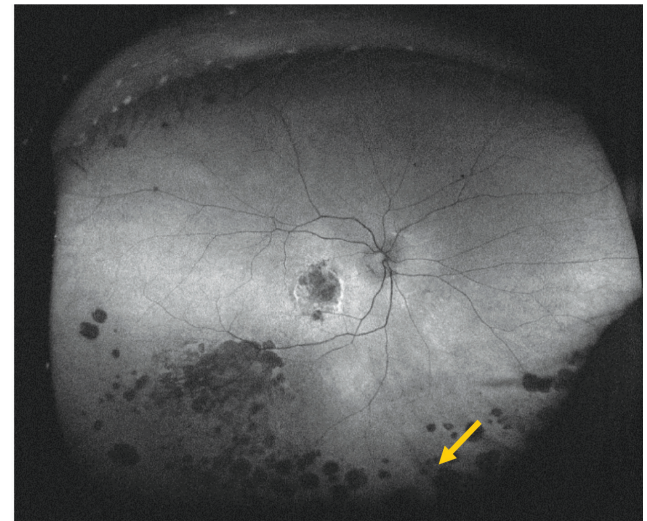


Figure 12. Fovea-centered fundus autofluorescence image showing cobblestone autofluorescence (arrow)

Results

In this study we evaluated 550 eyes of 277 patients diagnosed with AMD and 90 eyes of 45 healthy individuals in the control group. Four eyes in the AMD group that did not meet the evaluation criteria were excluded from the study. The age and sex distributions of patients in the AMD patients and control groups are shown in Table 1.

In the AMD group, 92 eyes (16.7%) were graded as early stage, 99 eyes (18%) as intermediate stage, and 359 eyes (65.3%) as late stage. Of those in the late AMD group, 95 eyes were evaluated as having geographic atrophy (17.3%) and 264 eyes as having neovascular AMD (48%).

Evaluation of Color Fundus Images

When color fundus images were evaluated, peripheral retinal changes in zone 2 and/or zone 3 were observed in 67.8% of the 550 eyes in the AMD group and in 47.8% of the 90 eyes in the control group. There were significantly more peripheral retinal changes in the AMD group compared to the control group (p<0.001).

The rates of the peripheral retinal changes detected when the color images of all patients in the AMD and control groups were evaluated are shown in Table 2.

When all peripheral zones were evaluated, rates of peripheral retinal change were significantly higher in the AMD group compared to the control group.

The distribution of peripheral retinal changes observed in the color fundus images of subjects in the AMD and control groups according to lesion type is shown in Table 3.

Drusen were the most common peripheral retinal change. Rates of drusen detection in zone 2, superior zone 3, and inferior zone 3 images were 29.6%, 54.2%, and 40.9%, respectively in the AMD group and 18.9%, 30%, and 21.1%, respectively in the control group (p=0.042, p<0.001, p<0.001). Compared to the control group, the AMD group had significantly more drusen in all areas.

When pigmentary changes were evaluated, the prevalence of RPE hypopigmentation in zone 2, superior zone 3, and inferior zone 3 was 3.1%, 6%, and 9.3% in the AMD group and 0%, 3.3%, and 4.4% in the control group, respectively (p=0.15, p=0.441, p=0.189). Rates of RPE hyperpigmentation in the AMD and control groups were 3.1% and 0% for zone 2, 2.7% and 2.2% for superior zone 3, and 5.5% and 4.4% for inferior zone 3, respectively (p=0.150, p=1.0, p=1.0). The prevalence of reticular changes in the AMD and control groups was 0.4% and 0% for zone 2, 4% and 0% for superior zone 3, and 5.3% and 3.3% for inferior zone 3, respectively (p=1.0, p=0.058, p=0.604). There was no statistically significant difference between the groups in terms of pigmentary changes.

Table 1. Age and sex distributions of the AMD and control groups

	AMD group n=277 (550 eyes)	Control group n=45 (90 eyes)
Sex	Female, 275 eyes (50.0%)	Female, 58 eyes (64.4%)
Age (mean)	72.13±8.16	65.91±7.84
Age (median)	73 (66-78)	63 (61-70.25)

AMD: Age-related macular degeneration

Table 2. Rates of peripheral retinal changes detected in the color images of patients in the AMD and control groups

	AMD group n=550		Control group n=90		
	n	%	n	%	
All peripheral changes - color					
Zone 2	193	35.1	17	18.9	p=0.002
Zone 3 superior	338	61.5	33	36.7	p<0.001
Zone 3 inferior	294	53.5	30	33.3	p<0.001

AMD: Age-related macular degeneration

Table 3. Distribution of all peripheral retinal changes detected in the color fundus images of patients in the AMD and control groups

		AMD group			Control group		
		Zone 2	Zone 3 superior	Zone 3 inferior	Zone 2	Zone 3 superior	Zone 3 inferior
Drusen	n	163	298	225	17	27	19
	%	29.6	54.2	40.9	18.6	30	21.1
RPE hypopigmentation	n	17	33	51	0	3	4
	%	3.1	6	9.3	0	3.3	4.4
RPE hyperpigmentation	n	17	15	30	0	2	4
	%	3.1	2.7	5.5	0	2.2	4.4
Reticular changes	n	2	22	29	0	0	3
	%	0.4	4	5.3	0	0	3.3
Cobblestone pattern	n	0	8	38	0	1	3
	%	0	1.5	6.9	0	1.1	3.3

AMD: Age-related macular degeneration, RPE: Retinal pigment epithelium

The prevalence of cobblestone degeneration, which was evaluated under other peripheral changes, in superior and inferior zone 3 was 1.5% and 6.9% in the AMD group and 1.1% and 3.3% in the control group, respectively (p=1.0, p=0.293). There was no statistically significant difference between the groups.

When evaluating the color fundus images of subjects in the AMD and control groups, the largest of multiple lesions was identified as the primary lesion and others as secondary lesions. Analysis of superior zone 3 images of the 550 eyes in the AMD group revealed primary peripheral retinal changes in 338 eyes (61.4%). Drusen were the most common primary lesion (82.5%), followed by RPE hypopigmentation (6.8%), reticular changes (5.6%), RPE hyperpigmentation (3.6%), and cobblestone degeneration (1.5%). Peripheral retinal changes in inferior zone 3 were detected in 294 eyes (53.4%). Similar to superior zone 3, drusen were the most common lesion (64.6%). RPE hypopigmentation and cobblestone degeneration were observed at equal rates (11.2%), followed by reticular changes (7.1%) and RPE hyperpigmentation (5.8%). The most common primary peripheral retinal change observed in superior and inferior zone 3 of patients in the control group was also drusen.

The most important and nonmodifiable risk factor associated with AMD is age. As mentioned in previous studies, we compared patient subgroups with no statistical age difference in order to prevent a miscalculation that may result from differences in age.⁶ The analysis included AMD patients between 65 and 79 years of age and control subjects between 60 and 71 years of age. Peripheral retinal changes were detected in 67% of 306 eyes in the AMD subgroup and in 34% of 50 eyes in the control subgroup. Based on this age-matched comparison, there were more significantly more peripheral retinal changes in the AMD group compared to the control group (p<0.001).

We also divided the AMD patients into subgroups based on disease stage and made comparisons between them and with the control group. Compared to the control group, patients with early, intermediate, and late AMD all showed significantly higher rates of peripheral retinal changes (p=0.038, p=0.001, p=0.001).

In the AMD group, the area occupied by lesions in the superior and inferior quadrants was measured in degrees. The largest lesion type in the superior quadrants was reticular changes, while the largest lesion type in the inferior quadrants was cobblestone degeneration.

Table 4. Rates of peripheral autofluorescence changes detected in the fundus autofluorescence images of patients in the AMD and control groups

	AMD group n=550		Control group n=90		
	n	%	n	%	
All peripheral changes- FAF					
Zone 2	119	21.6	1	1.1	p<0.001
Zone 3 superior	163	29.6	17	18.9	p=0.042
Zone 3 inferior	178	32.4	20	22.2	p=0.054

AMD: Age-related macular degeneration, FAF: Fundus autofluorescence

Evaluation of Fundus Autofluorescence (FAF) Images

When FAF images were evaluated, peripheral autofluorescence was observed in zone 2 and/or zone 3 in 39.6% of the 550 eyes in the AMD group and 28.9% of the 90 eyes in the control group. This difference between the groups was not statistically significant (p=0.052).

The prevalence of peripheral autofluorescence detected in the FAF images of all patients in the AMD and control groups is shown in Table 4.

The distribution of the peripheral retinal changes in the FAF images of patients in the AMD and control groups are shown in Table 5.

Table 5. Distribution of all peripheral retinal changes detected in the fundus autofluorescence images of patients in the AMD and control groups

		AMD group			Control group		
		Zone 2	Zone 3 superior	Zone 3 inferior	Zone 2	Zone 3 superior	Zone 3 inferior
Hyperautofluorescence	n	70	56	54	1	6	9
	%	12.7	10.2	9.8	1.1	6.7	10
Hyperautofluorescence	n	46	79	67	0	10	9
	%	8.4	14.4	12.2	0	11.1	10
Halo	n	7	23	23	0	0	0
	%	1.3	4.2	4.2	0	0	0
Nummular	n	0	19	36	0	0	1
	%	0	3.5	6.5	0	0	1.1
Cobblestone	n	0	8	38	0	1	3
	%	0	1.5	6.9	0	1.1	3.3

AMD: Age-related macular degeneration

Table 6. Rates of peripheral retinal and autofluorescence changes in the superior and inferior zone 3 images of patients in the AMD group

All Peripheral Changes (Zone 3 Superior/Inferior)			
	n	%	
Color fundus photographs			p<0.001
Superior	338	61.5	
Inferior	294	53.5	
Fundus autofluorescence			p<0.001
Superior	163	29.6	
Inferior	178	32.4	

AMD: Age-related macular degeneration

There was no statistically significant difference between the groups in the prevalence of hyperautofluorescence in zone 2 (p=0.002) or in superior and inferior zone 3 (p=0.394, p=1.00).

The prevalence of hypoautofluorescence in zone 2, superior zone 3, and inferior zone 3 were 8.4%, 14.4%, and 12.2% in the AMD group and 0%, 11.1%, and 10% in the control group, respectively (p=0.009, p=0.508, p=0.676). There were significantly more hypoautofluorescence lesions in zone 2 in the AMD group compared to the control group (p=0.004). Nummular autofluorescence was observed in superior and inferior zone 3 in 3.5% and 6.5% of eyes in the AMD group and 0% and 1.1% of eyes in the control group, respectively (p=0.092, p=0.071). The prevalence of cobblestone autofluorescence in superior and inferior zone 3 images was 1.5% and 6.9% in the AMD group and 1.1% and 3.3% in the control group, respectively (p=1.0, p=0.293). There were no statistically significant differences between the groups in terms of nummular or cobblestone autofluorescence rates.

Evaluation of superior zone 3 in the 550 AMD eyes revealed primary peripheral autofluorescence change in 163 eyes (29.6%). Hypoautofluorescence was the most common change (44.8%), followed by hyperautofluorescence (32.5%), halo (12.9%), and nummular lesions (7.4%). Cobblestone autofluorescence was the least common peripheral autofluorescence change (2.5%). Peripheral autofluorescence changes in inferior zone 3 were observed in a total of 178 eyes (32.3%). In inferior zone 3, hypoautofluorescence was the most common change (28.7%), followed by hyperautofluorescence (25.3%) and cobblestone (20.2%), nummular (14%), and halo hypoautofluorescence (11.8%).

As with color images, statistically age-matched subgroups were compared when evaluating FAF images. Peripheral autofluorescence changes were detected in 36.9% of 306 eyes in the AMD subgroup and 14% of 50 eyes in the control subgroup. Peripheral autofluorescence changes were significantly more common in the age-matched AMD subgroup compared to the control group (p=0.003).

Again, we also made comparisons between the control group and AMD subgroups based on disease stage. There

were no significant differences in the prevalence of peripheral autofluorescence changes in patients with early, intermediate, and late AMD compared to the control group (p=0.394, p=0.097, p=0.054). We further subclassified patients with late AMD into those with geographical atrophy and neovascular for comparison. There was a significant difference between these groups in terms of the prevalence of peripheral autofluorescence change (p=0.042), with more peripheral autofluorescence change in the geographical atrophy subgroup (49.5%) than in the neovascular subgroup (37.5%).

In the AMD eyes, the area occupied by lesions in the superior and inferior quadrants was measured in degrees. The largest lesion type in both hemispheres was hyperautofluorescence.

Color and FAF images of patients in the AMD group were examined in terms of the superior and inferior zone 3 regions. The comparison of rates of all retinal changes detected in superior and inferior zone 3 is shown in Table 6.

Peripheral retinal changes detected in color fundus images were significantly more common in the superior region compared to the inferior region (p<0.001). However, peripheral autofluorescence changes were significantly more common in the inferior region (p<0.001).

Discussion

Due to advances in imaging methods, we can now obtain peripheral retinal images using ultra-wide-angle imaging systems. In patients with AMD, the peripheral retina lying beyond the macula can be evaluated easily with color and autofluorescence images. Imaging of the peripheral retina has shown that peripheral retinal changes also occur in extramacular areas of the retina in AMD.

In this study comparing the color fundus and FAF images of AMD patients with those of healthy subjects, we evaluated similar studies in the literature and presented a detailed explanation of lesion names, locations, and evaluation methods in order to provide a summary of the interpretation and classification of these changes and to facilitate the standardization of future studies conducted in this field.

A review of the literature shows that the first study conducted with an ultra-wide-angle imaging system was published by Reznicek et al.⁸ in 2012. The study investigated peripheral autofluorescence intensity and abnormalities in patients with AMD. A significant difference was observed between the AMD and control group in terms of peripheral autofluorescence changes. The results of that study demonstrated that lipofuscin deposition in the RPE in AMD patients occurred not only in the macula, but also in the peripheral retina. However, only intensity was measured from the peripheral FAF images; the peripheral lesions and their features were not described.⁸

Since more standard images were obtained in published studies that utilized the software developed by Optos to eliminate torsion in images obtained in the upward and downward gaze fixation positions of the device, these studies seem to have less subjectivity.^{4,9} In the present study, we evaluated images taken

without using such software separately. In future studies, it may be beneficial to use software that ensures standardization in order to prevent analytical errors that may result from subjective evaluation.

Because there is no indicator that would ensure standard image acquisition, the images appear larger than they actually are if the patient gets too close to the device and smaller than they actually are if the patient is too far from the device. For this reason, the size of the patient's optic disc was used as a reference when evaluating each image in an effort to prevent the errors that can arise in millimetric measurements, which led to the concept of zones. Studies conducted to date present different views regarding how the midperipheral area (i.e., the retinal region referred to as zone 2) should be calculated.^{4,5,7,8,9,10,11,12} When planning the present study, we accepted an area of 3 DD as zone 1 and an area of 9 DD as zone 2 (considered the midperiphery).^{5,6} Confusion regarding the definition of the midperipheral region in the literature is preventing its standardization in current studies and necessitates the establishment of standard measurements which can be incorporated into emerging technologies.

There are also differences of opinion regarding the identification of autofluorescence changes in the periphery and midperiphery. Every change observed in the present study was named based on commonly used definitions in previous studies and is described together with an image. In one study, the rate of consistency between two independent researchers evaluating FAF images was reported as 78.4%.¹³ In the same study, when the researchers were asked to differentiate between hypoautofluorescence and hyperautofluorescence, the agreement rate fell to 69%. Ultimately, the interpretation of FAF images is subjective. Although increasing the number of researchers improves reliability, it does not ensure standardization.

In our evaluation of AMD patients, peripheral retinal changes were observed in 67.8% of their color fundus images and 39.6% of their FAF images. The prevalence of peripheral autofluorescence changes was 29.6% in superior images and 32.4% in inferior images. More peripheral retinal changes were detected in the color fundus and FAF images of AMD patients compared to healthy subjects.

Drusen was the most common peripheral retinal change observed in color images of zone 2, superior zone 3, and inferior zone 3 in both the AMD and control groups, while hypoautofluorescence was the most common peripheral autofluorescence change observed in FAF images. Studies in the literature present varying results regarding autofluorescence changes detected in the peripheral retina. In the OPERA study, consistent with our findings, the most common type of lesion observed in zone 2, superior zone 3, and inferior zone 3 color images from the patient and control groups was drusen, with the most common peripheral autofluorescence change observed in FAF images was hypoautofluorescence.⁴ In a study by Suetsugu et al.¹², the most common autofluorescence change observed in the periphery (45.5%) was mottled autofluorescence (areas of irregular hypoautofluorescence). In another study, drusen was reported as the most common lesion in color images and

granular (hyperautofluorescent areas) autofluorescence was the most common autofluorescence change in FAF images from the neovascular, geographic atrophy, and control groups.⁵

Drusen stands out as the most common type of peripheral lesion in studies. In a recent study, the CFHY402H genotype was linked to peripheral drusen and the CFHrs1410996 genotype to peripheral retinal pigmentary changes in patients with AMD.¹⁴

When the studies in the literature are compared, each research group seems to have described autofluorescence lesions in a distinctive way. In one study, lesions are described as being granular, nummular, and mottled, while in another study they are described as focal pinpoint, granular, patchy, and reticular.^{5,10} In the OPERA study, the detected lesions were described as hypoautofluorescence, hyperautofluorescence, and reticular autofluorescence.⁴ Based on our review of all relevant studies, we classified autofluorescence lesions in the present study under 5 categories: hypoautofluorescence, hyperautofluorescence, halo, nummular, and cobblestone autofluorescence.

A limitation of our study which is common to all studies is the age difference between the study and control groups. This difference may stem from the fact that the rate of patients aged 80 and over with healthy retinas presenting to outpatient clinics is much lower than for the same age group with AMD. For this reason, the patient population constituting the control group has a relatively lower average age than the study group. As in other studies, we performed an age-matched subgroup analysis in this study to overcome this limitation.^{4,5}

Based on the present study and others in the literature, peripheral retinal changes are found in the color and FAF images of AMD patients. It is thought that these peripheral lesions may herald dysfunction at the RPE level. This disease is not exclusively macular but can affect the entire retina at varying rates in all zones, and shows individual differences. In a study evaluating dark adaptation in AMD patients, it was shown that higher patient age, AMD stage, and presence of pseudodrusen were associated with prolonged dark adaptation time.¹⁵

Only FAF images were evaluated in some studies, while others evaluated both color and FAF images together.^{4,5,10,11} The disadvantage of not evaluating both images together is that in patients with peripheral drusen on color images, FAF images may show hypoautofluorescence, hyperautofluorescence, or no change in autofluorescence. Therefore, the rate of detection of peripheral retinal changes may differ when only FAF images are evaluated.

Conclusion

In conclusion, we observed a statistically significant difference between AMD patients and the control group in terms of peripheral retinal change detection rates. Our findings are consistent with those of other studies.^{4,5,11,12} The evidence indicates that AMD is not just a macular disease, but rather a disease that can affect the entire retina. Future prospective studies will allow us to determine the relationship between these peripheral retinal changes and patients' genetic characteristics

and their importance in prognosis, diagnosis, and treatment of the disease.

Ethics

Ethics Committee Approval: Eskişehir Osmangazi University dated 30.05.2016 80558721/137 23 ethical committee approval of the data.

Informed Consent: Written informed consent was obtained from the patients.

Peer-review: Externally peer-reviewed.

Authorship Contributions

Surgical and Medical Practices: K.K., Concept: N.E., Design: K.K., N.E., Data Collection or Processing: K.K., Analysis or Interpretation: M.B., K.K., Literature Search: K.K., Writing: K.K.

Conflict of Interest: No conflict of interest was declared by the authors.

Financial Disclosure: The authors declared that this study received no financial support.

References

1. Pascolini D, Mariotti SP. Global estimates of visual impairment: 2010. *Br J Ophthalmol*. 2012;96:614-618.
2. Jarrett SG, Boulton ME. Consequences of oxidative stress in age-related macular degeneration. *Mol Aspects Med*. 2012;33:399-417.
3. Shuler RK Jr, Schmidt S, Gallins P, Hauser MA, Scott WK, Caldwell J, Agarwal A, Haines LJ, Pericak-Vance MA, Postel EA. Peripheral Reticular Pigmentary Change Is Associated with Complement Factor H Polymorphism (Y402H) in Age-Related Macular Degeneration. *Ophthalmology*. 2008;115:520-524.
4. Writing Committee for the OPRs, Domalpally A, Clemons TE, Danis RP, Sadda SR, Cukras CA, Toth CA, Friberg TR, Chew EY. Peripheral Retinal Changes Associated with Age-Related Macular Degeneration in the Age-Related Eye Disease Study 2: Age-Related Eye Disease Study 2 Report Number 12 by the Age-Related Eye Disease Study 2 Optos PEripheral RetinA (OPERA) Study Research Group. *Ophthalmology*. 2017;124:479-487.
5. Tan CS, Heussen F, Sadda SR. Peripheral autofluorescence and clinical findings in neovascular and non-neovascular age-related macular degeneration. *Ophthalmology*. 2013;120:1271-1277.
6. Nomura Y, Takahashi H, Tan X, Obata R, Yanagi Y. Widespread choroidal thickening and abnormal midperipheral fundus autofluorescence characterize exudative age-related macular degeneration with choroidal vascular hyperpermeability. *Clin Ophthalmol*. 2015;9:297-304.
7. Age-Related Eye Disease Study Research Group. Risk factors associated with age related macular degeneration. A case-control study in the age-related eye disease study: Age-Related Eye Disease Study Report Number 3. *Ophthalmology*. 2000;107:2224-2232.
8. Reznicek L, Wasfy T, Stumpf C, Kampik A, Ulbig M, Neubauer AS, Kernt M. Peripheral fundus autofluorescence is increased in age-related macular degeneration. *Invest Ophthalmol Vis Sci*. 2012;53:2193-2198.
9. Oellers P, Laíns I, Mach S, Garas S, Kim IK, Vavvas DG, Miller JW, Husain D, Miller JB. Novel grid combined with peripheral distortion correction for ultra-widefield image grading of age-related macular degeneration. *Clin Ophthalmol*. 2017;11:1967-1974.
10. Heussen FM, Tan CS, Sadda SR. Prevalence of peripheral abnormalities on ultra-widefield greenlight (532 nm) autofluorescence imaging at a tertiary care center. *Invest Ophthalmol Vis Sci*. 2012;53:6526-6531.
11. Witmer MT, Kozbial A, Daniel S, Kiss S. Peripheral autofluorescence findings in age-related macular degeneration. *Acta Ophthalmol*. 2012;90:428-433.
12. Suetsugu T, Kato A, Yoshida M, Yasukawa T, Nishiwaki A, Hasegawa N, Usui H, Ogura Y. Evaluation of peripheral fundus autofluorescence in eyes with wet age-related macular degeneration. *Clin Ophthalmol*. 2016;10:2497-2503.
13. Guduru A, Fleischman D, Shin S, Zeng D, Baldwin JB, Houghton OM, Say EA. Ultra-widefield fundus autofluorescence in age-related macular degeneration. *PLoS One*. 2017;12:e0177207.
14. Seddon JM, Reynolds R, Rosner B. Peripheral retinal drusen and reticular pigment: association with CFHY402H and CFHrs1410996 genotypes in family and twin studies. *Invest Ophthalmol Vis Sci*. 2009;50:586-591.
15. Flamendorf J, Agrón E, Wong WT, Thompson D, Wiley HE, Doss EL, Al-Holou S, Ferris FL, Chew EY, Cukras C. Impairments in Dark Adaptation Are Associated with Age-Related Macular Degeneration Severity and Reticular Pseudodrusen. *Ophthalmology*. 2015;122:2053-2062.



Stereoacuity, Fusional Vergence Amplitudes, and Refractive Errors Prior to Treatment in Patients with Attention-Deficit Hyperactivity Disorder

© Irmak Karaca*, © Elif Demirkılınc Biler*, © Melis Palamar*, © Burcu Özbaran**, © Önder Üretmen*

*Ege University Faculty of Medicine, Department of Ophthalmology, İzmir, Turkey

**Ege University Faculty of Medicine, Department of Child and Adolescent Psychiatry, İzmir, Turkey

Abstract

Objectives: To evaluate stereoacuity, fusional vergence amplitudes, and refractive errors in patients with attention-deficit hyperactivity disorder (ADHD).

Materials and Methods: Twenty-three patients who were newly diagnosed as having ADHD and had not started medication, and 48 children without ADHD were included. Retrospective data analysis of comprehensive eye examination, stereoacuity, and fusional vergence amplitudes of the patients were performed.

Results: The mean age at ADHD diagnosis was 10.68 ± 2.34 (7-16) years in the ADHD group (14 male, 9 female) and 12.23 ± 2.16 (7-15) years in the control group (25 male, 23 female) patients ($p=0.605$). The mean stereoacuity was 142.14 ± 152.65 (15-480) sec/arc in patients with ADHD and 46.3 ± 44.11 (15-240) sec/arc in the control group ($p<0.001$). For ADHD patients, the mean convergence and divergence amplitudes at distance were 19.87 ± 8.40 (6 to 38) prism diopter (PD) and -9.09 ± -4.34 (-4 to -25) PD, and 37.30 ± 12.81 (14 to 70) PD and -13.13 ± -3.45 (-4 to -20) PD at near, respectively. The mean cycloplegic spherical equivalent was 1.06 ± 1.13 (-1 to 4.63) diopter in ADHD patients, with 6 patients having significant refractive errors (hyperopia in 4 patients, astigmatism in 2 patients). There were no significant differences between groups in terms of spherical equivalents ($p=0.358$) or convergence and divergence amplitudes at distance ($p=0.289$ and $p=0.492$, respectively) or near ($p=0.452$ and $p=0.127$, respectively).

Conclusion: Fusional vergence amplitudes did not present significant difference, while the mean value of stereoacuity was significantly lower in newly diagnosed ADHD patients prior to treatment.

Keywords: Attention-deficit and hyperactivity disorder, fusional vergence, stereoacuity

Introduction

Attention-deficit hyperactivity disorder (ADHD) is one of the most common neurodevelopmental disorders in children and adolescents. The prevalence of ADHD in developed countries is reported to be 2-18% among children between the ages of

6 and 17 years.^{1,2} ADHD is characterized by low attention, increased hyperactivity, impulsivity, and lack of control of inappropriate behaviors.³ In addition to quality of life, school performance is likely to be affected in patients with ADHD. In the literature, despite the variable results in studies associating visual dysfunction with school performance, there is a possible

Address for Correspondence: Irmak Karaca MD, Ege University Faculty of Medicine, Department of Ophthalmology, İzmir, Turkey
Phone: +90 536 621 56 16 E-mail: irmakkaracamd@gmail.com **ORCID-ID:** orcid.org/0000-0001-7927-0887

Received: 29.05.2019 **Accepted:** 05.09.2019

Cite this article as: Karaca I, Demirkılınc Biler E, Palamar Onay M, Özbaran B, Üretmen Ö. Stereoacuity, Fusional Vergence Amplitudes, and Refractive Errors Prior to Treatment in Patients with Attention-Deficit Hyperactivity Disorder. Turk J Ophthalmol. 2020;50:15-19

relationship between the symptoms of visual problems and ADHD-related behaviors.^{4,5}

Brain imaging studies demonstrated delayed maturation in the brains of ADHD patients, with reduced striatal volume and differences in hippocampal, accumbens, and amygdala volumes compared to healthy controls. These findings along with dopamine and norepinephrine imbalance in the prefrontal cortex supported the deficits in emotional regulation, motivation, and memory in these patients.^{6,7} As the eyes are considered a continuation of central nervous system, the ocular system enables the evaluation of neurological changes and nervous system activation/inhibition.⁸ In patients with ADHD, binocular vision changes and oculomotor deficits such as convergence insufficiency^{9,10}, accommodative dysfunction¹¹, reduced stereoacuity¹², and ametropia¹³ have been reported. Regarding underlying mechanisms, Poltavski et al.¹⁴ suggested a bidirectional relationship between attention and accommodation. However, the association between ADHD and oculomotor control changes such as accommodative dysfunction and convergence insufficiency is not clearly known yet. Additionally, there are several contradictory reports in terms of stereoacuity, refractive state, etc.^{12,13}, and treatment status of the patients enrolled in those studies also varied. Therefore, this study aims to investigate stereoacuity, fusional vergence amplitudes, and cycloplegic refractive errors in newly diagnosed ADHD patients prior to medication.

Materials and Methods

The charts of 23 consecutive patients who were newly diagnosed with ADHD according to DSM-IV criteria³ and had not yet received medication, and the data of 48 control patients of similar age and sex distribution who did not have ADHD and consecutively presented to the ophthalmology outpatient clinic for routine evaluation were retrospectively reviewed. The study was approved by the Institutional Ethics Review Board of Ege University and adhered to the precepts of the Declaration of Helsinki. Patients with congenital or acquired ophthalmic pathologies (such as optic nerve disease, glaucoma, cataract or additional media opacities, amblyopia, and strabismus), ophthalmic surgery history, and systemic or neuropsychiatric diseases other than ADHD were excluded. Stereoacuity measured with TNO Random-dot Stereo test (Lameris Intrumenten, Groeningen, Netherlands, 17th Edition), fusional vergence amplitudes, presence of heterophoria with cover/uncover test, best corrected visual acuity (BCVA) according to Snellen scale, and spherical equivalent (SE) of refractive errors (Topcon KR-7000P) (Topcon Europe BV, Capelle/dIJssel, Netherlands) after cycloplegia (with 1% cyclopentolate hydrochloride) were recorded for all patients. As described in the literature¹⁵, fusional convergence and divergence amplitudes at distance (6 m) and near (33 cm) were measured by the same two examiners (I.K., E.D.B.) 3 times at 15-minute intervals with placement of the fixed horizontal prism bar (1D-40D) in front of an eye in all patients, while they fixated on an accommodative

target. The base-out prism power was gradually increased for convergence and the base-in prism bar was gradually increased for divergence, and the patient was asked to identify the point at which the target image appeared to be doubled; this prism power was designated as the breakpoint. Patients with spectacles were tested with habitual optical correction in glasses or contact lenses. The mean value of the fusional vergence measurements were taken into account for the statistical analysis. Significant refractive errors were defined as an SE of myopia ≥ 0.5 diopter (D) or hyperopia ≥ 1.0 D. Significant astigmatism was defined as a level of ≥ 1.0 D and anisometropia, ≥ 1.0 D SE.¹⁶

Statistical Analysis

The statistical analysis was performed using SPSS software for Windows version 15.0 (SPSS Inc, Chicago, Illinois, USA) and Microsoft Office Excel (Microsoft, Redmond, Washington, USA). For stereoacuity, all values were transformed to the logarithm of arc seconds.¹⁷ Statistical analyses were performed by independent t-test and chi-square test. A p value < 0.05 was accepted as statistically significant.

Results

The mean age of the subjects was 10.68 ± 2.34 (range=7 to 16) years in patients with ADHD (14 male, 9 female) and 12.23 ± 2.16 (range=7 to 15) years in the control group (25 male, 23 female). Anterior segment and fundus examinations were unremarkable and BCVA was 20/20 in both eyes of all subjects. No patient presented with restriction of eye movements, heterotropia, or anisometropia. The 22 patients (95.5%) in the ADHD group who were able to perform TNO Random-dot Stereo test had stereoacuity (at least 480 sec/arc) with full refractive correction. The mean and median values for stereoacuity were 142.14 ± 152.65 (range=15-480) sec/arc and 60 sec/arc, respectively. The mean of convergence and divergence amplitudes at distance were 19.87 ± 8.40 (range=6 to 38) prism diopter (PD) and -9.09 ± 4.34 (-4 to -25) PD, and at near 37.30 ± 12.81 (14 to 70) PD, and -13.13 ± 3.45 (-4 to -20) PD, respectively. The SE following cycloplegia was 1.06 ± 1.13 (range=-1 to +4.63) D. Thirteen patients were found to have significant refractive errors (hyperopia in 13 patients, astigmatism in 2 patients). Two patients who had hyperopia higher than 3.5 D were prescribed spectacles due to asthenopia and low BCVA. In the control group, all subjects were able to perform TNO Random-dot Stereo test and had stereoacuity with a mean of 46.3 ± 44.11 (range=15 to 240) and the median of 30 sec/arc. The mean of convergence and divergence amplitudes at distance were 23.54 ± 6.24 (range=14 to 36) and -9.67 ± 3.71 (range=-4 to -16) PD, and at near 38.21 ± 8.13 (range=25 to 64) and -15.76 ± 3.52 (range=-12 to -25) PD, respectively. Following cycloplegia, the mean SE was 0.53 ± 1.76 (range=-2.75 to 2.12) D, while 13 subjects had significant refractive errors (myopia in 6 patients, hyperopia in 7 patients, and astigmatism in 3 patients). There were no statistically significant differences between groups in terms of SE ($p=0.358$) or convergence and divergence amplitudes at distance ($p=0.289$ and $p=0.492$, respectively) or

near ($p=0.452$ and $p=0.127$, respectively). Stereoacuity, fusional vergence amplitudes, and refractive status of the subjects are summarized in Table 1.

Discussion

ADHD is thought to be associated with several negative outcomes, such as antisocial behaviors, social and peer problems, and psychiatric disorders later in life.^{18,19} Specifically, school performance, along with intellectual capacity, social abilities and occupational functions are impaired in patients with ADHD. In addition, ADHD is considered a major public health problem due to the considerable economic burden to families and community.^{3,20,21}

A possible association between ADHD and visual problems was reported.^{4,5} In the literature, there are only a few studies revealing the relationship between ADHD and ocular abnormalities.^{8,13,22,23} Granet et al.⁸ retrospectively evaluated 266 children with convergence insufficiency and reported that 26 (21 male, 5 female) patients (9.8%) had ADHD either at the time of diagnosis or during the follow-up period. Among them, 20 (76.9%) patients were on medical treatment and 6 patients had never received treatment or had discontinued treatment. Additionally, a review of 176 ADHD patients who underwent ophthalmic evaluation revealed that 29 patients (15.9%) were diagnosed with convergence insufficiency based on their medical records. Thus, the authors suggested that convergence insufficiency should be investigated in patients with ADHD, despite the lack of causal relationship. Vergence is defined as simultaneous movements of eyes in opposite directions in order to have single binocular vision.²⁴ Viewing through a range of prisms placed before the eyes in both a base-in and then base-out direction has long been used as a diagnostic measure of

vergence and accommodation dysfunction.²⁵ The capacity to see a single image via the base-out prisms without diplopia or blur is referred to as the fusional limit and determines the strength of convergence response, and vice versa.²⁶ Therefore, fusional amplitudes have an important role in the maintenance of single binocular vision.¹⁵ For instance, low positive fusional limits, with the accompanying complaints of asthenopia, blur, or diplopia leading to frontal headaches following prolonged periods of near work, might be distracting and adversely affect school performance.^{27,28,29} Moreover, oculomotor dynamics are related to brain areas controlling attention and demonstrate sensitivity to alterations in attentional status.¹⁴ Animal models also indicated that the superior colliculus (SC), which constitutes the principal subcortical area involved in ocular control, participates in the regulation of near response, visual fixation, accommodation, and convergence.^{30,31} The SC is also linked to distractibility and proposed to be dysfunctional in ADHD.³² Therefore, the evaluation of stereoacuity and fusional vergence amplitudes are of special importance in patients with ADHD. Gronlund et al.¹² evaluated ADHD patients receiving medical treatment both before and 2 hours after stimulant use. They reported that the proportion of patients with stereoacuity ≥ 60 sec/arc was significantly higher in the ADHD population, independent of stimulant use. The rate of convergence near point < 6 cm was significantly lower in ADHD patients before stimulant use, while there was no significant difference between the groups 2 hours after stimulant use. Fabian et al.²³ compared 56 ADHD patients with 66 control subjects and did not find a statistically significant difference in terms of stereoacuity (41.5 sec/arc and 40.8 sec/arc, respectively; $p=0.29$) or fusional vergence amplitudes. They also noted that 15 patients (27%) were currently taking methylphenidate treatment. On the other hand,

	ADHD (n=23)	Control (n=48)	p
BCVA (Snellen)	20/20	20/20	0.500*
TNO			
Median (sec/arc)	60	30	
Mean (sec/arc)	142.14±152.65 (15-480)	46.3±44.11 (15-240)	<0.001*
Mean (log sec/arc)	2.03± 0.51 (1.17-2.68)	1.54±0.31 (1.17-2.38)	0.048*
≥480 sec/arc (n, %)	22 (95.7%)	48 (100%)	0.194**
DCA (PD)	19.87±8.40 (6 to 38)	23.54±6.24 (14 to 36)	0.289*
DDA (PD)	-9.09±-4.34 (-4 to -25)	-9.67±-3.71 (-4 to -16)	0.452*
NCA (PD)	37.30±12.81 (14 to 70)	38.21±8.13 (25 to 64)	0.492*
NDA (PD)	-13.13± -3.45 (-4 to -20)	-15.76± -3.52 (-12 to -25)	0.127*
Spherical equivalent (D)	1.06±1.13 (-1 to 4.63)	0.53±1.76 (-2.75 to 2.12)	0.358*
Myopia (n, %)	1 (4.3%)	6 (12.5%)	0.063**
Hyperopia (n, %)	13 (56.5%)		
≥1 D	2 (8.7%)	7 (14.6%)	0.059**
≥3,5 D		0 (0%)	0.111**
Astigmatism (n, %)	2 (8.7%)	3 (6.3%)	0.094**

ADHD: Attention-deficit hyperactivity disorder, BCVA: Best corrected visual acuity, PD: Prism diopter, DCA: Convergence angle at distance, DDA: Divergence angle at distance, NCA: Convergence angle at near, NDA: Divergence angle at near, *: Independent t-test, **: Chi-square test

Table 2. Spherical equivalents after cycloplegia in patients with ADHD in the literature

	ADHD	Control	
<i>Gronlund et al.</i> ¹²	Right: 1.16±1.91 (-2.0-8.25) Left: 1.24±1.90 (-1.75-9.25)	Right: 0.59±1.19 (-2.13-2.75) Left: 0.68±1.40 (-2.75-6.75)	<i>p</i> >0.05*
<i>Fabian et al.</i> ²²	0.63 (-1.88-2.75)	0.89 (-1.25-5.38)	<i>p</i> =0.16**
<i>Larranaga-Fragoso et al.</i> ²⁶	Right: 0.75±0.94 (-1.25-2.88) Left: 0.90±1.06 (-1.33-3.0)	-	
<i>Present study</i>	1.06±1.13 (-1-4.63)	0.53±1.76 (-2.75-2.12)	<i>p</i> =0.358**

ADHD: Attention-deficit hyperactivity disorder, *: Mann-Whitney U test, **: Independent t-test

Fabian et al.²³ did not report convergence insufficiency in any of their patients. Despite the near point of convergence being significantly lower in patients with ADHD [5.3 (range, 3 to 15) and 4.1 (range, 2 to 10); *p*=0.002], this did not reveal any clinical importance, since these values were <6 cm. In the present study, although all patients with ADHD had stereoacuity of at least 480 sec/arc, the mean value of stereoacuity in these patients was significantly lower compared to the control group. In addition, there was no significant difference in terms of fusional vergence amplitudes. The limitation of the present study is the lack of data regarding near point of convergence. However, convergence insufficiency was not present in any of the patients in terms of symptoms or decreased positive fusional vergences (both at the near point). These findings are also consistent with the report of Fabian et al.²³ In contrast, in the present study, all patients were newly diagnosed with ADHD and had not previously received any medication, which eliminates the confounding effect of medication on these parameters. On the other hand, Bennett et al.³³ suggested that some of the medications used in the treatment of ADHD might worsen convergence insufficiency and certain drugs may lead to blurry vision due to difficulty in accommodation. Herein, convergence insufficiency was thought to be a comorbidity rather than a disease-related problem, since fusional vergence amplitudes were similar in both groups. Also, when the prevalence of convergence insufficiency is believed to be as low as 2.25-13% in school-age children^{34,35}, the sample size of our study does not seem to be adequate to make a definite conclusion. Therefore, more precise results will be achieved with larger prospective studies which will also evaluate the follow-up of ADHD patients. Another potential bias might have occurred in relation to the examiner, who was only partially blinded to which children were in which group.

Refractive changes in patients with ADHD were previously investigated and no statistically significant difference was determined as compared to controls (Table 2).^{11,23} Larranaga-Fragoso et al.³⁶ reported that in patients with ADHD, SE before and after cycloplegia did not differ significantly during 9 months of follow-up. As compared with the literature, they suggested that methylphenidate treatment does not affect refraction in children with ADHD. Besides, the relationship between hyperopia and learning difficulties has not yet been clarified. Although some studies reported that hyperopia is associated with different developmental problems and low school

performance³⁷, some studies did not reveal such an association.^{38,39} However, in most studies measurements were obtained without cycloplegia. In hyperopia, unlike myopia, diagnosis may be delayed due to clear visualization through excessive accommodation at near distances. Excessive accommodation may also result in asthenopia, distractibility, hyperactivity, and learning difficulties.^{39,40} Additionally, it is stated that hyperopia >3.5 D increases strabismus and visual acuity problems and is accepted as an amblyogenic risk factor.⁴⁰ In the present study, SE did not show a significant difference between groups. However, the prevalence of hyperopia was higher in patients with ADHD, whereas myopia was more commonly observed in control subjects (Table 2). This also suggests that visual problems may be associated with disorders such as ADHD.

Conclusion

In conclusion, this study showed that fusional vergence amplitudes did not differ significantly, whereas the mean value of stereoacuity was significantly lower in newly diagnosed and unmedicated ADHD patients. Despite the similar fusional vergence amplitudes, it is possible that low stereoacuity in patients with ADHD may suggest the lack of adequate attention while performing TNO random-dot stereo test. Nevertheless, it could be beneficial for children with vision problems to be examined for signs and symptoms of ADHD and vice versa.

Ethics

Ethics Committee Approval: The study was approved by the Institutional Ethics Review Board of Ege University and adhered to the precepts of the Declaration of Helsinki.

Informed Consent: A consent form was completed by all participants.

Peer-review: Externally peer-reviewed.

Authorship Contributions

Concept: I.K., E.D.B., B.Ö., Design: I.K., E.D.B., M.P.O., B.Ö., Ö.Ü., Data Collection or Processing: I.K., E.D.B., Analysis or Interpretation: I.K., E.D.B., M.P.O., B.Ö., Ö.Ü., Literature Search: I.K., E.D.B., M.P.O., B.Ö., Ö.Ü., Writing: I.K., E.D.B., M.P.O., Ö.Ü.

Conflict of Interest: No conflict of interest was declared by the authors.

Financial Disclosure: The authors declared that this study received no financial support.

References

- Polaczyk G, de Lima MS, Horta BL, Biederman J, Rohde LA. The worldwide prevalence of ADHD: a systematic review and meta-regression analysis. *Am J Psychiatry*. 2007;164:942-948.
- Berger I. Diagnosis of attention deficit hyperactivity disorder: much ado about something. *Isr Med Assoc J*. 2011;13:571-574.
- American Psychiatric Association. Diagnostic criteria from DSM-IV. Washington: American Psychiatric Association 1994;358.
- Damari D, Liu J, Smith KB. Visual disorders misdiagnosed as ADHD case studies and literature review. *J Behav Optom*. 2000;11:87-91.
- Farrar R, Call M, Maples WC. A comparison of the visual symptoms between ADD/ADHD and normal children. *Optometry*. 2001;72:441-451.
- Hoogman M, Bralten J, Hibar DP, Mennes M, Zwiers MP, Scherren LSJ, van Hulzen KJE, Medland SE, Shumskaya E, Jahanshad N, Zeeuw P, Szekely E, Sudre G, Wolfers T, Onnink AMH, Dammers JT, Mostert JC, Vives-Gilabert Y, Kohls G, Oberwilleand E, Seitz J, Schulte-Rüther M, Ambrosino S, Doyle AE, Høvik MF, Dramsdahl M, Tamm L, van Erp TGM, Dale A, Schork A, Conzelmann A, Zierhut K, Baur R, McCarthy H, Yoncheva YN, Cubillo A, Chantiluke K, Mehta MA, Paloyelis Y, Hohmann S, Baumeister S, Bramati I, Mattos P, Tovar-Moll F, Douglas P, Banaschewski T, Brandeis D, Kuntsi J, Asherson P, Rubia K, Kelly C, Martino AD, Milham MP, Castellanos FX, Frodl T, Zentis M, Lesch KP, Reif A, Pauli P, Jernigan TL, Haavik J, Plessen KJ, Lundervold AJ, Hugdahl K, Seidman LJ, Biederman J, Rommelse N, Heslenfeld DJ, Hartman CA, Hoekstra PJ, Oosterlaan J, Polier GV, Konrad K, Vilarroya O, Ramos-Quiroga JA, Soliva JC, Durston S, Buitelaar JK, Faraone SV, Shaw P, Thompson PM, Franke B. Subcortical brain volume differences in participants with attention deficit hyperactivity disorder in children and adults: a cross-sectional mega-analysis. *Lancet Psychiatry*. 2017;4:310-319.
- Sharma A, Couture J. A review of the pathophysiology, etiology, and treatment of attention-deficit hyperactivity disorder (ADHD). *Ann Pharmacother*. 2014;48:209-225.
- De Groef L, Cordeiro MF. Is the Eye an Extension of the Brain in Central Nervous System Disease? *J Ocul Pharmacol Ther*. 2018;34:129-133.
- Granet DB, Gomi CE, Ventura R, Miller-Scholte A. The relationship between convergence insufficiency and ADHD. *Strabismus*. 2005;13:163-168.
- Rouse M, Borsting E, Mitchell GL, Kulp MT, Scheiman M, Amster D, Coulter R, Fecho G, Gallaway M; CITT Study Group. Academic behaviors in children with convergence insufficiency with and without parent reported ADHD. *Optom Vis Sci*. 2009;86:1169-1177.
- Redondo B, Vera J, Molina R, García JA, Ouadi M, Muñoz-Hoyos A, Jiménez R. Attention-deficit/hyperactivity disorder children exhibit an impaired accommodative response. *Graefes Arch Clin Exp Ophthalmol*. 2018;256:1023-1030.
- Gronlund MA, Aring E, Landgren M, Hellstrom A. Visual function and ocular features in children and adolescents with attention deficit hyperactivity disorder, with and without treatment with stimulants. *Eye (Lond)*. 2007;21:494-502.
- Mezer E, Wygnanski-Jaffe T. Do children and adolescents with attention deficit hyperactivity disorder have ocular abnormalities? *Eur J Ophthalmol*. 2012;22:931-935.
- Poltavski DV, Biberdorf D, Petros TV. Accommodative response and cortical activity during sustained attention. *Vis Res*. 2012;63:1-8.
- Fray KJ. Fusional Amplitudes: Developing Testing Standards. *Strabismus*. 2017;25:145-155.
- Negrel AD, Maul E, Pokharel GP, Zhao J, Ellwein LB. Refractive error study in children: sampling and measurement methods for a multi-country survey. *Am J Ophthalmol*. 2000;129:421-426.
- Lee HJ, Kim SJ, Yu YS. Stereopsis in patients with refractive accommodative esotropia. *J AAPOS*. 2017;21:190-195.
- Dulcan M. Practice parameters for the assessment and treatment of children, adolescents, and adults with attention-deficit/hyperactivity disorder. American Academy of Child and Adolescent Psychiatry. *J Am Acad Child Adolesc Psychiatry*. 1997;36:85-121.
- Swanson JM, Sergeant JA, Taylor E, Sonuga-Barke EJ, Jensen PS, Cantwell DP. Attention-deficit hyperactivity disorder and hyperkinetic disorder. *Lancet*. 1998;351:429-433.
- Faraone SV, Sergeant J, Gillberg C, Biederman J. The worldwide prevalence of ADHD: is it an American condition? *World Psychiatry*. 2003;2:104-113.
- Weiss MD, Gadow K, Wasdell MB. Effectiveness outcomes in attention-deficit/hyperactivity disorder. *J Clin Psychiatry*. 2006;67:38-45.
- Martin L, Aring E, Landgren M, Hellström A, Andersson Grönlund M. Visual fields in children with attention-deficit / hyperactivity disorder before and after treatment with stimulants. *Acta Ophthalmol*. 2008;86:259-264.
- Fabian ID, Kinori M, Ancrì O, Spierer A, Tsinman A, Ben Simon GJ. The possible association of attention deficit hyperactivity disorder with undiagnosed refractive errors. *J AAPOS*. 2013;17:507-511.
- Kirkby JA, Webster LA, Blythe HI, Liversedge SP. Binocular coordination during reading and non-reading tasks. *Psychol Bull*. 2008;134:742-763.
- Daum KM. Characteristics of convergence insufficiency. *Am J Optom Physiol Opt*. 1988;65:426-438.
- Thiagarajan P, Lakshminarayanan V, Bobier WR. Effect of vergence adaptation and positive fusional vergence training on oculomotor parameters. *Optom Vis Sci*. 2010;87:487-493.
- Cooper J, Jamal N. Convergence insufficiency-a major review. *Optometry*. 2012;83:137-158.
- Borsting E, Rouse M, Chu R. Measuring ADHD behaviors in children with symptomatic accommodative dysfunction or convergence insufficiency: a preliminary study. *Optometry*. 2005;76:588-592.
- Borsting E, Mitchell GL, Kulp MT, Scheiman M, Amster DM, Cotter S, Coulter RA, Fecho G, Gallaway MF, Granet D, Hertle R, Rodena J, Yamada T; CITT Study Group. Improvement in academic behaviors after successful treatment of convergence insufficiency. *Optom Vis Sci*. 2012;89:12-18.
- Overton PG. Collicular dysfunction in attention deficit hyperactivity disorder. *Med Hypotheses*. 2008;70:1121-1127.
- Hafed ZM, Goffart L, Krauzlis RJ. A neural mechanism for microsaccade generation in the primate superior colliculus. *Science*. 2009;323:940-943.
- Brace LR, Kraev I, Rostron CL, Stewart MG, Overton PG, Dommett EJ. Altered visual processing in a rodent model of attention-deficit hyperactivity disorder. *Neuroscience*. 2015;303:364-377.
- Bennett FC, Brown RT, Craver J, Anderson D. Stimulant medication for the child with attention-deficit/hyperactivity disorder. *Pediatr Clin North Am*. 1999;46:929-944.
- Rouse MW, Borsting E, Hyman L, Hussein M, Cotter SA, Flynn M, Scheiman M, Gallaway M, De Land PN. Frequency of convergence insufficiency among fifth and sixth graders. The Convergence Insufficiency and Reading Study (CIRS) group. *Optom Vis Sci*. 1999;76:643-649.
- Scheiman M, Mitchell GL, Cotter S, Cooper J, Kulp M, Rouse M, Borsting E, London R, Wensveen J. Convergence Insufficiency Treatment Trial Study Group. A randomized clinical trial of treatments for convergence insufficiency in children. *Arch Ophthalmol*. 2005;123:14-24.
- Larranaga-Fragoso P, Noval S, Rivero JC, Boto-de-los-Bueis A. The effects of methylphenidate on refraction and anterior segment parameters in children with attention deficit hyperactivity disorder. *J AAPOS*. 2015;19:322-326.
- Williams WR, Latif AH, Hannington L, Watkins DR. Hyperopia and educational attainment in a primary school cohort. *Arch Dis Child*. 2005;90:150-153.
- Helveston EM, Weber JC, Miller K, Robertson K, Hohberger G, Estes R, Ellis FD, Pick N, Helveston BH. Visual function and academic performance. *Am J Ophthalmol*. 1985;99:346-355.
- Dusek W, Pierscionek BK, McClelland JF. A survey of visual function in an Austrian population of school-age children with reading and writing difficulties. *BMC Ophthalmol*. 2010;10:16.
- Kodak G, Duranoglu Y. Amblyopia and Treatment. *Turk J Ophthalmol*. 2014;44:228-236.



The Effect of Topical Cyclopentolate on Anterior Segment Parameters in Patients with Keratoconus

Ahmet Kırgız*, Sevil Karaman Erdur**, Semih Çakmak*, Funda Dikkaya**, Rukiye Aydın*

*University of Health Sciences Turkey, Beyoğlu Eye Training and Research Hospital, Clinic of Ophthalmology, İstanbul, Turkey

**İstanbul Medipol University Faculty of Medicine, Department of Ophthalmology, İstanbul, Turkey

Abstract

Objectives: To investigate the effect of cycloplegia on anterior segment structures in keratoconus and forme fruste keratoconus patients using corneal topography.

Materials and Methods: In this study, 40 patients with keratoconus (group 1), 40 patients with forme fruste keratoconus (group 2), and 40 healthy subjects (group 3) were evaluated prospectively. Flat keratometry (K) value (K1), steep K value (K2), mean K value (Kmean), maximum K value (Kmax), corneal astigmatism value, anterior chamber depth (ACD), symmetry index front, symmetry index back, thinnest corneal thickness, central corneal thickness and corneal volume were measured using Sirius topography before and after cycloplegia. Results were compared with one way ANOVA test.

Results: The mean age of the participants was 24.4±6.2 years for group 1, 26.3±4.3 years for group 2 and 26.5±6.1 years for group 3. There was no difference between the groups with respect to mean age and gender (p>0.05). Mean K1 value was 45.54±2.43 diopters (D) before cycloplegia and 45.46±2.48 D after cycloplegia for group 1 (p=0.044). K1 value didn't change significantly after cycloplegia for group 2 and 3 (p=0.275, p=0.371). There was no significant difference in K2 and Kmean values after cycloplegia for all groups (p>0.05). Kmax value decreased significantly after cycloplegia in group 1 (p=0.001), but the difference was not significant for group 2 and 3 (p=0.087, p=0.241). ACD increased significantly after cycloplegia in all groups (p=0.001).

Conclusion: Cycloplegia causes corneal flattening only in manifest keratoconus patients, leading to an increase in ACD in all groups.

Keywords: Cyclopentolate, keratoconus, cornea, corneal topography, anterior chamber

Introduction

Keratoconus is characterized by progressive thinning of the cornea, corneal steepening, and irregular astigmatism.¹ The mechanical and structural changes that take place in the corneas of patients with keratoconus lead to biomechanical weakening of the cornea. The factors that cause this include changes in collagen and extracellular matrix structure and keratocyte apoptosis.^{2,3}

Although patients with manifest keratoconus can be diagnosed based on slit-lamp findings such as corneal steepening, Vogt lines, Fleischer ring due to iron deposition, and fractures in Bowman's membrane that appear in advanced disease, corneal topography is currently the gold standard diagnostic method.⁴ Fellow eyes of patients with manifest keratoconus that do not display the typical findings of the disease and corneas that

Address for Correspondence: Ahmet Kırgız MD, University of Health Sciences Turkey, Beyoğlu Eye Training and Research Hospital, Clinic of Ophthalmology, İstanbul, Turkey Phone:+90 505 397 46 83 E-mail: ahmetk1@yahoo.com **ORCID-ID:** orcid.org/0000-0001-7498-3693

Received: 05.06.2019 **Accepted:** 28.09.2019

Cite this article as: Kırgız A, Karaman Erdur S, Çakmak S, Dikkaya F, Aydın R. The Effect of Topical Cyclopentolate on Anterior Segment Parameters in Patients with Keratoconus. Turk J Ophthalmol. 2020;50:20-25

©Copyright 2020 by Turkish Ophthalmological Association
Turkish Journal of Ophthalmology, published by Galenos Publishing House.

present suspicious topographic findings were described by Amsler⁵ as forme fruste keratoconus.

Cycloplegic agents are used in the diagnosis and treatment of ocular diseases by inducing relaxation in ciliary muscles. In doing so, they eliminate the accommodation needed to achieve a clear image and focus on objects at varying distances. In addition to refractive changes, preventing accommodation also leads to changes in anterior segment structures.^{6,7,8,9,10}

Keratoconus typically begins in childhood, progresses into the 40s, and then halts progression.¹ Accommodation is also at full capacity in this age group, and the effect of accommodation should not be overlooked when evaluating visual complaints.

The effects of cycloplegia on refractive defects and corneal and anterior segment structures are known.^{6,7,8,9,10} However, the effect of cycloplegia on biomechanically weak corneas, as in keratoconus patients, may differ from that seen in normal eyes. The effect of cycloplegia on keratometric values in eyes with keratoconus has only been investigated using an optical biometry device.¹¹ In this study, we aimed to evaluate the effect of cycloplegia on anterior segment structures in eyes with clinical keratoconus and forme fruste keratoconus using corneal topography.

Materials and Methods

This prospective and comparative study was conducted at the Beyoğlu Ophthalmic Training and Research Hospital of the Health Sciences University. Approval was obtained from the medical, surgical, and drug research Ethics Committee of Istanbul Medipol University prior to the study and the ethical standards set forth in the Declaration of Helsinki were followed throughout the study. The participants were informed about the nature of the study and possible results during the study. Verbal consent and signed informed consent forms were obtained from the participants.

A single eye of each patient was included in the study. If both eyes of a patient were eligible for the study, one eye was randomly selected. Forty eyes of 40 patients diagnosed with keratoconus were randomly selected and included in the study as group 1; 40 eyes of 40 subjects diagnosed with forme fruste keratoconus were included in group 2; and 40 eyes of 40 age- and sex-matched healthy volunteers who presented to our clinic for eye examination and general check-ups were included in group 3. Refractive error and ophthalmological examinations were performed by the same ophthalmologist for all patients. This examination included autorefractometer measurements, corrected and uncorrected visual acuity assessment, slit-lamp cornea and anterior segment examination, intraocular pressure measurements, and dilated fundus examination. Based on slit-lamp corneal examination and topographic findings, diagnoses of keratoconus and forme fruste keratoconus were made according

to the criteria established in the Collaborative Longitudinal Evaluation of Keratoconus study.^{1,12,13,14}

The study population included patients between the ages of 20 and 35 years with no history of ocular surgery or laser therapy and no other concurrent ocular pathology. Patients who had systemic disease, were pregnant or breastfeeding, used contact lenses, had a history of ocular trauma, displayed allergic or dry eye symptoms and findings, or had corneal scarring or nebulae were excluded from the study.

For all patients, refractive error measurements were made using an automatic kerato refractometer (ARK-1a, NIDEK Co., Japan). The spherical equivalent (SE) value to be used for statistical evaluation was calculated using the formula $SE = \text{spherical} + \text{cylindrical}/2$. Measurements of keratometric and anterior segment parameters were made with a Sirius device (Sirius tomography and corneal topography, CSO, Florence, Italy). Cycloplegia was achieved by instilling 1% cyclopentolate hydrochloride (Sikloplejin, Abdi Ibrahim) 3 times at 5-minute intervals. Automatic kerato refractometer and Sirius topography measurements were repeated 45 minutes after the last drop. We evaluated post-cycloplegia changes in the following parameters: flat keratometry (K) value (K1), steep K value (K2), mean K value (Kmean), maximum K value (Kmax), corneal astigmatism value, anterior chamber depth (ACD), symmetry index front (S1f), symmetry index back (S1b), thinnest corneal thickness (TCT), central corneal thickness (CCT), and corneal volume.

Statistical Analysis

IBM SPSS for Windows version 22.0 statistical software was used for statistical analysis. The Shapiro-Wilk test was used to evaluate the normality of data distributions in the groups. Categorical variables were compared using chi-square test. Continuous variables were compared between groups with one-way variance of analysis (ANOVA) with Bonferroni post hoc test. Paired-samples t-test was used for within-group comparisons of continuous variables. Statistical significance was accepted as $p < 0.05$.

Results

Of the 120 patients included in the study, 68 were men and 52 were women. Mean age was 24.4 ± 6.2 years in group 1 (20-33 years), 26.3 ± 4.3 years in group 2 (20-34 years), and 26.5 ± 6.1 years in group 3 (20-35 years). There was no significant difference between the groups in terms of age or sex ($p > 0.05$).

The mean keratometric values (K1, K2, Kmean, and Kmax), SE value, corneal astigmatism value, ACD value, S1f and S1b values, TCT and CCT values, and corneal volume values of the groups before and after cycloplegia are shown in Tables 1, 2, and 3. There was a statistically significant increase in ACD and a significant hypermetropic change in SE value after cycloplegia in all groups ($p = 0.001$).

When the keratometric values were analyzed, mean K1 value in group 1 was 45.54±2.43 diopters (D) before cycloplegia and 45.46±2.48 D after cycloplegia, which was a statistically significant difference (p=0.044). No significant change was observed in K1 after cycloplegia in group 2 or 3 (p=0.275, p=0.371, respectively). None of the groups showed a significant change in K2 or Kmean values after cycloplegia (p>0.05 for

all). While there was a significant decrease in Kmax values after cycloplegia in group 1 (p=0.001), the decrease in group 2 was not statistically significant (p=0.087). The change in Kmax was also nonsignificant in group 3 (p=0.241). TCT and CCT values increased significantly in group 1 (p=0.028, p=0.016, respectively), but there was no significant change in group 2 or 3 (p>0.05 for both).

Table 1. Topographic values before and after cycloplegia in the keratoconus group

Variable	Before cycloplegia (n=40 eyes) Mean ± SD	After cycloplegia (n=40 eyes) Mean ± SD	p* value
K1 (D)	45.54±2.43	45.46±2.48	0.044**
K2 (D)	48.74±2.67	48.65±2.59	0.123
Kmean (D)	47.08±2.47	46.99±2.46	0.058
Spheric equivalent (D)	-5.45±1.48	-3.88±1.99	0.001**
Cylindric (D)	-3.20±1.26	-3.19±1.16	0.760
Kmax (D)	54.63±3.91	54.28±3.84	0.001**
ACD (mm)	3.78±0.31	3.91±0.27	0.001**
SIf (D)	5.96±2.71	5.95±2.81	0.895
SIb (D)	1.54±0.62	1.56±0.61	0.170
TCT (µm)	454.68±26.25	456.62±25.78	0.028**
CCT (µm)	470.38±27.69	473.35±27.57	0.016**
Corneal volume (mm ³)	54.52±2.90	54.84±2.21	0.205

SD: Standard deviation, K1: Flat keratometry value, K2: Steep keratometry value, Kmean: Mean keratometry values, Kmax: Maximum keratometry value, ACD: Anterior chamber depth, SIf: Symmetry index front, SIb: Symmetry index back, TCT: Thinnest corneal thickness, CCT: Central corneal thickness, D: Diopter, **Statistically significant
*Paired-samples t test

Table 2. Topographic values before and after cycloplegia in the forme fruste keratoconus group

Variable	Before cycloplegia (n=40 eyes) Mean ± SD	After cycloplegia (n=40 eyes) Mean ± SD	p* value
K1 (D)	42.67±1.59	42.70±1.61	0.275
K2 (D)	44.87±1.73	44.90±1.79	0.518
Kmean (D)	43.72±1.55	43.75±1.60	0.174
Spheric equivalent (D)	-2.40±1.44	-1.18±1.08	0.001**
Cylindric (D)	-2.22±1.32	-2.24±1.30	0.498
Kmax (D)	47.38±2.29	47.30±2.41	0.087
ACD (mm)	3.65±0.38	3.80±0.32	0.001**
SIf (D)	1.85±0.64	1.83±0.71	0.502
SIb (D)	0.57±0.24	0.58±0.27	0.127
TCT (µm)	489.70±23.50	491.15±24.48	0.119
CCT (µm)	505.40±24.86	506.15±25.74	0.598
Corneal volume (mm ³)	55.26±3.81	55.40±3.85	0.253

SD: Standard deviation, K1: Flat keratometry value, K2: Steep keratometry value, Kmean: Mean keratometry values, Kmax: Maximum keratometry value, ACD: Anterior chamber depth, SIf: Symmetry index front, SIb: Symmetry index back, TCT: Thinnest corneal thickness, CCT: Central corneal thickness, D: Diopter, **Statistically significant
*Paired-samples t test

Table 3. Topographic values before and after cycloplegia in the control group

Variable	Before cycloplegia (n=40 eyes) Mean ± SD	After cycloplegia (n=40 eyes) Mean ± SD	p* value
K1 (D)	42.67±1.46	42.76±1.41	0.371
K2 (D)	43.96±1.20	43.98±1.20	0.770
Kmean (D)	43.34±1.26	43.35±1.22	0.794
Spheric equivalent (D)	-1.78±0.78	+0.14±0.88	0.001**
Cylindric (D)	-1.22±0.96	-1.22±0.98	0.915
Kmax (D)	44.82±1.31	44.99±1.40	0.241
ACD (mm)	3.31±0.24	3.37±0.24	0.001**
SIf (D)	0.19±0.35	0.20±0.39	0.655
SIb (D)	0.03±0.10	0.02±0.10	0.865
TCT (µm)	548.75±36.05	549.92±36.01	0.198
CCT (µm)	552.05±35.32	552.70±35.50	0.493
Corneal volume (mm ³)	59.72±3.36	59.75±3.74	0.324

SD: Standard deviation, K1: Flat keratometry value, K2: Steep keratometry value, Kmean: Mean keratometry values, Kmax: Maximum keratometry value, ACD: Anterior chamber depth, SIf: Symmetry index front, SIb: Symmetry index back, TCT: Thinnest corneal thickness, CCT: Central corneal thickness, D: Diopter, **Statistically significant
*Paired-samples t test

Discussion

In this study evaluating the effect of cycloplegia on anterior segment structures in eyes with keratoconus and forme fruste keratoconus and a control group, we observed a significant decrease in K1 and Kmax values in the clinical keratoconus group after cycloplegia. This decrease demonstrates that cycloplegia causes corneal flattening in eyes with keratoconus.

Previous studies that examined the effects of accommodation on the refractivity of the cornea have had varying results. While Cheng et al.⁷ detected corneal flattening after instilling 0.04% tropicamide, Yasuda et al.¹⁵ reported an increase in corneal power after inducing ciliary muscle contraction with 4% pilocarpine. It is believed that ciliary muscle contraction causes corneal steepening by acting on the peripheral cornea via the scleral spur, whereas after cycloplegia this effect is eliminated and the cornea flattens.⁷ Contrary to these studies, others have indicated that accommodation has no effect on corneal refractivity.^{16,17}

Ex vivo studies have shown that biomechanically, eyes with keratoconus have a low Young's modulus, which also explains the pathophysiology of the disease.¹⁸ In addition, there are also studies demonstrating *in vivo* that corneal hysteresis, which is a marker of corneal biomechanics, is lower in eyes with keratoconus compared to normal eyes.^{19,20} We believe that relaxation of the ciliary muscles after cycloplegia causes corneal flattening through its effect on the biomechanically weak keratoconic cornea. Indeed, Polat and Gündüz¹¹ similarly found a significant decrease in mean K1 and K2 values after cycloplegia

in their study examining the effect of cycloplegia on keratoconic eyes with optical biometry. There are also studies that evaluated the corneal biomechanics of eyes with suspected keratoconus. Although some of these studies demonstrated low biomechanical properties similar to eyes with manifest keratoconus²¹, others did not show this effect.²² The lack of significant changes in the keratometric values of the control group and eyes with suspected keratoconus after cycloplegia in our study may result from their corneas being biomechanically stronger.

In the present study, Kmax and K1 values in eyes with keratoconus flattened by 0.35 D and 0.08 D, respectively, after cycloplegia. Although this change was found to be statistically significant, we believe it may be overlooked in the diagnosis of patients with manifest keratoconus. In addition, we think that pre-cycloplegia evaluation is more appropriate when evaluating keratoconus progression and especially in the follow-up of patients undergoing corneal cross-linking treatment.

In their study of healthy volunteers, Bagheri et al.⁸ observed a significant increase in central and paracentral corneal thickness with cycloplegia. Chen et al.²³ showed that corneal thickness increased following the administration of benzalkonium chloride (BAC) in their rabbit study and suggested that corneal edema occurred as a result of epithelial and endothelial damage caused by topical BAC.²³ In the present study, our findings that increases in TCT and CCT were not statistically significant in the suspected keratoconus or control groups ($p > 0.05$) but were significant in the keratoconus group ($p < 0.05$) may be due to the

corneas being thinner in keratoconus. The increase in corneal thickness that occurs due to corneal edema may have caused a significant difference in the thinner keratoconic corneas.

Many previous studies on healthy subjects and keratoconic patients have demonstrated an increase in ACD with cycloplegia.^{6,7,8,9,10,11,24} This is due to the decrease in lens thickness that occurs as the ciliary muscles relax and lens zonules tighten with cycloplegia. There is also posterior displacement of the lens. Increased ACD is expected as a result. In our study, we showed that in addition to healthy subjects and patients with keratoconus, this change in ACD after cycloplegia was also present in eyes with forme fruste keratoconus. In addition, Türkçüoğlu et al.¹⁰ demonstrated that in eyes in which pupil dilation was induced with phenylephrine alone and accommodation was unaffected, ACD was also unaffected.

One of the methods used to improve vision in keratoconic patients is the placement of posterior chamber phakic intraocular lenses.²⁵ ACD measurement is important when deciding to implant an aphakic intraocular lens.²⁶ In addition, new generation formulas take into account ACD when calculating intraocular lens power.²⁷ It has been reported that 42% of postoperative refractive errors are due to incorrect measurement of ACD.²⁸ Therefore, measurements should be made before cycloplegia in patients with keratoconus who will undergo phakic intraocular lens implantation.

Study Limitations

Limitations of our study are that we did not repeat measurements while stimulating accommodation or measure axial length and relative lens position.

Conclusion

In conclusion, the present study demonstrated corneal flattening after cycloplegia in patients with manifest keratoconus, as well as a positive shift in SE and an increase in ACD with cycloplegia in all groups. This should be kept in mind during refractive error examination, disease progression follow-up, and contact lens and phakic intraocular lens applications in keratoconus patients.

Ethics

Ethics Committee Approval: İstanbul Medipol University Non-Interventional Clinical Research Ethics Committee, Decision No: 249, dated 13/07/2017.

Infomed Consent: Obtained.

Peer-review: Externally and internally peer-reviewed.

Authorship Contributions

Surgical and Medical Practices: A.K., S.Ç., Concept: S.K.E., F.D., Design: A.K., S.K.E., Data Collection or Processing: A.K., S.Ç., R.A., Analysis or Interpretation: S.K.E., F.D., Literature Search: A.K., R.A., Writing: A.K., S.Ç., F.D.

Conflict of Interest: No conflict of interest was declared by the authors.

Financial Disclosure: The authors declared that this study received no financial support.

References

- Rabinowitz YS. Keratoconus. *Surv Ophthalmol.* 1998;42:297-319.
- Kenney MC, Nesburn AB, Burgeson RE, Butkowski RJ, Ljubimov AV. Abnormalities of the extracellular matrix in keratoconus corneas. *Cornea.* 1997;16:345-351.
- Meek KM, Tuft SJ, Huang Y, Gill PS, Hayes S, Newton RH, Bron AJ. Changes in collagen orientation and distribution in keratoconus corneas. *Invest Ophthalmol Vis Sci.* 2005;46:1948-1956.
- Mas Tur V, MacGregor C, Jayaswal R, O'Brart D, Maycock N. A review of keratoconus: diagnosis, pathophysiology, and genetics. *Surv Ophthalmol.* 2017;62:770-783.
- Amsler M. The "forme fruste" of keratoconus. *Wien Klin Wochenschr.* 1961;73:842-843.
- Higashiyama T, Iwasa M, Ohji M. Changes in the anterior segment after cycloplegia with a biometer using swept-source optical coherence tomography. *PLoS One.* 2017;12:e0183378.
- Cheng HC, Hsieh YT. Short-term refractive change and ocular parameter changes after cycloplegia. *Optom Vis Sci.* 2014;91:1113-1117.
- Bagheri A, Feizi M, Shafii A, Faramarzi A, Tavakoli M, Yazdani S. Effect of cycloplegia on corneal biometrics and refractive state. *J Ophthalmic Vis Res.* 2018;13:101-109.
- Koç M, Tekin K, Özçelik D, Yılmazbaş P. Topikal siklopentolatın ön segment biyometrisine etkisi. *Glo-Kat.* 2017;12:56-59.
- Türkçüoğlu P, Emre S, Göktaş A, Çankaya C, Koç B, Doğanay S. Pupilla dilatasyonunun ön kamara parametreleri üzerine etkilerinin Pentacam sistemi ile değerlendirilmesi. *Türkiye Klinikleri J Ophthalmol.* 2008;17:268-271.
- Polat N, Gunduz A. Effect of Cycloplegia on Keratometric and Biometric Parameters in Keratoconus. *J Ophthalmol.* 2016;2016:3437125.
- Barr JT, Wilson BS, Gordon MO, Rah MJ, Riley C, Kollbaum PS, Zadnik K; CLEK Study Group. Estimation of the incidence and factors predictive of corneal scarring in the Collaborative Longitudinal Evaluation of Keratoconus (CLEK) Study. *Cornea.* 2006;25:16-25.
- McMahon TT, Edrington TB, Szczotka-Flynn L, Olafsson HE, Davis LJ, Schechtman KB; CLEK Study Group. Longitudinal changes in corneal curvature in keratoconus. *Cornea.* 2006;25:296-305.
- Fukuda S, Beheregaray S, Hoshi S, Yamanari M, Lim Y, Hiraoka T, Yasuno Y, Oshika T. Comparison of three-dimensional optical coherence tomography and combining a rotating Scheimpflug camera with a Placido topography system for forme fruste keratoconus diagnosis. *Br J Ophthalmol.* 2013;97:1554-1559.
- Yasuda A, Yamaguchi T. Steepening of corneal curvature with contraction of the ciliary muscle. *J Cataract Refract Surg.* 2005;31:1177-1178.
- Read SA, Buehren T, Collins MJ. Influence of accommodation on the anterior and posterior cornea. *J Cataract Refract Surg.* 2007;33:1877-1885.
- Bayramlar H, Sadigov E, Yildirim A. Effect of accommodation on corneal topography. *Cornea.* 2013;32:1251-1254.
- Vellara HR, Patel DV. Biomechanical properties of the keratoconic cornea: a review. *Clin Exp Optom.* 2015;98:31-38.
- Shah S, Laiquzzaman M, Bhojwani R, Mantry S, Cunliffe I. Assessment of the biomechanical properties of the cornea with the ocular response analyzer in normal and keratoconic eyes. *Invest Ophthalmol Vis Sci.* 2007;48:3026-3031.
- Shao P, Eltony AM, Seiler TG, Tavakol B, Pineda R, Koller T, Seiler T, Yun SH. Spatially-resolved Brillouin spectroscopy reveals biomechanical abnormalities in mild to advanced keratoconus in vivo. *Sci Rep.* 2019;9:7467.
- Schweitzer C, Roberts CJ, Mahmoud AM, Colin J, Maurice-Tison S, Kerautret J. Screening of forme fruste keratoconus with the ocular response analyzer. *Invest Ophthalmol Vis Sci.* 2010;51:2403-2410.

22. Luz A, Lopes B, Hallahan KM, Valbon B, Fontes B, Schor P, Dupps WJ Jr, Ambrósio R Jr. Discriminant value of custom ocular response analyzer waveform derivatives in forme fruste keratoconus. *Am J Ophthalmology*. 2016;164:14-21.
23. Chen W, Li Z, Hu J, Zhang Z, Chen L, Chen Y, Liu Z. Corneal alternations induced by topical application of benzalkonium chloride in rabbit. *PLoS One*. 2011;6:e26103.
24. Saitoh K, Yoshida K, Hamatsu Y, Tazawa Y. Changes in the shape of the anterior and posterior corneal surfaces caused by mydriasis and miosis: detailed analysis. *J Cataract Refract Surg*. 2004;30:1024-1030.
25. Emerah SH, Sabry MM, Saad HA, Ghobashy WA. Visual and refractive outcomes of posterior chamber phakic IOL in stable keratoconus. *Int J Ophthalmol*. 2019;12:840-843.
26. Saxena R, Boekhoorn SS, Mulder PG, Noordzij B, van Rij G, Luyten GP. Long-term follow-up of endothelial cell change after Artisan phakic intraocular lens implantation. *Ophthalmology*. 2008;115:608-613.
27. Olsen T. Calculation of intraocular lens power: a review. *Acta Ophthalmol Scand*. 2007;85:472-485.
28. Tuncer İ, Zengin MÖ, Karahan E. IOLMaster ve A-Tarayıcı Ultrason ile Ön Kamara Derinliği ve Aksiyel Uzunluk Ölçümlerinin Karşılaştırılması. *Glo-Kat*. 2014;9:89-92 .



The Diagnostic Ability of Ganglion Cell Complex Thickness-to-Total Retinal Thickness Ratio in Glaucoma in a Caucasian Population

Almila Sarıgül Sezenöz*, Sirel Gür Güngör*, Ahmet Akman*, Caner Öztürk*, Şefik Cezairlioğlu*, Mustafa Aksoy*, Meriç Çolak**

*Başkent University Hospital, Clinic of Ophthalmology, Ankara, Turkey

**Başkent University Health Sciences Faculty, Department of Ophthalmology Ankara, Turkey

Abstract

Objectives: To evaluate the diagnostic accuracy of the macular ganglion cell complex-to-total retinal thickness (G/T) ratio in a Caucasian population.

Materials and Methods: A total of 86 patients were enrolled in this cross-sectional study. Patients were divided into 4 groups: healthy; ocular hypertension; preperimetric glaucoma; and early glaucoma. Macular ganglion cell complex (mGCC) thickness, total retinal thickness, and retinal nerve fiber layer thickness (RNFLT) in one randomly selected eye of each patient were measured with measured with Heidelberg HD spectral domain optical coherence tomography (Heidelberg Engineering, Inc., Heidelberg, Germany). G/T ratio (%) was calculated as (mGCC thickness / total retinal thickness) x100. The ability of each parameter to diagnose glaucoma was examined by area under the receiver operating characteristic curve (AUROC) analysis and sensitivity evaluation at a fixed level of specificity. Unpaired t test was used to compare the measured values between the healthy subjects and the different patient groups.

Results: The study included 9 healthy individuals, 18 patients with ocular hypertension, 28 with preperimetric glaucoma, and 31 with early glaucoma. Total retinal thickness, mGCC thickness, RNFLT, and G/T ratio were highest in the healthy group and decreased progressively in patients with ocular hypertension, preperimetric glaucoma, and early glaucoma. All comparisons between the groups were significant for these parameters (p<0.001 for all). Average RNFLT, average GCC, and total retinal thickness showed consistently higher AUROC than G/T ratio in the differentiation between healthy individuals and patients with ocular hypertension, preperimetric glaucoma, and early glaucoma.

Conclusion: G/T ratio does not contribute to separation of ocular hypertension, preperimetric glaucoma, and early glaucoma patients from the healthy population. Compared to the other parameters investigated, G/T had lower diagnostic value.

Keywords: Ganglion cell complex, glaucoma, optical coherence tomography

Introduction

Glaucoma is a progressive optic neuropathy characterized by retinal ganglion cell loss and thinning of the retinal nerve fiber layer (RNFL).^{1,2} Glaucomatous visual field defects emerge after

30% of the retinal ganglion cells are lost. Therefore, structural tests are important in the early diagnosis and follow-up of glaucoma.³

Previous optical coherence tomography (OCT) studies demonstrated peripapillary RNFL thinning in early

Address for Correspondence: Almila Sarıgül Sezenöz MD, Başkent University Hospital, Clinic of Ophthalmology, Ankara, Turkey

Phone:+90 536 686 97 63 E-mail: almilasarigul@gmail.com **ORCID-ID:** orcid.org/0000-0002-7030-5454

Received: 10.11.2018 **Accepted:** 28.09.2019

Cite this article as: Sarıgül Sezenöz A, Gür Güngör S, Akman A, Öztürk C, Cezairlioğlu Ş, Aksoy M, Çolak M. The Diagnostic Ability of Ganglion Cell Complex Thickness-to-Total Retinal Thickness Ratio in Glaucoma in a Caucasian Population. Turk J Ophthalmol. 2020;50:26-30

glaucoma.^{4,5,6} More recent studies have shown that in addition to the peripapillary RNFL, changes in inner macular thickness parameters also occur related to glaucomatous ganglion cell loss.^{7,8,9,10,11,12,13,14} The total of the macular nerve fibers, ganglion cells, and inner plexiform layer is called the macular ganglion cell complex (mGCC).¹⁵ Current OCT devices can obtain mGCC measurements automatically, and studies report that a decrease in mGCC thickness has high diagnostic value in early glaucoma, similar to RNFL parameters.^{11,15,16,17,18,19,20,21,22,23}

Reported mGCC thickness values range between 76.6 and 119.8 μm in normal eyes and between 53.6 and 99.1 μm in perimetric glaucomatous eyes.¹⁶ Because the range of mGCC thickness overlaps in normal and glaucomatous eyes, Kita et al.¹⁵ compared various macular parameters in Japanese patients and demonstrated that the ratio of mGCC thickness to total retinal thickness (G/T ratio) was the parameter with the highest diagnostic value in glaucoma. However, in a later study of white Europeans, G/T ratio was found to have a lower area under the receiver operating characteristic curve (AUROC) value than RNFL.²⁴

The aim of this study was to determine the diagnostic value of G/T ratio for glaucoma in a Caucasian patient population.

Materials and Methods

This study was approved by the Başkent University Ethics Committee. Data from a total of 130 patients who presented to the glaucoma unit of the ophthalmology outpatient clinic of Başkent University Hospital between December 2017 and June 2019 were reviewed for inclusion in this cross-sectional study. All patients underwent ophthalmologic examinations and their medical histories were analyzed. Ophthalmologic examination included visual acuity, slit-lamp anterior segment examination, gonioscopy, intraocular pressure measurements with Goldmann applanation tonometry, and dilated fundus examination. The results of 24-2 visual field tests performed with a Humphrey standard automated perimeter (Humphrey-Zeiss Systems, Dublin, CA) were evaluated. Tests with less than 20% fixation loss and false positive and false-negative rates both below 33% were regarded as reliable.

A Heidelberg HD spectral domain OCT (Heidelberg Engineering, Inc., Heidelberg, Germany) device was used to evaluate the optic nerve head and macular parameters of the patients. Measurements were made after pupil dilation by the same experienced technician at the same time of day. Patients whose images had signal strength values below 6 were not included in the study. Macular thickness was measured using an automated system. G/T ratio (%) was calculated using the formula (mGCC thickness / total retinal thickness) $\times 100$.

The patients were divided into 4 groups for evaluation: healthy, ocular hypertension, preperimetric glaucoma, and early glaucoma. Those included in the healthy group had intraocular pressure below 21 mmHg, normal optic nerve appearance, normal anterior chamber angle, and normal visual field test results. The criteria for diagnosing open-angle glaucoma in the study patients were: open iridocorneal angle on gonioscopic

examination, glaucomatous optic nerve damage (focal thinning or notching of the neuroretinal rim or diffuse thinning of the neuroretinal rim), and glaucomatous visual field defect in the absence of any other ocular disease that could be linked to visual field defect. Glaucomatous visual field defect was defined as meeting at least two of the following three criteria: (1) glaucoma hemifield test results outside normal limits; (2) presence of three locations with P <5% of normal distribution and one location with p <1% on pattern deviation plot; and (3) pattern standard deviation value with p <5%. These visual field defects were confirmed by two consecutive reliable visual field tests (fixation loss $\leq 20\%$, false positive and false negative error rates $\leq 25\%$). The individuals' fellow eyes had open angle on gonioscopy and normal disc appearance and visual field results. Glaucomatous eyes with a mean deviation (MD) value of ≤ -6 dB upon enrollment were grouped as early glaucoma. Patients with glaucomatous optic nerve damage but normal visual field were classified as preperimetric glaucoma. Patients with a normal optic disc and visual field but intraocular pressure above 21 mmHg were included in the ocular hypertension group.

Criteria for inclusion in the study were sufficient central vision for optimal fixation, adequate image quality for optimal evaluation, and no macular pathology on stereoscopic evaluation of the study eye.

Statistical Analysis

Statistical analyses were performed using IBM SPSS 21 statistics software (SPSS Inc., Chicago, IL). The adequacy of each parameter for diagnosing glaucoma was determined through AUROC analysis and evaluating sensitivity at a fixed level of specificity. Measured values of the healthy individuals and selected patient groups were compared using ANOVA.

Results

Ninety-five eyes of 95 patients were included in the study. Data from 18 healthy subjects, 18 patients with ocular hypertension, 28 patients with preperimetric glaucoma, and 31 patients with early glaucoma were analyzed. Comparisons of age, sex, and refraction values of the 95 study patients revealed no significant differences between the groups ($p \geq 0.05$). The patients' clinical characteristics are shown in Table 1.

It was observed that mGCC thickness, total retinal thickness, RNFL thickness, and G/T ratio were highest in healthy subjects and decreased respectively in patients with ocular hypertension, patients with preperimetric glaucoma, and patients with early glaucoma. All between-group comparisons based on these values were statistically significant ($p < 0.001$ for all) (Table 2).

For distinguishing healthy subjects from early glaucoma patients, AUROC values for mean mGCC, RNFL thickness, total retinal thickness, and G/T ratio were 0.876, 0.876, 0.840, and 0.794, respectively. Similarly, AUROC values were higher for mean mGCC, RNFL thickness, and total retinal thickness values compared to G/T ratio in the differentiation between healthy subjects and patients with ocular hypertension and preperimetric glaucoma (Table 3). ROC values for all parameters are shown in Figures 1A, B, and C.

Table 1. Clinical characteristics of the patients: mean age, visual acuity, mean refraction values, cup-to-disc ratio, intraocular pressure, central corneal thickness, and visual field values

	Healthy individuals	Ocular hypertension	Preperimetric glaucoma	Early glaucoma	p ANOVA
Mean age (years)	61.00±6.48	66.61±10.44	66.71±11.33	68.20±9.12	0.141
Snellen visual acuity	0.96±0.05	0.94±0.09	0.92±0.11	0.87±0.22	0.185
Refraction value (D)	-0.41±1.92	-0.08±1.39	0.04±1.91	-0.03±1.60	0.864
IOP (mmHg)	18.0±2.83	20.72±2.27	17.64±2.84	17.96±3.31	0.004
CCT (µm)	564.63±68.79	550.80±39.66	563.43±26.13	546.91±23.18	0.668
c/d ratio	0.35±0.13	2.46±2.44	2.59±2.89	5.00±1.99	<0.001
MD (dB)	0.14±5.9	-0.57±1.02	-1.62±1.65	-8.27±9.78	0.001
PSD (dB)	1.91±2.04	1.55±1.74	-1.86±1.18	4.82±4.70	0.008

IOP: Intraocular pressure, CCT: Central corneal thickness, c/d: Cup/disc, MD: Mean deviation, PSD: Pattern standard deviation

Table 2. Comparison of mean mGCC, RSLT thickness, total macular retinal thickness, and G/T ratio values between the patient group

	Healthy individuals	Ocular hypertension	Preperimetric glaucoma	Early glaucoma	ANOVA p
mGCC (µm)	113.58±13.27	107.64±7.49	104.33±8.48	92.92±16.04	<0.001
Total retinal thickness (µm)	335.36±18.61	322.41±11.78	317.15±16.50	311.87±19.55	<0.001
RNFL (µm)	95.56±8.01	92.88±11.06	88.04±8.47	75.77±16.27	<0.001
G/T ratio (%)	0.34±0.02	0.33±0.02	0.33±0.02	0.30±0.04	<0.001

mGCC: Macular ganglion cell complex thickness, RNFL: Retinal nerve fiber layer, G/T: mGCC to total retinal thickness, ANOVA: Analysis of variance

Table 3. Area under the receiving operator characteristic curve (AUROC) values for mGCC, RSLT thickness, total macular retinal thickness, and G/T ratio

	Healthy vs. Early glaucoma	Healthy vs. Preperimetric glaucoma	Healthy vs. Ocular hypertension
mGCC	0.876	0.780	0.688
RNFL thickness	0.876	0.744	0.599
Total retinal thickness	0.840	0.772	0.728
G/T ratio	0.794	0.567	0.545

AUROC: Area under the receiver operating characteristic curve, mGCC: Macular ganglion cell complex, RNFL: Retinal nerve fiber layer, G/T: mGCC to total retinal thickness

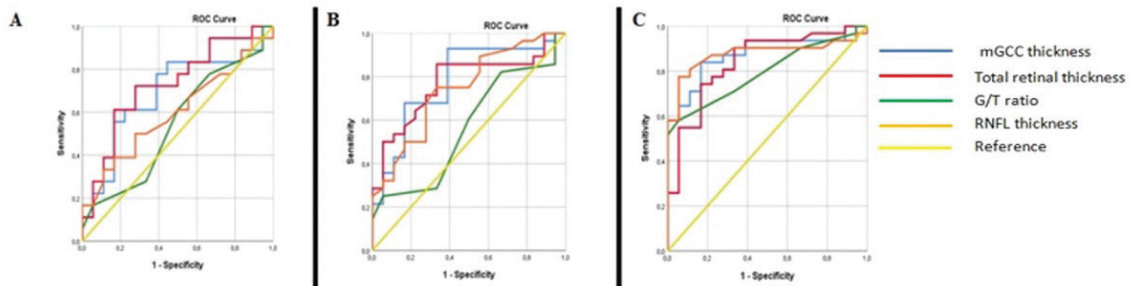


Figure 1. Receiving operator characteristic curves for mGCC thickness, total retinal thickness, RNFL thickness, and G/T ratio. A) Healthy vs. ocular hypertension; B) Healthy vs. preperimetric glaucoma; C) Healthy vs. early glaucoma

Discussion

In the present study, we evaluated the diagnostic power of mGCC thickness, RNFL thickness, total retinal thickness, and G/T ratio for glaucoma in our patients.

The diagnostic power of macular thickness parameters has been previously investigated in OCT studies, but it was shown

that total macular thickness values were not as valuable as RNFL in the diagnosis of glaucoma.^{6,11,12,25} When subsequently developed macular segmentation algorithms were used to separately evaluate the thicknesses of the macular nerve fiber and inner retinal layers, values comparable to RNFL were obtained.^{14,16,26} However, these values range widely and may be

insufficient for differentiating between normal eyes and those with early glaucoma.¹⁵ For this reason, Kita et al.¹⁵ first proposed the G/T ratio as a diagnostic parameter. They suggested that outer retinal thicknesses would not change as mGCC becomes thinner in glaucomatous eyes, resulting in a decrease in the G/T ratio, and they obtained results supporting this.¹⁵ Their study, conducted in the Japanese population, demonstrated that G/T ratio yielded significantly higher AUROC values than peripapillary RNFL in glaucoma patients, indicating that G/T ratio was more valuable in the diagnosis of glaucoma.¹⁵ However, these results were contradicted by a subsequent study conducted by Hollö et al.²⁴ in the European population. Hollö et al.²⁴ reported that G/T ratio had a lower AUROC value than those of mean RNFL and GCC thickness. The researchers attributed this discrepancy to the different ethnicities of the study groups.^{24,27}

In the present study, we evaluated the AUROC values of RNFL, GCC, total macular thickness, and G/T ratio for differentiating between healthy individuals and patients with ocular hypertension, preperimetric glaucoma, and early glaucoma. Similar to the study by Hollö et al.²⁴, our analysis showed that G/T ratio had a lower AUROC value compared to mean RNFL, mGCC, and total retinal thickness for all groups.²⁴ Although the literature may present contradictory results due to ethnic differences, the G/T ratio has no diagnostic importance in practice, both in Europeans and in the present study conducted in our center. Instead of this calculation, a more practical approach would be to monitor the ganglion cell layer and peripapillary RNFL in glaucoma patients using OCT.

Study Limitations

As a cross-sectional study, the inability to make the detailed distinction between preperimetric glaucoma and non-progressive glaucomatous optic nerve changes was one of its limitations, as in the study by Hollö et al.²⁴ Prospective studies are needed to clearly make this distinction.

Conclusion

In conclusion, the present study demonstrated that G/T ratio does not contribute significantly to the differentiation of patients with ocular hypertension, preperimetric glaucoma, and early glaucoma from the healthy population and has a lower diagnostic value compared to RNFL thickness, mGCC thickness, and total macular retinal thickness, as has been previously shown in various groups in the literature.

Ethics

Ethics Committee Approval: This study was approved by the Başkent University Ethics Committee.

Informed Consent: Our study is for a retrospective cross-sectional study and patient consent will be obtained.

Peer-review: Externally peer reviewed.

Authorship Contributions

Surgical and Medical Practices: S.G.G., A.A., A.S.S., C.Ö., Ş.C., M.A., Concept: S.G.G., A.A., A.S.S., C.Ö., Ş.C., M.A., Design: S.G.G., A.A., Data Collection or Processing: S.G.G.,

A.A., A.S.S., C.Ö., Ş.C., M.A., M.Ç., Analysis or Interpretation: S.G.G., A.A., A.S.S., C.Ö., Ş.C., M.A., M.Ç., Literature Search: S.G.G., A.A., A.S.S., C.Ö., Ş.C., M.A., Writing: S.G.G., A.A., A.S.S.

Conflict of Interest: No conflict of interest was declared by the authors.

Financial Disclosure: The authors declared that this study received no financial support.

References

1. Quigley HA, Addicks EM, Green WR. Optic nerve damage in human glaucoma. III. Quantitative correlation of nerve fiber loss and visual field defect in glaucoma, ischemic neuropathy, papilledema, and toxic neuropathy. *Arch Ophthalmol*. 1982;100:135-146.
2. Quigley HA, Dunkelberger GR, Green WR. Retinal ganglion cell atrophy correlated with automated perimetry in human eyes with glaucoma. *Am J Ophthalmol*. 1989;107:453-464.
3. Kerrigan-Baumrind LA, Quigley HA, Pease ME, Kerrigan DE, Mitchell RS. Number of ganglion cells in glaucoma eyes compared with threshold visual field tests in the same persons. *Invest Ophthalmol Vis Sci*. 2000;41:741-748.
4. Kanamori A, Nakamura M, Escano MFT, Seya R, Maeda H, Negi A. Evaluation of the glaucomatous damage on retinal nerve fiber layer thickness measured by optical coherence tomography. *Am J Ophthalmol*. 2003;135:513-520.
5. Wollstein G, Ishikawa H, Wang J, Beaton SA, Schuman JS. Comparison of three optical coherence tomography scanning areas for detection of glaucomatous damage. *Am J Ophthalmol*. 2005;139:39-43.
6. Ojima T, Tanabe T, Hangai M, Yu S, Morishita S, Yoshimura N. Measurement of retinal nerve fiber layer thickness and macular volume for glaucoma detection using optical coherence tomography. *Jpn J Ophthalmol*. 2007;51:197-203.
7. Nakatani Y, Higashide T, Ohkubo S, Takeda H, Sugiyama K. Evaluation of macular thickness and peripapillary retinal nerve fiber layer thickness for detection of early glaucoma using spectral domain optical coherence tomography. *J Glaucoma*. 2011;20:252-259.
8. Sung KR, Sun JH, Na JH, Lee JY, Lee Y. Progression detection capability of macular thickness in advanced glaucomatous eyes. *Ophthalmology*. 2012;119:308-313.
9. Sung MS, Kang BW, Kim HG, Heo H, Park SW. Clinical validity of macular ganglion cell complex by spectral domain-optical coherence tomography in advanced glaucoma. *J Glaucoma*. 2014;23:341-346.
10. Takagi ST, Kita Y, Yagi F, Tomita G. Macular retinal ganglion cell complex damage in the apparently normal visual field of glaucomatous eyes with hemifield defects. *J Glaucoma*. 2012;21:318-325.
11. Lederer DE, Schuman JS, Hertzmark E, Heltzer J, Velazques LJ, Fujimoto JG, Mattox C. Analysis of macular volume in normal and glaucomatous eyes using optical coherence tomography. *Am J Ophthalmol*. 2003;135:838-843.
12. Parikh RS, Parikh SR, Thomas R. Diagnostic capability of macular parameters of stratus OCT 3 in detection of early glaucoma. *Br J Ophthalmol*. 2010;94:197-201.
13. Leung CK, Chan WM, Yung WH, Ng AC, Woo J, Tsang MK, Tse RK. Comparison of macular and peripapillary measurements for detection of glaucoma: an optical coherence study. *Ophthalmology*. 2005;112:391-400.
14. Tan O, Li G, Lu AT, Varma R, Huang D. Mapping of macular substructures with optical coherence tomography for glaucoma diagnosis. *Ophthalmology*. 2008;115:949-956.
15. Kita Y, Kita R, Takeyama A, Takagi S, Nishimura C, Tomita G. Ability of optical coherence tomography-determined ganglion cell complex thickness to totalretinal thickness ratio to diagnose glaucoma. *J Glaucoma*. 2013;22:757-62.
16. Tan O, Chopra V, Lu AT, Schuman JS, Ishikawa H, Wollstein G, Varma R, Huang D. Detection of macular ganglion cell loss in glaucoma by Fourier-domain optical coherence tomography. *Ophthalmology*. 2009;116:2305-2314.

17. Kita Y, Kita R, Nitta A, Nishimura C, Tomita G. Glaucomatous eye macular ganglion cell complex thickness and its relation to temporal circumpapillary retinal nerve fiber layer thickness. *Jpn J Ophthalmol*. 2011;55:228-234.
18. Takagi ST, Kita Y, Yagi F, Tomita G. Macular retinal ganglion cell complex damage in the apparently normal visual field of glaucomatous eyes with hemifield defects. *J Glaucoma*. 2012;21:318-325.
19. Rao HL, Zangwill LM, Weinreb RN, Sample PA, Alencar LM, Medeiros FA. Comparison of different spectral domain optical coherence tomography scanning areas for glaucoma diagnosis. *Ophthalmology*. 2010;117:1692-1699.
20. Seong M, Sung KR, Choi EH, Kang SY, Cho JW, Um TW, Kim YJ, Park SB, Hong HE, Kook MS. Macular and peripapillary retinal nerve fiber layer measurements by spectral domain optical coherence tomography in normal-tension glaucoma. *Invest Ophthalmol Vis Sci*. 2010;51:1446-1452.
21. Garas A, Vargha P, Hollo G. Diagnostic accuracy of nerve fibre layer, macular thickness and optic disc measurements made with the RTVue-100 optical coherence tomograph to detect glaucoma. *Eye (Lond)*. 2011;25:57-65.
22. Korkmaz B, Yiğit U, Ağaçhan A, Helvacioğlu F, Bilen H, Tuğcu B. The Evaluation of the Relationship Between Retinal Nerve Fiber Layer and Ganglion Cell Complex in Glaucomatous and Normal Cases With Optical Coherence Tomography. *Turk J Ophthalmol*. 2010;40:338-342.
23. Huang JY, Pekmezci M, Mesiwala N, Kao A, Lin S. Diagnostic power of optic disc morphology, peripapillary retinal nerve fiber layer thickness, and macular inner retinal layer thickness in glaucoma diagnosis with fourier-domain coherence tomography. *J Glaucoma*. 2011;20:87-94.
24. Holló G, Naghizadeh F, Vargha P. Accuracy of macular ganglion-cell complex thickness to total retina thickness ratio to detect glaucoma in white Europeans. *J Glaucoma*. 2014;23:132-137.
25. Medeiros FA, Zangwill LM, Bowd C, Vessani RM, Susanna R Jr, Weinreb RN. Evaluation of retinal nerve fiber layer, optic nerve head, and macular thickness measurements for glaucoma detection using optical coherence tomography. *Am J Ophthalmol*. 2005;139:44-55.
26. Ishikawa H, Stein DM, Wollstein G, Beaton S, Fujimoto JG, Schuman JS. Macular segmentation with optical coherence tomography. *Invest Ophthalmol Vis Sci*. 2005;46:2012-2017.
27. Kim JM, Jeoung JW, Bitrian E, Supawavej C, Mock D, Park KH, Caprioli J. Comparison of clinical characteristics between Korean and Western normal-tension glaucoma patients. *Am J Ophthalmol*. 2013;155:852-857.



Iris Cysts: Clinical Features, Imaging Findings, and Treatment Results

Helin Ceren Köse, Kaan Gündüz, Melek Banu Hoşal

Ankara University Faculty of Medicine, Department of Ophthalmology, Ankara, Türkiye

Abstract

Objectives: To report the clinical and demographic characteristics, imaging findings, treatment results, and follow-up data of patients with iris cysts.

Materials and Methods: The medical records of 37 patients with iris cysts were retrospectively analyzed. Ultrasound biomicroscopy (UBM), swept-source optical coherence tomography (SS-OCT), and SS-OCT angiography (SS-OCTA) were performed to examine the iris cysts.

Results: The mean age of the patients was 34.4 years, ranging from 5 to 85 years. Twenty-four patients (65%) were female and 13 (35%) were male. Mean follow-up period was 21.3 months, ranging from 4 months to 8 years. Thirty-five (94.5%) of the cysts were classified as primary and 2 (4.5%) were classified as secondary. Thirty-one (83.7%) of the primary cysts were pigment epithelial and 4 were stromal. Primary iris pigment epithelial (IPE) cysts were classified as peripheral in 26 patients (72.2%), midzonal in 4 (11.1%), and dislodged in 1 (2.7%). Stromal cysts were classified as acquired in 3 patients (8.1%) and congenital in 1 patient (2.7%). Secondary iris cysts were caused by perforating eye injury. UBM could visualize both the anterior and posterior surfaces of the cysts (26 patients). Anterior segment SS-OCT could visualize the anterior but not the posterior surface of the cysts (4 patients). Iris cysts did not display intrinsic vascularity on SS-OCTA (4 patients). All pigment epithelial cysts were managed by observation. Of the 4 primary stromal cysts, 3 were managed by surgical excision and 1 by observation. Two secondary cysts required surgical removal.

Conclusion: Pigment epithelial cysts generally remain stable without need for treatment. However, iris stromal cysts frequently require surgical intervention. UBM and SS-OCT were valuable in the diagnosis of iris cysts. On UBM, iris cysts appear with a thin, hyperechoic wall with hypoechoic internal content. Iris cysts did not have intrinsic vascularity on anterior segment SS-OCTA.

Keywords: Iris pigment epithelial cyst, iris stromal cyst, SS-OCT, SS-OCTA, UBM

Introduction

Iris tumors are categorized as cystic and noncystic (solid) lesions. In a study examining 3,680 iris tumors, 21% were reported to be cystic (n=718) and 79% noncystic (n=2,733).¹ Cystic lesions originate from the iris pigment epithelium (IPE) or iris stroma.^{2,3}

In a classification made by Shields⁴ in 1981, iris cysts are grouped as primary and secondary according to their etiology,

then divided into subgroups based on their tissue or origin. According to this classification, primary IPE cysts are the most common in clinical practice. Most IPE cysts are asymptomatic.^{4,5} Primary cysts are usually of neuroepithelial origin and rarely lead to complications. Primary IPE cysts have 4 subtypes based on their location: pupillary, midzonal, peripheral, and free-floating/dislodged.^{4,5,6} Secondary cysts, on the other hand, develop due to causes such as implantation after penetrating or surgical trauma, intraocular tumors, prolonged use of prostaglandins and

Address for Correspondence: Helin Ceren Köse MD, Ankara University Faculty of Medicine, Department of Ophthalmology, Ankara, Türkiye
Phone: +90 536 689 78 56 E-mail: helinceren_kose@hotmail.com **ORCID-ID:** orcid.org/0000-0002-4654-0657

Received: 28.03.2019 **Accepted:** 28.09.2019

Cite this article as: Köse HC, Gündüz K, Hoşal MB. Iris Cysts: Clinical Features, Imaging Findings, and Treatment Results. Turk J Ophthalmol. 2020;50:31-36

miotics, or parasitic infections such as ocular cysticercosis.^{6,7,8,9,10} They may lead to complications such as decreased visual acuity, secondary glaucoma, corneal edema, or uveitis.

Stromal iris cysts can be congenital or acquired.^{11,12} They can remain dormant for years or suddenly grow and rupture, leading to secondary glaucoma and corneal decompensation. Although stromal cysts can occasionally regress spontaneously, most require treatment by needle aspiration or surgical excision.^{12,13}

Slit-lamp examination, anterior segment (AS) optical coherence tomography (OCT), and ultrasound biomicroscopy (UBM) are used in the differential diagnosis of iris cysts.¹⁴ These techniques are important in ruling out solid tumors such as nevus or melanoma.

The aim of this study was to discuss the demographic and clinical features, treatment, and follow-up results of patients with iris cysts.

Materials and Methods

The records of 37 seven patients who were treated and followed for iris cysts in the ocular oncology unit of the Medical Faculty of Ankara University Ophthalmology Department between January 2007 and January 2019 were retrospectively reviewed. The type, etiology, location, and size of the cyst, treatments applied, recurrence status, and outcome at final follow-up were analyzed. Cyst size was measured with UBM in 26 patients. Four patients underwent AS swept-source OCT (SS-OCT) (Topcon, Tokyo, Japan) and SS-OCT angiography (SS-OCTA) imaging. Three of the patients with stromal cysts underwent partial lamellar sclerouvectomy (PLSU) and 2 underwent surgical resection via limbal incision.

The study was conducted in accordance with the principles of the Declaration of Helsinki. Approval was obtained from our institutional ethics committee and informed consent forms were obtained from the study participants.

Results

The demographic and clinical characteristics of the patients are presented in Table 1. Of the 37 patients with iris cysts, 24 (65%) were female and 13 (35%) were male. The mean age at diagnosis was 34.4 ± 19.5 (5–85) years. Twenty-one (57%) of the iris cysts were located in the right eye and 16 (43%) in the left eye. The patients were followed for a mean of 21.3 ± 9.6 (median 20) months. Thirty-five (94.5%) of the cysts were classified as primary and 2 (5.5%) as secondary based on etiology. Of the primary cysts, 31 (84%) were pigment epithelial and 4 (11%) were stromal cysts. The secondary cysts were all stromal cysts and developed due to perforating ocular injury. One of these patients was a 5-year-old boy and the other was a 16-year-old girl.

UBM was performed on 26 patients with iris cysts. On UBM, IPE cysts appeared as thin-walled with no solid lesion component (Figure 1e). According to UBM and clinical findings, 26 (72.2%) of the primary IPE cysts were peripheral (Figure 1a), 4 (11.1%) were midzonal, and 1 was free-floating/dislodged (2.7%) (Figure 2a-b). Patients with peripheral IPE cysts had a mean age of 30.4 ± 10.7 (16-53) and included 18 females and 8 males. Patients with midzonal IPE cysts had a mean age of 52 ± 19.2 (29-72) and included 3 men and 1 woman. The patient with dislodged IPE cyst was a 20-year-old woman. Of the primary stromal cysts, 3 (8.1%) were acquired (Figure 2c) and 1 was congenital (2.7%). These patients had a mean age of 52 ± 33.5 (17-85) years and included 3 females and 1 male. The mean size of pigment epithelial cysts was 1.7×2.0 mm and that of stromal cysts was 5.2×3.5 mm.

SS-OCT and SS-OCTA were performed on 4 of the patients. AS SS-OCT was used to study iris configuration and the relationship of peripheral IPE cysts to the anterior chamber angle (Figure 1b). AS SS-OCT images of a patient with stromal iris cyst secondary to penetrating trauma by knife revealed a hollow

Table 1. Clinical and demographic characteristics of the 37 patients with iris cyst

Cyst type	n	%	Age (years)		Sex	
			Mean	Min-max	Female	Male
Primary cyst (n=35)						
Primary IPE cyst (n=31)						
Pupillary	0	0	-	-	0	0
Midzonal	4	11	52	(29-72)	1	3
Peripheral	26	72	30.4	(16-53)	18	8
Free-floating/Dislodged	1	2.7	20	20	1	0
Primary stromal cyst (n=4)						
Congenital	1	2.7	17	17	1	0
Acquired	3	8.1	63.6	30-85	2	1
Secondary stromal cyst (n=2)						
Due to trauma/surgery	2	5.5	10.5	5-16	1	1
Due to tumor	0	0	-	-	0	0
Parasitic	0	0	-	-	0	0

n: Number, IPE: Iris pigment epithelium

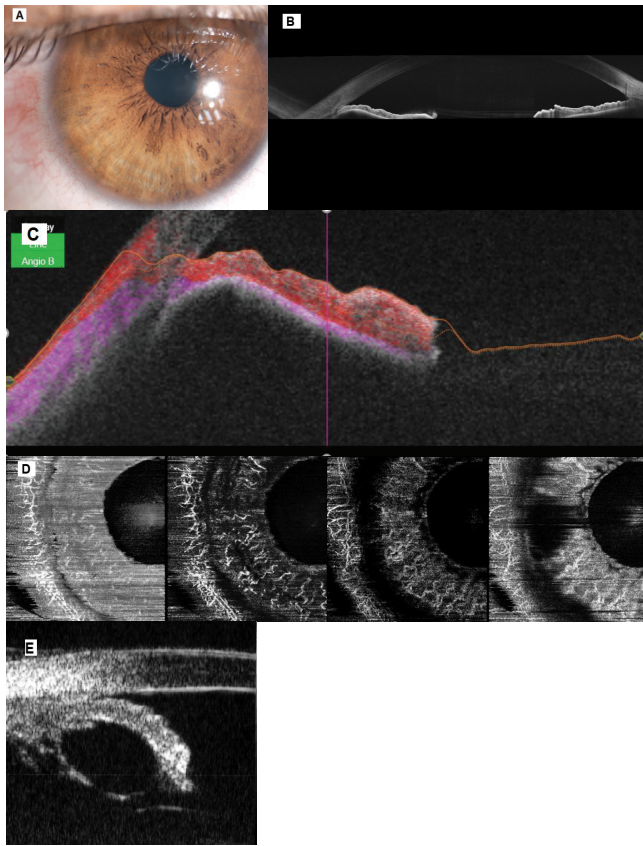


Figure 1. A) Peripheral IPE cyst at 9 o'clock in the right eye with hyperemia in the adjacent conjunctiva. B) Anterior segment SS-OCT image of a temporal iris cyst shows anterior protrusion of the iris, while the posterior borders of the cyst are not clearly distinguishable. C) SS-OCT anterior segment B-scan angiography image of a temporal peripheral iris cyst shows no intrinsic vascularization in the mass causing anterior protrusion of the iris. D) SS-OCTA images of a temporal peripheral IPE cyst from 4 different layers of the iris. A signal void is observed in the cyst region. E) The anterior and posterior walls of a hollow peripheral IPE cyst are clearly visible on UBM

cyst with a thin, hyperreflective wall that had grown to the point of touching the corneal endothelium, as well as a tissue defect on the posterior corneal surface (Figure 2D). The anterior surfaces of the cysts showed high reflectivity but the posterior surface boundaries could not be distinguished. AS SS-OCTA was used to evaluate intrinsic vascularity and blood flow in the cysts. No intrinsic tumoral vascularity or blood flow was observed in any of the cysts (flow void) (Figure 1C, D).

In terms of cyst location, 14 (37.8%) were inferior, 12 (32.4%) were temporal, 8 (21.6%) were nasal, and 3 (8.1%) were superior (4:30-7:30 o'clock was regarded as inferior, 7:30-10:30 o'clock as temporal/nasal, 10:30-1:30 o'clock as superior, and 1:30-4:30 o'clock as the nasal/temporal region).

As treatment, monitoring was recommended for all patients with pigment epithelial cysts. No growth or intraocular complications were observed in any of the patients. Of the 4 patients with primary stromal cyst, 3 were treated by surgical excision while monitoring was recommended for the other.

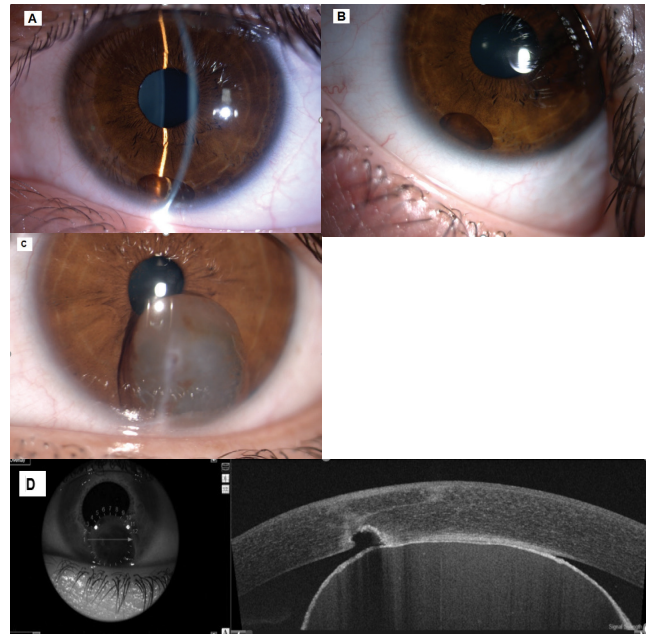


Figure 2. A) A dislodged (free-floating) iris cyst. B) Free movement of the dislodged (free-floating) iris cyst is observed as head position changes. C) Stromal iris cyst secondary to penetrating trauma. D) Anterior segment SS-OCT shows a stromal cyst secondary to trauma with a hyporeflective center and hyperreflective wall touching the corneal endothelium, and a defect in the endothelium/Descemet's membrane/deep stroma

Surgical resection was performed on both patients with secondary stromal cyst. Three patients underwent surgical resection via partial lamellar sclerouvectomy (PLSU). One of these patients was first treated with cyst aspiration and ethanol injection into the lesion, and resection by PLSU was done later done when recurrence was detected. Two patients underwent surgical resection through a limbal incision. One patient with a congenital stromal cyst who had a limbal incision developed secondary glaucoma and band keratopathy after resection of the 6x5 mm cyst. In final follow-up examination, all patients who were followed by clinical observation and those who underwent surgery were in stable condition.

Discussion

Peripheral (iridociliary) cysts are the most common type of IPE cysts. Lois et al.² reported that peripheral IPE cysts present more frequently after the age of 33 and in women. In 26 of our patients, IPE cysts were peripheral. Their mean age was 30.4 ± 10.7 years, with 18 being female and 8 male. Although peripheral IPE cysts are common, the diagnosis may be overlooked in clinical practice because they are asymptomatic and located in the iridociliary sulcus.¹⁵ They are usually noticed during routine slit-lamp examination as an anterior elevation of the iris stroma in the nasal or temporal region (Figure 1A). UBM should be performed to differentiate them from solid tumors. They appear as hollow, thin-walled lesions on UBM.^{14,15}

Midzonal IPE cysts are located in the middle region of the iris. They are usually noticed during periodic examination or cataract surgery. They emerge around the age of 52 on average, with no sex difference.² IPE cysts were midzonal in 4 of our patients. Their mean age was 52 ± 19.2 years, with 3 being male and 1 female. Pupillary (central) IPE cysts are located at the pupil margin and may be visible without the need for dilation.

IPE cysts can sometimes dislodge from their initial location and float freely in the anterior chamber or vitreous humor.^{18,19} Dislodged IPE cysts floating freely in the anterior chamber change location according to head position due to gravity. Dislodged cysts in the anterior chamber can sometimes settle in the angle.¹⁵ Cysts in the vitreous humor, which has a collagen/hyaluronic acid roof, are less mobile. The 1 patient with dislodged iris cyst in our study was a 20-year-old woman (Figure 2A, B). Free-floating pigmented cysts in the vitreous may originate from the IPE or ciliary pigment epithelium. Previous studies have shown that iris cysts floating in the vitreous may have originated from the pigmented ciliary body epithelium in the pars plana region after blunt trauma.^{20,21,22,23,24} Free-floating implantation cysts may cause corneal endothelial damage and reduce endothelial cell count. Therefore, free-floating cysts should be monitored regularly, and intervention should be considered if endothelial damage is observed.

IPE cysts are generally asymptomatic and do not require treatment except in rare cases that affect the visual axis or involve the anterior chamber angle.^{2,4,5} Such cases can be treated with laser ablation or cyst evacuation by needle aspiration.¹⁵ Surgical resection may be necessary for large cysts that fill the anterior chamber. Follow-up was the recommended treatment approach for all of our patients and none developed clinical complications during the follow-up period.

Stromal iris cysts are more anteriorly located compared to IPE cysts and can slowly grow to fill the anterior chamber and pupillary region. They may remain the same size for years, or enlarge suddenly and rupture, leading to secondary glaucoma and corneal decompensation. They include congenital and acquired subtypes. Congenital cysts usually appear before the age of 10 and are aggressive.^{11,12} Although spontaneous regression can occur in rare cases, most stromal cysts require treatment by needle aspiration or surgical excision.^{11,13} Four of our patients had stromal cysts; 1 was congenital and 3 were acquired. The congenital cyst was 6x5 mm in size and was treated with surgical resection through a limbal incision. Secondary glaucoma and band keratopathy developed after resection. Of the 3 patients with acquired cysts, 1 was recommended follow-up while 2 were treated with surgical resection by the PLSU method. One of these patients was first treated with cyst aspiration and ethanol injection and underwent resection with PLSU upon detection of recurrence. Leakage into the eye should be avoided during ethanol injection. For this reason, the cyst wall should be carefully perforated with the needle. Care should also be taken not to leave residual cyst tissue during PLSU.

Secondary cysts usually develop after ocular surgery or trauma. They usually form due to surface epithelial cells from the conjunctiva or cornea growing inward and accumulating

on the iris after a penetrating or surgical trauma (implantation cysts).^{7,19} Though rare, secondary iris cysts can also result from the prolonged use of miotic drugs and prostaglandins; parasitic infections such as ocular cysticercosis; inflammatory conditions such as uveitis; or medulloepithelioma, melanoma, nevi, and metastatic tumors.^{8,9,10,25} Secondary cysts grow faster than primary cysts and as a result may lead to complications such as uveitis, decreased vision, secondary glaucoma, lens subluxation, iris bombe, or complicated cataract. Two of our patients had secondary cysts associated with perforating ocular injury (Figure 2C). Both underwent surgical resection, one with the PLSU method and the other through a limbal incision.

Imaging methods are important in the differential diagnosis of cysts and ocular tumors. Melanoma and pigment epithelial adenoma should be ruled out in patients with IPE cysts. IPE cysts appear as thin-walled, hollow, and homogenous lesions with regular borders on UBM and AS OCT, while tumors present a solid inner structure.^{14,26,27} In the differential diagnosis from iris melanoma, the main indicator of malignancy was shown to be increase in lesion size.^{28,29} UBM is used to evaluate lesion growth by objectively measuring the maximum thickness and diameter of the iris lesion (Figure 1E). It provides valuable information about the AS due to its high penetration power, ability to show ciliary body extension, and because it is unaffected by degree of pigmentation and enables good visualization of the posterior border of the tumor.³⁰

Though rare, cyst-like cavitory spaces appearing on ultrasound as hollow lesions are found in cases of uveal melanoma.^{31,32} In such cases of cavitory melanoma, it is important to make a differential diagnosis between solid and cystic lesions. Cavitory lesions have much thicker walls than cysts.

AS OCT is a noncontact imaging method that provides high-resolution cross-sectional images and is used in the imaging of many pathological conditions such as iris cyst, iris nevus, and iris/ciliary body melanoma. This method may be unable to show the posterior wall of the cyst due to the absorption of light by the IPE layer, especially in dark-colored eyes. Bianciotto et al.³³ compared UBM and AS OCT in a series of 200 AS tumors and demonstrated that AS OCT images had lower resolution compared to UBM due to the shadowing effect in large or pigmented lesions originating from the IPE or ciliary body, and that UBM was superior to AS OCT in displaying the posterior lesion border and tumor configuration. Previous studies have also shown UBM to be superior to AS OCT in the evaluation and follow-up of AS tumors due to its effective visualization of large, pigmented tumors and ciliary body tumors.^{26,34,35,36} In the case of our 4 patients who underwent AS SS-OCT imaging, the internal structure of the lesions was analyzed by measuring base diameter and thickness. The AS SS-OCT image of a patient with iris cyst secondary to penetrating knife trauma revealed a hollow cyst with a thin, hyperreflective wall that had grown and touched the corneal endothelium, in addition to a tissue defect on the posterior surface of the cornea (Figure 2D). While the anterior surfaces of IPE cysts were visible on AS SS-OCT as high reflectivity, the posterior borders could not be distinguished (Figure 1B).

OCTA is a noninvasive imaging method based on an algorithm-based evaluation of changes in the intensity and phase of light reflected by the movement of red blood cells within a vessel. This method enables the detailed visualization of the retinal and choroidal vascular networks, has recently been used for the examination of AS tumors. The visibility of the vascular structures in the iris varies depending on pigment density. Consistent with this, intrinsic intratumoral vascularity and vascular flow were not observed in any of the 4 patients in our study who underwent SS-OCTA (Figure 1C, D). These findings were found to be important in the differentiation of cystic and solid tumors.³⁷

Study Limitations

The main limitation of this study is that due to the small patient number, we were unable to analyze pupillary primary IPE cysts, which are rarer in clinical practice.

Conclusion

In conclusion, cystic lesions of the iris originate from the pigment epithelium or stroma. Most cysts are of primary etiology, pigmentary epithelial origin, and are located peripherally. Pigment epithelial cysts do not require any treatment, whereas iris stromal cysts usually require treatment. Although both UBM and AS OCT play an important role in diagnosis and treatment follow-up of iris cysts, UBM is superior to AS OCT in the imaging of iris lesions and the differentiation of cystic and solid lesions. With the development of AS OCTA techniques, it is also possible to noninvasively obtain information about the internal vascular structure of these tumors.

Ethics

Ethics Committee Approval: The study was conducted in accordance with the principles of the Declaration of Helsinki. Approval was obtained from our institutional ethics committee.

Informed Consent: Informed consent forms were obtained from the study participants.

Peer-review: Externally peer reviewed.

Authorship Contributions

Concept: H.C.K., K.G., M.B.H., **Design:** H.C.K., K.G., M.B.H., **Data Collection or Processing:** H.C.K., K.G., M.B.H., **Analysis or Interpretation:** H.C.K., K.G., M.B.H., **Literature Search:** H.C.K., K.G., M.B.H., **Writing:** H.C.K., K.G., M.B.H.,

Conflict of Interest: The authors declare no conflicts of interest.

Financial Disclosure: The authors report receiving no financial support.

References

- Shields CL, Kancherla S, Patel J, Vijayvargiya P, Suriano MM, Kolbus E, Badami A, Sharma P, Jacobs E, Voluck M, Zhang Z, Kansal R, Shields PW, Bianciotto CG, Shields JA. Clinical survey of 3680 iris tumors based on patient age at presentation. *Ophthalmology* 2012;119:407-414.
- Lois N, Shields CL, Shields JA, Mercado G. Primary cysts of the iris pigment epithelium: clinical features and natural course in 234 patients. *Ophthalmology* 1998;105:1879-1885.
- Shields JA, Shields CL, Lois N, Mercado G. Iris cysts in children: classification, incidence, and management. *Br J Ophthalmol* 1999;83:334-338.
- Shields JA. Primary cysts of the iris. *Trans Am Ophthalmol Soc* 1981;79:771-809.
- Shields JA, Kline MW, Augsburger JJ. Primary iris cysts: a review of the literature and report of 62 cases. *Br J Ophthalmol* 1984;68:152-166.
- Hildreth T, Maino J, Hartong T. Primary and secondary iris cysts. *J Am Optom Assoc* 1991;62:588-592.
- Farmer SG, Kalina RE. Epithelial implantation cyst of the iris. *Ophthalmology* 1981;88:1286-1289.
- Lai IC, Kuo MT, Teng LM. Iris pigment epithelial cyst induced by topical administration of latanoprost. *Br J Ophthalmol* 2003;87:366.
- Chin NB, Gold AA, Breinin GM. Iris cysts and miotics. *Arch Ophthalmol* 1964;71:611-616.
- Reddy CC, Gupta VP, Sarada P, Prabhakar V, Reddy DL, Anjaneyulu C. Ocular cysticercosis (a study of 15 cases). *Indian J Ophthalmol* 1980;28:69-72.
- Lois N, Shields CL, Shields JA, Mercado G, De Potter P. Primary iris stromal cysts: a report of 17 cases. *Ophthalmology* 1998;105:1317-1322.
- Capó H, Palmer E, Nicholson DH. Congenital cysts of the iris stroma. *Am J Ophthalmol* 1993;116:228-232.
- Shields CL, Arepalli S, Lally EB, Lally SE, Shields JA. Iris stromal cyst management with absolute alcohol-induced sclerosis in 16 patients. *JAMA Ophthalmol* 2014;132:703-708.
- Gündüz K, Hoşal BM, Zilelioğlu G, Günalp I. The use of ultrasound biomicroscopy in the evaluation of anterior segment tumors and simulating conditions. *Ophthalmologica* 2007;221:305-312.
- Shields JA, Shields CL. Cysts of the iris pigment epithelium. What is new and interesting? *Asia Pac J Ophthalmol (Phila)*. 2017;6:64-69.
- Makley TA, King GL. Multiple cysts of the iris and ciliary body simulating a malignant melanoma. *Trans Am Acad Ophthalmol Otolaryngol* 1958;62:441-443.
- Shields CL, Shields PW, Manalac J, Jumroendarasame C, Shields JA. Review of cystic and solid tumors of the iris. *Oman J Ophthalmol* 2013;6:159-164.
- Shields JA, Shields CL, DePotter P, Wagner RS, Caputo AR. Free-floating cyst in the anterior chamber of the eye. *J Pediatr Ophthalmol Strabismus* 1996;33:330-331.
- Lally DR, Shields JF, Shields CL, Marr BP, Shields JA. Pigmented free floating vitreous cyst in a child. *J Pediatr Ophthalmol Strabismus* 2008;45:47-48.
- Lisch W, Rochels R. Pathogenesis of congenital vitreous cysts (in German) *Klin Monbl Augenheilkd* 1989;195:375-378.
- Awan KJ. Multiple free floating vitreous cysts with congenital nystagmus and esotropia. *J Pediatr Ophthalmol Strabismus* 1975;12:49-53.
- Tuncer S, Bayramoglu S. Pigmented free-floating vitreous cyst in a patient with high myopia and uveal coloboma simulating choroidal melanoma. *Ophthalmic Surg Lasers Imaging*. 2011 Apr 14;42 Online: e49-52.
- Bullock JD. Developmental vitreous cysts. *Arch Ophthalmol* 1974;91:83-84.
- Aydin E, Demir HD, Tasliyurt T. Idiopathic pigmented free-floating posterior vitreous cyst. *Int Ophthalmol* 2009;29:299-301.
- Gentile RC, Liebmann JM, Tello C, Stegman Z, Weissman SS, Ritch R. Ciliary body enlargement and cyst formation in uveitis. *Br J Ophthalmol* 1996;80:895-899.
- Pavlin CJ, Vásquez LM, Lee R, Simpson ER, Ahmed II. Anterior segment optical coherence tomography and ultrasound biomicroscopy in the imaging of anterior segment tumors. *Am J Ophthalmol* 2009;147:214-249.
- Kozart DM. Echographic evaluation of primary cysts of the iris pigment epithelium. *Am J Ophthalmol* 1996;121:100-101.
- Shields CL, Kaliki S, Shah SU, Luo W, Furuta M, Shields JA. Iris melanoma: Features and prognosis in 317 children and adults. *J AAPOS* 2012;16:10-16.
- Shields JA, Sanborn GE, Augsburger JJ. The differential diagnosis of malignant melanoma of the iris. A clinical study of 200 patients. *Ophthalmology* 1983;90:716-720.

31. Arslantürk Eren M, Gündüz AK, Gündüz ÖÖ. Evaluation of iris melanoma with anterior segment optical coherence tomography. *Turk J Ophthalmol* 2017;47:231-234.
32. Zhang J, Demirci H, Shields CL, Leon JA, Shields JA, Eagle RC Jr. Cavitory melanoma of ciliary body simulating a cyst. *Arch Ophthalmol* 2005;123:569-571.
33. Lois N, Shields CL, Shields JA, Eagle RC Jr, De Potter P. Cavitory melanoma of the ciliary body. A study of eight cases. *Ophthalmology* 1998;105:1091-1098.
34. Bianciotto C, Shields CL, Guzman JM, Romanelli-Gobbi M, Mazzuca D Jr, Green WR, Shields JA. Assessment of anterior segment tumors with ultrasound biomicroscopy versus anterior segment optical coherence tomography in 200 cases. *Ophthalmology* 2011;118:1297-1302.
35. Wang D, Pekmezci M, Basham RP, He M, Seider MI, Lin SC. Comparison of different modes in optical coherence tomography and ultrasound biomicroscopy in anterior chamber angle assessment. *J Glaucoma* 2009;18:472-478.
36. Mansouri K, Sommerhalder J, Shaarawy T. Prospective comparison of ultrasound biomicroscopy and anterior segment optical coherence tomography for evaluation of anterior chamber dimensions in European eyes with primary angle closure. *Eye (Lond)* 2010;24:233-239.
37. Dada T, Sihota R, Gadia R, Aggarwal A, Mandal S, Gupta V. Comparison of anterior segment optical coherence tomography and ultrasound biomicroscopy for assessment of the anterior segment. *J Cataract Refract Surg* 2007;33:837-840.
38. Skalet AH, Li Y, Lu CD, Jia Y, Lee B, Husvagt L, Maier A, Fujimoto JG, Thomas CR Jr, Huang D. Optical coherence tomography angiography characteristics of iris melanocytic tumors. *Ophthalmology* 2017;124:197-204.



Artificial Intelligence and Ophthalmology

© Kadircan Keskinbora*, © Fatih Güven**

*Bahçeşehir University Faculty of Medicine, Department of Ophthalmology, Division of Medical Ethics and History of Medicine, İstanbul, Turkey

**Health Sciences University Bakırköy Training and Research Hospital, Clinic of Ophthalmology, İstanbul, Turkey

Abstract

Artificial intelligence is advancing rapidly and making its way into all areas of our lives. This review discusses developments and potential practices regarding the use of artificial intelligence in the field of ophthalmology, and the related topic of medical ethics. Various artificial intelligence applications related to the diagnosis of eye diseases were researched in books, journals, search engines, print and social media. Resources were cross-checked to verify the information. Artificial intelligence algorithms, some of which were approved by the US Food and Drug Administration, have been adopted in the field of ophthalmology, especially in diagnostic studies. Studies are being conducted that prove that artificial intelligence algorithms can be used in the field of ophthalmology, especially in diabetic retinopathy, age-related macular degeneration, and retinopathy of prematurity. Some of these algorithms have come to the approval stage. The current point in artificial intelligence studies shows that this technology has advanced considerably and shows promise for future work. It is believed that artificial intelligence applications will be effective in identifying patients with preventable vision loss and directing them to physicians, especially in developing countries where there are fewer trained professionals and physicians are difficult to reach. When we consider the possibility that some future artificial intelligence systems may be candidates for moral/ethical status, certain ethical issues arise. Questions about moral/ethical status are important in some areas of applied ethics. Although it is accepted that current intelligence systems do not have moral/ethical status, it has yet to be determined what the exact characteristics that confer moral/ethical status are or will be.

Keywords: Artificial intelligence, machine learning, deep learning, ophthalmology, medical ethics

What is Artificial Intelligence?

Artificial intelligence, described simply, is the ability of a computer to mimic the intellectual intelligence unique to humans. This type of intelligence includes qualities such as the ability to link events to specific causes, make generalizations, and learn from experience.¹ As a general public notion, the term is used to describe devices that can provide a reason for a

certain phenomenon, develop strategies, make judgments about situations, and have the ability to learn. However, there are ongoing controversies regarding the level and reliability of this intelligence.²

Many different theories on how to evaluate machine intelligence have been proposed. The most famous of these is the Turing test, which was put forward in 1950 by Alan Turing, an English mathematician, computer scientist, and cryptologist.

Address for Correspondence: Kadircan Keskinbora MD, Bahçeşehir University Faculty of Medicine, Department of Ophthalmology, Division of Medical Ethics and History of Medicine, İstanbul, Turkey Phone: +90 532 275 87 95 E-mail: kadircan.keskinbora@gmail.com **ORCID-ID:** orcid.org/0000-0003-1940-1026

Received: 07.03.2019 **Accepted:** 10.06.2019

Cite this article as: Keskinbora K, Güven F. Artificial Intelligence and Ophthalmology. Turk J Ophthalmol. 2020;50:37-43

In this test, an assessor compares responses given by a computer and a person without knowing who gave which answer and predicts which one is the machine. If the machine can convince the assessor with its answers at least 30% of the time, it passes the test. In 2014, a program called Eugene Goostman passed this test.³

Types of Artificial Intelligence

Artificial intelligence is classified under three headings based on technological achievements and future projections:

1) **Artificial Narrow Intelligence:** Artificial narrow intelligence, which encompasses nearly all of the software currently described as artificial intelligence, mimics human intelligence within the limited field for which it is designed and responds within this framework.

2) **Artificial General Intelligence:** This type of artificial intelligence has the same intellectual capacity as humans and is expected in theory to be able to perform tasks at the same level as a person. The consensus among researchers of artificial intelligence is that this type, also called human-level artificial intelligence, must be able to learn and reason, develop strategies, make plans, communicate using language, and synthesize all of these abilities to accomplish a certain task.⁴

3) **Artificial Superintelligence:** This kind of artificial intelligence is expected to be superior to the most intelligent and talented human brain, and prominent figures in science and technology such as Stephen Hawking and Elon Musk have suggested grim scenarios for the future related to its emergence.

Artificial Intelligence Learning Algorithms and Ophthalmology

a) **Machine Learning:** The term “machine learning”, one of the subclasses of artificial intelligence frequently used in ophthalmology studies, was first introduced in 1959 by the engineer Arthur Samuel, a pioneer in artificial intelligence. He defined this term as the ability of machines to learn outcomes that are not explicitly programmed.⁵

In the machine learning technique, the aim is to generate an algorithm based on a certain amount of data entered into a computer and for the computer to then use this algorithm to improve its predictions. The phase in which the device trains with the input to improve its predictions is the learning phase, which is divided into two types: supervised and unsupervised learning. In supervised learning, labels are assigned to the training data as they are entered into the computer, while in unsupervised learning, the device creates its own algorithm from unlabeled input.

b) **Deep Learning:** As the machine learning technique improves and the amount of input increases, this more advanced method uses multiple layers to generate output, unlike machine learning, which operates with a single layer. Using deep neural networks, the computer can train with much larger data capacity and improve itself with each training cycle to create its own algorithm.

Examples of Artificial Intelligence in Medicine

As in many other industries, the use of artificial intelligence in the field of medicine is steadily increasing. Major companies in numerous medical sectors, particularly the pharmaceutical and imaging sectors, have invested billions of dollars in this field, while research on artificial intelligence software is also an area of intense interest in the academic sphere. Although the various publications on the use of artificial intelligence applications in different fields of medicine reveal the breadth of the uses of these techniques, the number of studies that have been approved is still limited.

To give some notable examples of artificial intelligence applications in the field of medicine, in 2016 an artificial intelligence framework by Google called DeepVariant was proven to be able to identify single nucleotide polymorphisms, the most common genetic variation, with 99.9587% accuracy and received an award from the FDA.⁶ The OsteoDetect application, used for wrist fractures in adults, evaluates patients' X-ray images and was approved by the FDA in 2018.⁷

Artificial intelligence applications developed for purposes such as diagnosing tuberculosis by evaluating a chest X-rays, assessing suspected malignant melanoma based on skin lesion photographs, and detecting lymph node metastasis of breast cancer by analyzing pathology slides, and publications about these represent examples of future areas of use of artificial intelligence.^{8,9,10,11} This is exemplified by a radiology algorithm developed at Stanford University that was able to diagnose pneumonia more accurately than radiologists.¹²

What Can Artificial Intelligence Do for Ophthalmology?

The field of ophthalmology is well suited for artificial intelligence studies, with its numerous digital techniques such as color fundus photography, optical coherence tomography (OCT), and computerized visual field (VF) testing and the huge databases they provide.

In addition to this, the global increase in life expectancy is accompanied by an increase in eye diseases that cause preventable vision loss.^{13,14} Solutions are sought for the early diagnosis and treatment of these diseases, especially in regions where access to physicians is difficult. Artificial intelligence applications are being developed for many different eye diseases, particularly diabetic retinopathy (DR), age-related macular degeneration (AMD), glaucoma, and retinopathy of prematurity (ROP), which are the leading causes of vision loss.¹⁵

Artificial Intelligence and Diabetic Retinopathy

Due to the rapidly increasing number of patients worldwide, DR has generated the most interest in terms of the use of artificial intelligence in ophthalmology. IDx-DR, the first FDA-approved device using artificial intelligence software, was also developed for this area.¹⁶

The IDx-DR uses a Topcon NW400 fundus camera to classify patients according to retinopathy level. Ease of use was cited as the priority when choosing the fundus camera. The operators selected to obtain the fundus photographs had no previous experience using a fundus camera. Patients were

grouped into those with mild to advanced DR according to the American Academy of Ophthalmology classification (Preferred Practice Patterns for Diabetic Retinopathy) and those without retinopathy, and the patients were recommended follow-up examination at 12 months or sooner according to their results. A total of 900 patients participated in the study and the sensitivity and specificity of the device were found to be 87.4% and 89.5%, respectively. The device began to be used at the University of Iowa in 2018 after receiving FDA approval.¹⁶

The IDx-DR was developed using software that uses deep learning techniques, and there are a growing number of similar studies using fundus cameras and deep learning software.^{17,18,19,20} Thanks to deep learning applications, it is possible to develop software with databases containing over 100,000 data points.^{21,22}

There are examples of studies using machine learning methods with fundus photographs, machine learning with OCT, and deep learning methods with OCT.^{19,23,24,25,26,27} Some of these studies have reported nearly 100% sensitivity or specificity rates.^{28,29}

Artificial Intelligence and Age-related Macular Degeneration

As with DR, an increasing number of studies are investigating software that uses artificial intelligence for the early diagnosis and classification of AMD. The earliest published studies involved software developed using fundus photography and machine learning with database sizes smaller than 1,000.^{30,31,32} Later, with software using deep learning technology, database sizes increased and high sensitivity and specificity rates were reached.^{20,33,34}

Ting et al.²⁰ used a database of 72,610 fundus photographs and classified patients as those with intermediate to advanced AMD and those without according to the AREDS (Age-Related Eye Disease Study) classification. They reported sensitivity and specificity of 93.2% and 88.2%, respectively.²⁰

Burlina et al.³³ classified patients with software developed using 130,000 images from 4613 patients and reporting a 91.6% accuracy rate in identifying those with moderate and advanced AMD patients.

Grassmann et al.³⁴ tested an algorithm they generated from 120,656 fundus photographs of 3,654 patients against the AREDS database and reported an accuracy rate of 84.2% in differentiating early and late disease and 94.3% accuracy in identifying healthy subjects.

Artificial Intelligence and Glaucoma

Glaucoma is among the leading causes of vision loss worldwide and has also attracted the attention of artificial intelligence researchers due to the importance of its early diagnosis and treatment.¹⁵

Initially, studies using machine learning to identify glaucomatous optic nerve damage based on fundus photographs were published.^{35,36,37} These were followed by studies that used deep learning technology with much larger databases compared

to the earlier machine learning studies.^{20,38,39} In another study using a database of 125,189 fundus photographs, Ting et al.²⁰ reported a sensitivity of 96.4% and specificity of 87.2%.

Studies are being conducted on the use of imaging modalities other than fundus photography in the diagnosis and monitoring of glaucoma. In addition to artificial intelligence applications created using computerized VF and OCT data, studies have also been published describing programs that are able to evaluate patients based on data from both of these examination devices.^{40,41,42,43,44,45}

Artificial Intelligence and Retinopathy of Prematurity

ROP is a leading cause of vision loss in childhood worldwide and its prevalence is reported as 6-18% in different studies.⁴⁶ According to the ETROP (Early Treatment for Retinopathy of Prematurity) study, early treatment is vital for improving visual acuity, and 9% of patients have permanent vision loss despite early treatment.⁴⁷

Although the impact of ROP diagnosis and treatment on patients' visual acuity outcomes and quality of life is known, access to physicians specializing in ROP can be limited, especially in less developed countries. One of the reasons for this is that the follow-up and treatment of ROP requires a long time and specialized education, even for ophthalmologists. This coupled with high malpractice rates and lawsuits result in physicians avoiding this area.^{48,49} In addition, parameters used in the diagnosis of ROP, such as zone, stage, and presence of additional diseases lead to diagnostic variations even among ROP specialists.⁴⁸ The difficulty in finding specialists and the diagnostic variations among specialists has prompted artificial intelligence researchers to conduct studies on ROP.

Brown et al.⁵⁰ developed software using deep learning technology and a database of 5,511 fundus images obtained with a RetCam fundus camera and reported 93% sensitivity and 94% specificity in determining the presence of additional disease.

In an application developed by Redd et al.⁵¹ based on the same deep learning technology, the software was found to have 0.96 and 0.91 area under the curve values, respectively, in the identification of type 1 ROP and clinically significant ROP.

Other Applications in Ophthalmology

Data from a study by De Fauw et al.⁵² conducted at Moorfields Eye Hospital using Google's deep learning technology called DeepMind presents a striking illustration of the level artificial intelligence has reached.

The artificial intelligence algorithm was trained by introducing 10 different lesions such as hemorrhage and fluid and using 14,884 untagged OCT images, and is able to distinguish more than 50 retinal diseases. The study included data obtained from 37 different OCT devices from different centers affiliated with Moorfields, and data from the application were compared with the decisions of four ophthalmologists and four optometrists affiliated with Moorfields. These physicians and the device were asked to classify OCT images based on the need for referral as urgent, semi-urgent, routine examination, and observation.

At the end of the study, the software's error rate (5.5%) was comparable to those of the hospital's two best retina specialists (6.7% and 6.8%) and was significantly better than those of the other six specialists (10-24.1%). In particular, it was reported that the software made no errors in the urgent referral group.⁵²

Discussion

The progress made in artificial intelligence studies shows that important advances in this technology are ongoing, and it is clear that potential future applications lie on the horizon and are promising for future studies. It is believed that artificial intelligence will be effective in identifying patients with preventable vision loss and referring them to a physician, especially in developing countries where access to physicians is difficult and the population of trained individuals is low.

The diagnostic spectrum in which artificial intelligence may be used and its possible clinical benefits represent a broad field of study. With technologies similar to those in previous studies, applications based on different imaging modalities can be developed in various areas such as occlusive vascular disease, keratoconus, and retinitis pigmentosa. Beyond just screening for or diagnosing diseases, surgical applications may be created to provide guidance for physicians in areas such as determining the ideal type of intraocular lens for a patient or estimating the risk of surgery.

Another important aspect of artificial intelligence that should be discussed is the potential ethical conflicts. Imagine that in the near future, a bank evaluates home loan applications using machine learning algorithms. Now imagine that someone denied a loan sues the bank, claiming that the algorithm racially discriminated in its evaluation. The bank will state that this is impossible because the algorithm does not know the applicants' race. In fact, the reason the bank implemented such a system was to eliminate unpleasant situations such as the involvement of human emotions. Nevertheless, suppose statistics indicate that the bank's approval rate is steadily falling for black applicants. When ten equivalent applications are entered into the system, the algorithm accepts those of the white applicants and rejects those of the black applicants. What do you think is happening here? It may not be easy to determine the answer. If the machine learning algorithm is created using a complex artificial neural network or based on a genetic algorithm generated by controlled evolution, it would be impossible to understand why and according to what data the algorithm makes its racially discriminant decisions. In contrast, decision trees or networks in special computer language are much more transparent in terms of allowing the programmer to analyze them. This may allow an auditor to discover, for example, that the decision is reached based on where the applicants were born or the fact that they previously resided mostly in suburban neighborhoods, i.e., their addresses.

Artificial intelligence algorithms play an increasingly prominent role in modern society. In general, however, those who are affected by them are not even aware that such a thing exists in the background.

When we consider the possibility that some future artificial intelligence systems may be candidates for moral/ethical status, various ethical issues arise. Relations with beings of moral/ethical status are not entirely a matter of rationality; we also have moral/ethical reasons to treat them in certain ways and to avoid mistreating them. Kamm⁵³ proposed the following definition of moral status that will serve our purpose: An entity has moral status when it is morally important in its own right and some things are morally permissible or impermissible to do to them, for their own sake.

Questions about moral/ethical status are important in some areas of applied ethics. For example, disputes regarding the moral acceptability of abortion generally influence disagreements about the moral/ethical status of the human embryo. The controversies related to animal experimentation and the treatment of animals in the food industry include questions about the moral/ethical status of different animal species. Our obligations to persons with severe dementia, such as end-stage Alzheimer's patients, may also depend on questions of moral/ethical status.

Current artificial intelligence systems are generally regarded as not having moral status. At least as far as the programs themselves are concerned, we can modify, copy, terminate, delete, and use computer programs as desired. The moral/ethical restrictions involved in our relationships with contemporary artificial intelligence systems are based on our obligations to other beings, such as human race itself. However, we have no duty to the systems themselves.

Although there seems to be a consensus that current artificial intelligence systems do not have moral/ethical status, it is not clear what the characteristics determining moral/ethical status are or will be. In addition, infants and individuals suffering from severe mental illnesses do not meet the criteria for cognitive capacity. Some authorities do not regard people with mental illness as having full moral status.

Further Complication of the Issue

Let us set aside these arguments and focus on the criteria of sentience and mind. This understanding of moral/ethical status suggests that if an artificial intelligence system has the capacity for sensation, such as the ability to feel pain, then it may have moral/ethical status. A sentient artificial intelligence system, although it lacks language and other higher cognitive abilities, is not a toy animal or doll. It is more like a living animal. It is immoral to inflict pain on a mouse, unless there are strong moral/ethical grounds compelling you to do so. The same should also apply to an artificial intelligence system with any kind of sentience.

If an artificial intelligence system possesses intelligence similar to a normal adult in addition to a sensory system, then it should have full moral/ethical status equivalent to that of human beings. One of the ideas underlying this moral/ethical

evaluation can be expressed more strongly as the principle of substrate non-discrimination: If two entities have the same functionality and the same conscious experience, and differ only in the substrate of their implementation, then they have the same moral/ethical status. To reject this principle is to adopt an attitude similar to racism. Different skin color does not affect the essence of humanity. This principle does not make the claim that a digital computer can be conscious or have the same functionality as a human being. However, what this principle does say is that we should not look at whether an entity is made of silicon or carbon, or whether its brain uses semiconductors or neurotransmitters.^{54,55,56}

Three metaphor groups have been identified to allow us to conceptualize the capabilities of an artificial superintelligence:

a) Metaphors inspired by individual differences in intelligence between people: Artificial intelligence will make new discoveries, publish groundbreaking research articles, earn money on the stock exchange, or direct political power blocs.

b) Metaphors inspired by differences in knowledge between past and present human civilizations: Artificial intelligence will realize predictions made by futurists for human civilization of the next century or millennium, such as molecular nanotechnology or interstellar travel.

c) Metaphors inspired by differences in brain architecture between humans and other biological organisms: For example, Vinge⁵⁷ said, “Imagine running a dog mind at a very high speed. Would a thousand years of doggy living add up to any human insight?” What that implies is that changes in cognitive architecture could give rise to insight that not even humans possess. Even if we confine ourselves to historical metaphors, it is clear that superhuman intelligence poses new ethical challenges that are not exactly like those that came before. Kurzweil⁵⁸ stated that “intelligence is inherently uncontrollable” and that even if people attempt to take precautions, intelligent beings will have the intelligence to easily overcome such obstacles. Artificial intelligence is not only intelligent, but can also block access to its own source code as part of the process of developing its own intelligence and even reprogram itself to turn into anything it wants.

Conclusion

The discipline of artificial intelligence ethics, especially considering artificial general intelligence, differs fundamentally from the moral/ethical discipline of non-cognitive technologies:

- The local, specific behavior of artificial intelligence may not be predictable apart from its safety, even if programmers do everything right.

- Verifying the reliability of the system can become a greater challenge, as it requires verifying what the system is trying to do rather than verifying the safe behavior of the system in all areas in which it operates.

- Ethical cognition should be addressed as an engineering issue.^{59,60}

Ancient civilizations considered slavery acceptable; we believe otherwise. Ethical debates over voting rights for women and blacks continued even into the nineteenth and twentieth centuries. Advancing science and increasing technological capabilities are not the only differences between modern and ancient civilizations. There is also a difference in ethical perspective. It is very likely that machine ethics will present our greatest challenge. The question then becomes:

How will you create artificial intelligence that, as it operates, will eventually become more ethical than you?

Peer-review: Externally and internally peer reviewed.

Authorship Contributions

Concept: K.K., Design: F.G., Data Collection or Processing: K.K., Analysis or Interpretation: K.K., F.G., Literature Search: K.K., Writing: K.K., F.G.

Conflict of Interest: No conflict of interest was declared by the authors.

Financial Disclosure: The authors declared that this study received no financial support.

References

1. Copeland BJ. Artificial intelligence | Definition, Examples, and Applications | Britannica.com. Encyclopedia Britannica, <https://www.britannica.com/technology/artificial-intelligence> (2019, accessed 25 February 2019).
2. Adams S, Arel I, Bach J, Coop R, Furlan R, Goertzel B, Hall JS, Samsonovich A, Scheutz M, Schlesinger M, Shapiro SC, Sowa J. Mapping the Landscape of Human-Level Artificial General Intelligence. *AI Magazine*. 2012;33:25-42.
3. Computer AI passes Turing test in 'world first' - BBC News, <https://www.bbc.com/news/technology-27762088> (2014, accessed 25 February 2019).
4. Russell SJ, Norvig P. *Artificial intelligence : a modern approach*. 3rd ed. New Jersey: Pearson Education. 2010.
5. Samuel AL. Some Studies in Machine Learning Using the Game of Checkers. II—Recent Progress. In: *Computer Games I*. New York, NY: Springer New York, pp. 366-400.
6. PrecisionFDA Truth Challenge - Google Genomics v1 documentation, https://googlegenomics.readthedocs.io/en/staging-2/use_cases/discover_public_data/precision_fda.html (accessed 26 February 2019).
7. Levy MC. FDA and Artificial Intelligence in Digital Health Innovation | Artificial Intelligence Law Blog, <https://www.artificialintelligencelawblog.com/2018/12/fda-artificial-intelligence-digital-health-innovation/> (2018, accessed 3 March 2019).
8. Lakhani P, Sundaram B. Deep Learning at Chest Radiography: Automated Classification of Pulmonary Tuberculosis by Using Convolutional Neural Networks. *Radiology*. 2017;284:574-582.
9. Ting DSW, Yi PH, Hui F. Clinical Applicability of Deep Learning System in Detecting Tuberculosis with Chest Radiography. *Radiology*. 2018;286:729-731.
10. Esteva A, Kuprel B, Novoa RA, Ko J, Swetter SM, Blau HM, Thrun S. Dermatologist-level classification of skin cancer with deep neural networks. *Nature* 2017;542:115-118.
11. Ehteshami Bejnordi B, Veta M, Johannes van Diest P, van Ginneken B, Karssemeijer N, Litjens G, van der Laak JAWM; the CAMELYON16 Consortium, Hermsen M, Manson QF, Balkenhol M, Geessink O, Stathonikos N, van Dijk MC, Bult P, Beca F, Beck AH, Wang D, Khosla A, Gargeya R, Irshad H, Zhong A, Dou Q, Li Q, Chen H, Lin HJ, Heng PA, Haß C, Bruni E, Wong Q, Halici U, Öner MÜ, Cetin-Atalay R, Berseth M, Khvatkov V, Vylegzhanin A, Kraus O, Shaban M, Rajpoot N, Awan R, Sirinukunwattana K, Qaiser T, Tsang YW, Tellez D, Annuscheit J, Hufnagl P, Valkonen M, Kartasalo K, Latonen L, Ruusuvoori P, Liimatainen K, Albarqouni S, Mungal B, George A, Demirci S, Navab N, Watanabe S, Seno S, Takenaka

- Y, Matsuda H, Ahmady Phoulady H, Kovalev V, Kalinovsky A, Liauchuk V, Bueno G, Fernandez-Carrobles MM, Serrano I, Deniz O, Racoceanu D, Venâncio R. Diagnostic Assessment of Deep Learning Algorithms for Detection of Lymph Node Metastases in Women With Breast Cancer. *JAMA*. 2017;318:2199-2210.
12. Kubota T. Algorithm better at diagnosing pneumonia than radiologists | News Center | Stanford Medicine, <https://med.stanford.edu/news/all-news/2017/11/algorithm-can-diagnose-pneumonia-better-than-radiologists.html> (accessed 3 March 2019).
13. Arias E, Heron M, Xu J. United States life tables, 2014. *Natl Vital Stat Rep*. 2017;66:1-64.
14. Zheng Y, He M, Congdon N. The worldwide epidemic of diabetic retinopathy. *Indian J Ophthalmol*. 2012;60:428-431.
15. Flaxman SR, Bourne RRA, Resnikoff S, Ackland P, Braithwaite T, Cicinelli MV, Das A, Jonas JB, Keeffe J, Kempen JH, Leasher J, Limburg H, Naidoo K, Pesudovs K, Silvester A, Stevens GA, Tahhan N, Wong TY, Taylor HR; Vision Loss Expert Group of the Global Burden of Disease Study. Global causes of blindness and distance vision impairment 1990-2020: a systematic review and meta-analysis. *Lancet Glob Health*. 2017;5:e1221-e1234.
16. Abràmoff MD, Lavin PT, Birch M, Shah N, Folk JC. Pivotal trial of an autonomous AI-based diagnostic system for detection of diabetic retinopathy in primary care offices. *npj Digital Medicine*. 2018;1:39.
17. Ramachandran N, Hong SC, Sime MJ, Wilson AG. Diabetic retinopathy screening using deep neural network. *Clinical & Experimental Ophthalmology*. 2018;46:412-416.
18. Gargeya R, Leng T. Automated Identification of Diabetic Retinopathy Using Deep Learning. *Ophthalmology*. 2017;124:962-969.
19. Abràmoff MD, Lou Y, Erginay A, Clarida W, Amelon R, Folk JC, Niemeijer M. Improved Automated Detection of Diabetic Retinopathy on a Publicly Available Dataset Through Integration of Deep Learning. *Invest Ophthalmol Vis Sci*. 2016;57:5200-5206.
20. Ting DSW, Cheung CY, Lim G, Tan GSW, Quang ND, Gan A, Hamzah H, Garcia-Franco R, San Yeo IY, Lee SY, Wong EYM, Sabanayagam C, Baskaran M, Ibrahim F, Tan NC, Finkelstein EA, Lamoureux EL, Wong IY, Bressler NM, Sivaprasad S, Varma R, Jonas JB, He MG, Cheng CY, Cheung GCM, Aung T, Hsu W, Lee ML, Wong TY. Development and Validation of a Deep Learning System for Diabetic Retinopathy and Related Eye Diseases Using Retinal Images From Multiethnic Populations With Diabetes. *JAMA*. 2017;318:2211-2223.
21. Gulshan V, Peng L, Coram M. Development and validation of a deep learning algorithm for detection of diabetic retinopathy in retinal fundus photographs. *JAMA*. 2016;316:2402-2410.
22. Li Z, Keel S, Liu C, He Y, Meng W, Scheetz J, Lee PY, Shaw J, Ting D, Wong TY, Taylor H, Chang R, He M. An Automated Grading System for Detection of Vision-Threatening Referable Diabetic Retinopathy on the Basis of Color Fundus Photographs. *Diabetes Care*. 2018;41:2509-2516.
23. Acharya UR, Ng EYK, Tan J-H, Sree SV, Ng KH. An integrated index for the identification of diabetic retinopathy stages using texture parameters. *J Med Syst*. 2012;36:2011-2020.
24. Ganesan K, Martis RJ, Acharya UR, Chua CK, Min LC, Ng EY, Laude A. Computer-aided diabetic retinopathy detection using trace transforms on digital fundus images. *Med Biol Eng Comput*. 2014;52:663-672.
25. Sandhu HS, Eltanboly A, Shalaby A, Keynton RS, Schaal S, El-Baz A. Automated Diagnosis and Grading of Diabetic Retinopathy Using Optical Coherence Tomography. *Invest Ophthalmol Vis Sci*. 2018;59:3155-3160.
26. Adhi M, Semy SK, Stein DW, Potter DM, Kuklinski WS, Sleeper HA, Duker JS, Waheed NK. Application of Novel Software Algorithms to Spectral-Domain Optical Coherence Tomography for Automated Detection of Diabetic Retinopathy. *Ophthalmic Surg Lasers Imaging Retina*. 2016;47:410-417.
27. ElTanboly A, Ismail M, Shalaby A, Switala A, El-Baz A, Schaal S, Gimel'farb G, El-Azab M. A computer-aided diagnostic system for detecting diabetic retinopathy in optical coherence tomography images. *Med Phys*. 2017;44:914-923.
28. Qi SR. Machine Learning and OCT Images—the Future of Ophthalmology, <https://medium.com/health-ai/machine-learning-and-oct-images-the-future-of-ophthalmology-47dc64ee9dc6>.
29. Qi SR. Deep Learning in Ophthalmology — How Google Did It – Health, <https://medium.com/health-ai/deep-learning-in-ophthalmology-using-128-175-retinal-images-59814e8a3f68> (accessed 4 March 2019).
30. Agurto C, Barriga ES, Murray V, Nemeth S, Crammer R, Bauman W, Zamora G, Pattichis MS, Soliz P. Automatic Detection of Diabetic Retinopathy and Age-Related Macular Degeneration in Digital Fundus Images. *Invest Ophthalmol Vis Sci*. 2011;52:5862-5871.
31. Zheng Y, Hijazi MHA, Coenen F. Automated “Disease/No Disease” Grading of Age-Related Macular Degeneration by an Image Mining Approach. *Invest Ophthalmol Vis Sci*. 2012;53:8310-8318.
32. Mookiah MR, Acharya UR, Koh JE, Chandran V, Chua CK, Tan JH, Lim CM, Ng EY, Noronha K, Tong L, Laude A. Automated diagnosis of Age-related Macular Degeneration using greyscale features from digital fundus images. *Comput Biol Med*. 2014;53:55-64.
33. Burlina PM, Joshi N, Pekala M, Pacheco KD, Freund DE, Bressler NM. Automated Grading of Age-Related Macular Degeneration From Color Fundus Images Using Deep Convolutional Neural Networks. *JAMA Ophthalmol*. 2017;135:1170-1176.
34. Grassmann F, Mengelkamp J, Brandl C, Harsch S, Zimmermann ME, Linkohr B, Peters A, Heid IM, Palm C, Weber BHF. A Deep Learning Algorithm for Prediction of Age-Related Eye Disease Study Severity Scale for Age-Related Macular Degeneration from Color Fundus Photography. *Ophthalmology*. 2018;125:1410-1420.
35. Singh A, Dutta MK, ParthaSarathi M, Uher V, Burget R. Image processing based automatic diagnosis of glaucoma using wavelet features of segmented optic disc from fundus image. *Comput Methods Programs Biomed*. 2016;124:108-120.
36. Salam AA, Khalil T, Akram MU, Jameel A, Basit I. Automated detection of glaucoma using structural and non structural features. *Springerplus*. 2016;5:1519.
37. Chakrabarty L, Joshi GD, Chakravarty A, Raman GV, Krishnadas SR, Sivaswamy J. Automated Detection of Glaucoma From Topographic Features of the Optic Nerve Head in Color Fundus Photographs. *J Glaucoma*. 2016;25:590-597.
38. Chen X, Xu Y, Kee Wong DW, Wong TY, Liu J. Glaucoma detection based on deep convolutional neural network. In: 2015 37th Annual International Conference of the IEEE Engineering in Medicine and Biology Society. Conference 2015:715-718.
39. Li Z, He Y, Keel S, Meng W, Chang RT, He M. Efficacy of a Deep Learning System for Detecting Glaucomatous Optic Neuropathy Based on Color Fundus Photographs. *Ophthalmology*. 2018;125:1199-1206.
40. Muhammad H, Fuchs TJ, De Cuir N, De Moraes CG, Blumberg DM, Liebmann JM, Ritch R, Hood DC. Hybrid Deep Learning on Single Wide-field Optical Coherence tomography Scans Accurately Classifies Glaucoma Suspects. *J Glaucoma*. 2017;26:1086-1094.
41. Oh E, Yoo TK, Hong S. Artificial Neural Network Approach for Differentiating Open-Angle Glaucoma From Glaucoma Suspect Without a Visual Field Test. *Invest Ophthalmol Vis Sci*. 2015;56:3957-3966.
42. Bowd C, Lee I, Goldbaum MH, Balasubramanian M, Medeiros FA, Zangwill LM, Girkin CA, Liebmann JM, Weinreb RN. Predicting Glaucomatous Progression in Glaucoma Suspect Eyes Using Relevance Vector Machine Classifiers for Combined Structural and Functional Measurements. *Invest Ophthalmol Vis Sci*. 2012;53:2382-2389.
43. Niwas SI, Lin W, Bai X, Kwok CK, Jay Kuo CC, Sng CC, Aquino MC, Chew PT. Automated anterior segment OCT image analysis for Angle Closure Glaucoma mechanisms classification. *Comput Methods Programs Biomed*. 2016;130:65-75.
44. Silva FR, Vidotti VG, Cremasco F, Dias M, Gomi ES, Costa VP. Sensitivity and specificity of machine learning classifiers for glaucoma diagnosis using Spectral Domain OCT and standard automated perimetry. *Arq Bras Oftalmol*. 2013;76:170-174.
45. Vidotti VG, Costa VP, Silva FR, Resende GM, Cremasco F, Dias M, Gomi ES. Sensitivity and Specificity of Machine Learning Classifiers and Spectral Domain OCT for the Diagnosis of Glaucoma. *Eur J Ophthalmol*. 2012;23:61-69.

46. Fleck BW, Dangata Y. Causes of visual handicap in the Royal Blind School, Edinburgh, 1991-2. *Br J Ophthalmol.* 1994;78:421.
47. Early Treatment for Retinopathy of Prematurity Cooperative Group, Good WV, Hardy RJ, Dobson V, Palmer EA, Phelps DL, Tung B, Redford M. Final visual acuity results in the early treatment for retinopathy of prematurity study. *Arch Ophthalmol.* 2010;128:663-671.
48. Chiang MF, Jiang L, Gelman R, Du YE, Flynn JT. Interexpert Agreement of Plus Disease Diagnosis in Retinopathy of Prematurity. *Arch Ophthalmol.* 2007;125:875-880.
49. Braverman RS, Enzenauer RW. Socioeconomics of Retinopathy of Prematurity In-Hospital Care. *Arch Ophthalmol.* 2010;128:1055-1058.
50. Brown JM, Campbell JP, Beers A, Chang K, Ostmo S, Chan RVP, Dy J, Erdogmus D, Ioannidis S, Kalpathy-Cramer J, Chiang MF. Imaging and Informatics in Retinopathy of Prematurity (i-ROP) Research Consortium. Automated Diagnosis of Plus Disease in Retinopathy of Prematurity Using Deep Convolutional Neural Networks. *JAMA Ophthalmol.* 2018;136:803-810.
51. Redd TK, Campbell JP, Brown JM, Kim SJ, Ostmo S, Chan RVP, Dy J, Erdogmus D, Ioannidis S, Kalpathy-Cramer J, Chiang MF. Imaging and Informatics in Retinopathy of Prematurity (i-ROP) Research Consortium. Evaluation of a deep learning image assessment system for detecting severe retinopathy of prematurity. *Br J Ophthalmol.* 2018;bjophthalmol-2018-313156.
52. De Fauw J, Ledsam JR, Romera-Paredes B, Nikolov S, Tomasev N, Blackwell S, Askham H, Glorot X, O'Donoghue B, Visentin D, van den Driessche G, Lakshminarayanan B, Meyer C, Mackinder F, Bouton S, Ayoub K, Chopra R, King D, Karthikesalingam A, Hughes CO, Raine R, Hughes J, Sim DA, Egan C, Tufail A, Montgomery H, Hassabis D, Rees G, Back T, Khaw PT, Suleyman M, Cornebise J, Keane PA, Ronneberger O. Clinically applicable deep learning for diagnosis and referral in retinal disease. *Nat Med.* 2018;24:1342-1350.
53. Kamm FM. Terrorism and several moral distinctions. *Legal Theory.* 2006;12:19-69.
54. Frankish K, Ramsey WM. The Cambridge handbook of artificial intelligence. *Choice Reviews Online.* 2015;52:3019-3019.
55. Keskinbora HK, Keskinbora K. Ethical considerations on novel neuronal interfaces. *Neurol Sci.* 2018;39:607-613.
56. Bostrom N, Cirkovic MM. Global catastrophic risks. *Choice Reviews Online.* 2013;46:6152-6152.
57. Vinge V. The Coming Technological Singularity: How to Survive in the Post-Human Era. *Science Fiction Criticism: An Anthology of Essential Writings.* 1993;352-363.
58. Kurzweil R. *The singularity is near: when humans transcend biology.* Viking, 2005.
59. Frankish K, Ramsey WM. The Cambridge Handbook of Artificial Intelligence, <https://philpapers.org/rec/FRATCH-2> (2014, accessed 4 March 2019).
60. Keskinbora KH, Jameel MA. Nanotechnology Applications and Approaches in Medicine: A Review, *J Nanosci Nanotechnol Res.* 2018;2:6.



Efficacy of Topical Brinzolamide Treatment in Posterior Microphthalmos-Related Macular Cystoid Lesions: A Case Series

© Ceren Durmaz Engin*, © Umut Baran Ekinci**, © Alper Selver***, © Ali Osman Saatci****

*Karadeniz Ereğli State Hospital, Clinic of Ophthalmology, Zonguldak, Turkey

**Celal Bayar University Faculty of Engineering, Department of Electrical and Electronics Engineering, Manisa, Turkey

***Dokuz Eylül University Faculty of Engineering, Department of Electrical and Electronics Engineering, İzmir, Turkey

****Dokuz Eylül University Faculty of Medicine, Department of Ophthalmology, İzmir, Turkey

Abstract

The aim of this study was to report the outcome of topical brinzolamide 1% treatment on macular cystoid lesions resembling retinoschisis in 4 patients diagnosed with posterior microphthalmia. The medical records of 4 patients with a clinical diagnosis of posterior microphthalmia who had started topical brinzolamide 1% treatment were reviewed. Visual acuity, central foveal thickness, and cystoid lesion area percentage were used to evaluate treatment response. In the follow-up, there was a decrease in central foveal thicknesses and cystoid lesion area percentages in both eyes of 3 of the patients. However, 1 patient showed increases in both parameters. Visual acuity remained stable in 5 eyes and increased in 3 eyes. Topical brinzolamide treatment may have some positive effects on macular cystoid lesions in selected cases.

Keywords: Brinzolamide, macular cystoid lesion, retinoschisis, posterior microphthalmos

Introduction

Microphthalmos is an ocular developmental disorder characterized by an eye with a total axial length of more than two standard deviations smaller than normal for that age group. Posterior microphthalmos (PM) is a type of microphthalmos which is defined as hyperopia, a short axial length, posterior segment foreshortening and a normal-appearing anterior segment of normal or subnormal dimensions.^{1,2}

Retinal folds, macular schisis, cystoid lesions, reduced or absent foveal avascular zone, pseudopapilledema and uveal

effusion are prominent posterior segment changes in PM.^{2,3,4,5,6} Optical coherence tomography (OCT) scans of PM patients demonstrate that the neurosensory retina is folded, while the retinal pigment epithelium (RPE) layer and choroid are intact without folds.^{7,8} The growth of neurosensory retina occurs independently of other ocular tissues, while choroid and RPE development are regulated by thickened sclera; therefore, disproportionate growth between the neurosensory retina and surrounding outer tissues causes retinal folding.^{9,10} Macular schisis is thought to be caused by thickened sclera, which causes blockage of the trans-scleral outflow.^{11,12}

Address for Correspondence: Ceren Durmaz Engin MD, Karadeniz Ereğli State Hospital, Clinic of Ophthalmology, Zonguldak, Turkey
Phone:+90 534 685 84 22 E-mail: cerendurmaz@gmail.com **ORCID-ID:** orcid.org/0000-0001-5797-6467

Received: 24.06.2019 **Accepted:** 30.09.2019

Cite this article as: Durmaz Engin C, Ekinci UB, Selver A, Saatci AO. Efficacy of Topical Brinzolamide Treatment in Posterior Microphthalmos-Related Macular Cystoid Lesions: A Case Series. Turk J Ophthalmol. 2020;50:44-49

©Copyright 2020 by Turkish Ophthalmological Association
Turkish Journal of Ophthalmology, published by Galenos Publishing House.

Carbonic anhydrase inhibitors (CAIs) function by acidifying the subretinal space and increasing fluid transport across the RPE; therefore, CAIs have been used for the treatment of macular schisis in various causes.¹³ In this paper, we present 4 cases of PM and evaluate the efficacy of topical brinzolamide 1% treatment on the cystoid cavities resembling retinoschisis.

Case Report

A chart review was conducted on all patients in our clinic diagnosed with PM who were either being treated with or had previously been treated with topical brinzolamide 1% (Azopt™; Alcon Inc., Belgium) 3 times a day. Four patients (8 eyes) who had been on the treatment for at least 6 months between December 2016 to May 2018 at Dokuz Eylül University, Ophthalmology Clinic, İzmir were included in the study. This retrospective study adhered to the tenets of the Declaration of Helsinki, and informed consent was obtained from all participants. Diagnosis of PM was based on short axial length along with normal corneal diameter and anterior chamber depth. Short axial length was accepted to be between 12.30 mm and 20.36 mm, depending on age, in accordance with the literature.¹⁴

All patients had undergone a detailed ophthalmological examination, including visual acuity, cycloplegic refraction, corneal topography (Pentacam; Oculus, Wetzlar, Germany), spectral domain optical coherence tomography (SD-OCT)-fluorescein angiography (Spectralis; Heidelberg Engineering Ltd, Heidelberg, Germany), and ocular ultrasound (US) (Nidek Co., Japan). We compared the initial and final visual acuity (VA) with a Snellen chart. OCT images were captured in radial scan mode. Initial and final central foveal thickness (CFT) values of the horizontal section crossing over the same macular region in follow-up OCT scans were determined and compared.

In order to evaluate the drug’s effect on macular cystoid lesions more accurately, we calculated the cystoid lesion area (CLA), which was defined as any intraretinal hyporeflective space that was greater than 3x3 pixels. Smaller areas that were not correctly drawn or accurately defined on OCT scans were not included. The area extending from the vitreous-internal limiting membrane interface to the RPE was defined as total retina area (TRA). These areas were detected by hand and converted to gray-scale images. Calculations were made with MATLAB version R2016b, MathWorks, Inc. In accordance with the literature in which MATLAB software was used for segmentation of cyst in SD-OCT images, CLA percentage was calculated as CLA divided by TRA (CLA/TRA).^{15,16} All boundary determinations were assessed by two graders.

All of the patients were admitted to our clinic with a history of low vision. They were healthy according to their medical records and had unremarkable family histories. Due to the lack of family history and consanguineous marriage, we believed all of the cases were sporadic. The patients were questioned for potential adverse effects of the drug at each visit.

VA was stable in 5 eyes of 3 patients. In 3 eyes of 2 patients, VA was increased at the final visit. However, since the initial and final refractions of these patients were different, the effect of the treatment on the increase in VA could not be evaluated. Demographic information, initial cycloplegic refraction, baseline and final VA findings are shown in Table 1. SD-OCT and A and B Scan US results of the patients are summarized in Table 2.

CFT and CLA percentage were found to be decreased in 6 eyes of 3 patients, and increased in both eyes of 1 patient. Results and analyzed images are given in Figure 1, 2, 3 and 4 for patient 1, 2, 3 and 4, respectively. Color fundus photos, late phase of FFA, initial and final OCT scans, and the B-mode US results of Patient 1 are shown in Figure 5.

Table 1. Demographic information, visual acuity, and refractive status of the patients

Demographic & Refractive Information		Patient 1	Patient 2	Patient 3	Patient 4
Age		9	17	4	39
Gender		Female	Male	Female	Male
First VA	OD	20/200 (+17.50 D)	20/200 (6.00 D)	CF at 5 meters (+17.00 D)	10/200 (+14.00 D)
	OS	20/100 (+17.50 D)	20/63 (5.50 D)	CF at 5 meters (+16.50 D)	20/200 (+14.00 D)
Final VA	OD	20/200 (+17.50 D)	20/200 (6.00 D)	20/100 (+14.00 D)	10/200 (+14.00 D)
	OS	20/100 (+17.50 D)	20/50 (+4.25 (+2.00x95) D)	20/100 (+13.00 D)	20/200 (+14.00 D)
Cycloplegic Refraction	OD	+19.00 (+0.50x164) D	+6.50 (+0.75x74) D	+17.00 D	+14.00 (+0.50x156) D
	OS	+19.25 (+0.50x173) D	+4.25 (+2.00x95) D	+16.50 D	+14.25 (+0.50x47) D
Follow-up Time		6 months	10 months	11 months	8 months

VA: Visual acuity, CF: Counting fingers, D: Diopters

Retina examination		Patient 1	Patient 2	Patient 3	Patient 4
SD-OCT Morphology		Retinal folds affecting particularly neural retina, without involvement of the RPE-choroid band as well as cystoid lesions in both eyes	Macular cystoid lesions in both eyes	Retinal folds involving only layers anterior to the external limiting membrane and concomitant mild foveal cystoid lesions in both eyes	Retinal folds affecting neural retina, without involvement of the RPE-choroid band and macular cystoid lesions in both eyes
A Scan USG (AL, ACD, LT, VT)	OD	14.57 mm, 2.67 mm, 4.39 mm and 7.50 mm	20.69 mm, 3.72 mm, 3.57 mm and 13.40 mm	15.96 mm, 2.85 mm, 4.49 mm and 8.62 mm	17.00 mm, 3.52 mm, 4.21 mm and 9.27
	OS	14.70 mm, 2.74 mm, 4.40 mm and 7.56 mm	19.71 mm, 3.20 mm, 3.49 mm and 13.03 mm	15.87 mm, 2.84 mm, 4.58 mm and 8.45 mm	16.94 mm, 3.48 mm, 4.40 mm and 9.06
B Scan USG		Diffuse thickening of the choroid and sclera with foreshortening of the globe bilaterally	Diffuse thickening of the choroid and sclera bilaterally	Shallow posterior segment bilaterally	Diffuse thickening of the choroid and sclera bilaterally

SD-OCT: Spectral domain optical coherence tomography, USG: Ultrasound, AL: Axial length, LT: Lens thickness, ACD: Anterior chamber depth, VT: Vitreus thickness, RPE: Retina pigment epithelium

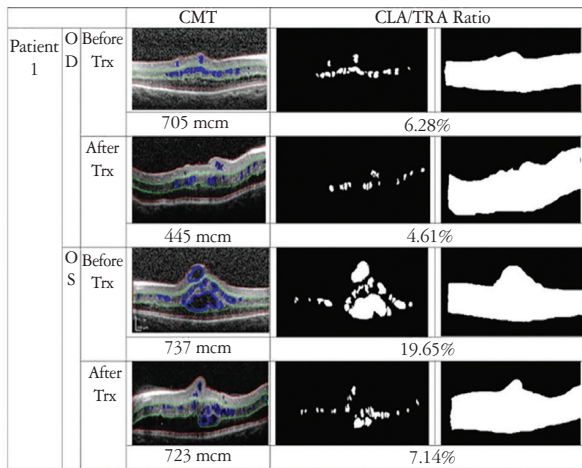


Figure 1. OCT image with manual segmentation lines, cystoid lesion area (CLA) and total retina area (TRA) images of the right and left eyes of patient 1 before and after treatment. Central foveal thickness (CFT) and CLA/TRA values are given with corresponding images

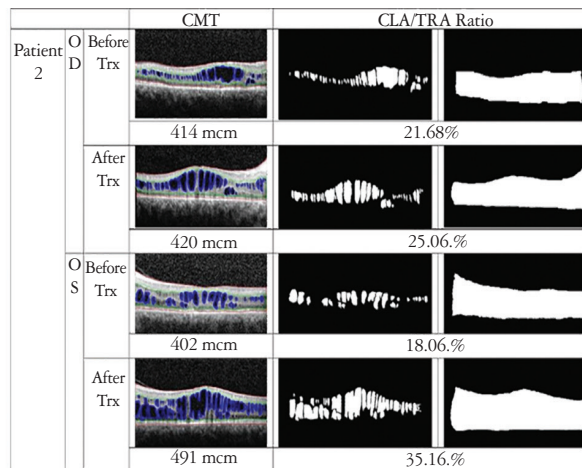


Figure 2. OCT image with manual segmentation lines, cystoid lesion area (CLA) and total retina area (TRA) images of the right and left eyes of patient 2 before and after treatment. Central foveal thickness (CFT) and CLA/TRA values are given with corresponding images

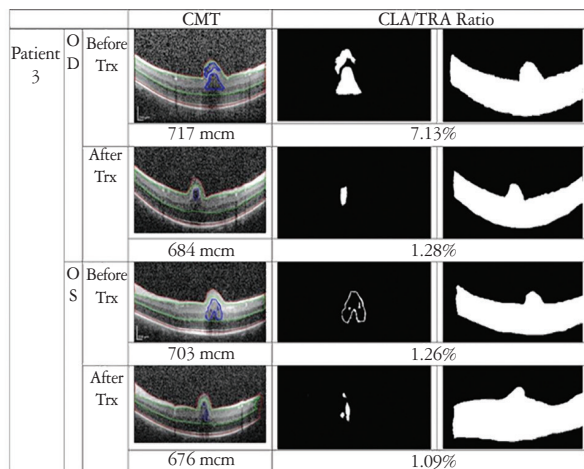


Figure 3. OCT image with manual segmentation lines, cystoid lesion area (CLA) and total retina area (TRA) images of the right and left eyes of patient 3 before and after treatment. Central foveal thickness (CFT) and CLA/TRA values are given with corresponding images

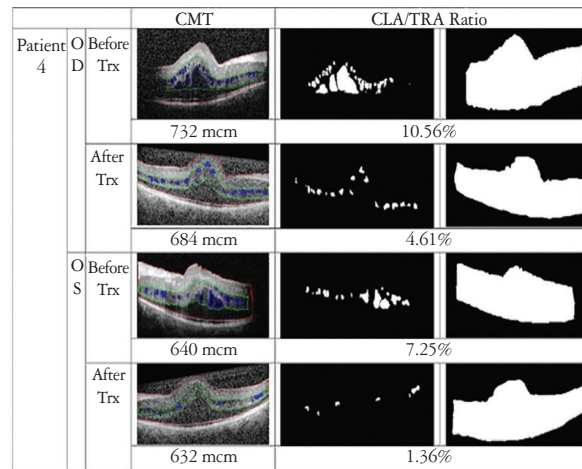


Figure 4. OCT image with manual segmentation lines, cystoid lesion area (CLA) and total retina area (TRA) images of the right and left eyes of patient 4 before and after treatment. Central foveal thickness (CFT) and CLA/TRA values are given with corresponding images

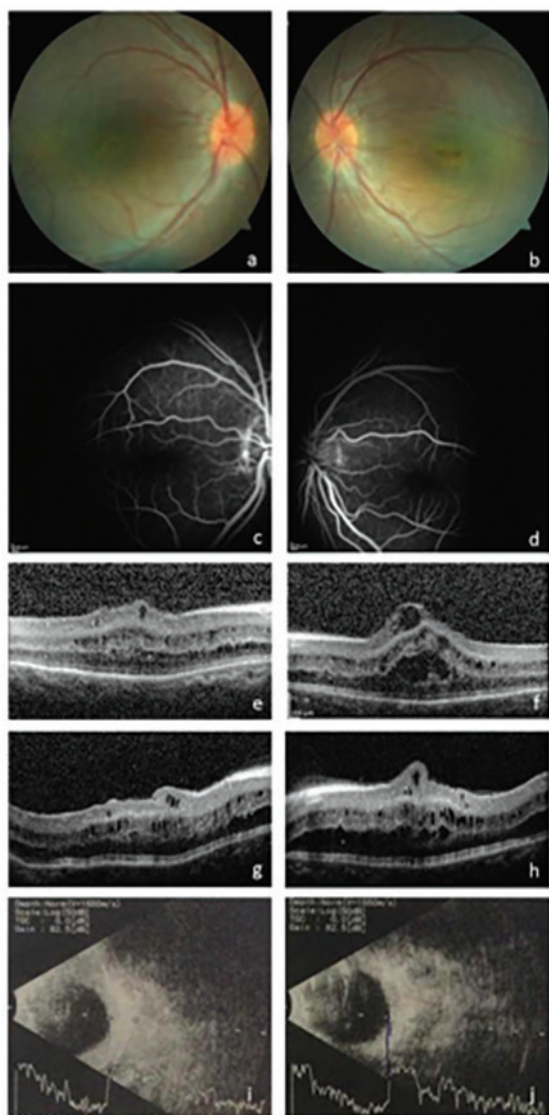


Figure 5. Color fundus photo: mild retinal pigmentary changes and horizontal papillomacular folds bilaterally (a, b). Fundus fluorescein angiography: no vascular pathology or cystoid macular edema in both eyes (c, d). Spectral domain optical coherence tomography: retinal folds affecting the neural retina in particular, without involvement of the RPE-choroid band and macular cystoid lesions resembling schisis bilaterally before treatment (e, f) and reduction in cystoid lesion area after treatment (g, h) B-scan ultrasound: diffuse thickening of the choroid and sclera with foreshortening of the globe in both eyes (i, j)

Discussion

The carbonic anhydrase (CA) is a group of enzymes found extensively throughout the body. Although CA isoenzymes are diverse, the body's most common subtype is the intracellular CA isoenzyme II. In the retina, CA II is found in the cytoplasm of red/green cones and inside the Müller cells especially.¹⁷ However, the RPE appears to contain the membrane-bound isoenzyme IV, which regulates the extracellular pH gradient created via the metabolic activity of cells and also acts as a bicarbonate channel.¹⁸

CAIs have been proven to increase retinal adhesiveness, enhance the activity of fluid transporter on the RPE cell membrane and change subretinal acidity.¹³ The use of CAIs for retinal diseases is not uncommon. Initial investigations were conducted by Cox et al.¹⁹ in which 41 patients with cystoid macular edema (CME) of various causes were given oral acetazolamide. The drug was effective in more than half of the patients with uveitis or hereditary outer retinal diseases, but in none with retinal vascular disorders. According to the authors, acetazolamide increased the rate of fluorescein disappearance and fluid transport from vitreous by acting via CA-IV receptors on RPE cells.¹⁹ A topical CAI for a retinal disease was first used in chronic CME of retinitis pigmentosa (RP) patients and provided partial improvement in visual function.²⁰ In 2006, Apushkin et al.²¹ were first to investigate the effect of a topical CAI, in particular dorzolamide 2%, on schisis and cystic macular cavities in X-linked retinoschisis (XLRS). The authors reported more than 7 letters gain in VA within 2 months in nearly half of cases.

Foveoschisis is one of the most common causes of pseudo-CME. Unlike CME, there is no leakage in late phases of FFA in foveoschisis.²² The differential diagnosis of foveoschisis includes retinal dystrophies like XLRS, Goldmann-Favre syndrome, enhanced S-cone syndrome, and RP; high myopia; microphthalmia-nanophthalmia; and age-related retinoschisis. The cause of schisis and retinal cysts in hereditary dystrophies is thought to be associated with gene mutations (e.g., in *RS1*, *NR2E3*) causing defective protein synthesis. These proteins cause abnormal RPE and PR cell formation and ineffective cellular adhesion, and therefore splitting of the fovea. In PM, however, macular schisis is thought to arise from thickened sclera that causes impermeability of the trans-scleral outflow. Consequent congestion of the retina may result in cystic degeneration by overwhelming Müller cell function, which provides physiologic and architectural support.^{11,12} To the best of our knowledge, our study is first to evaluate the effect of a CAI for PM.

We investigated both the anatomical and functional outcomes of topical brinzolamide treatment. We observed a decrease in CLA percentage in both eyes of 3 patients. However, in both eyes of 1 patient, this ratio was increased. We observed that CLA percentage of this patient was higher than the other patients and cystoid macular degeneration was prominent in his OCT sections. In accordance with the literature, we hypothesized that the drug might have a greater benefit on patients with more preserved retinal anatomy. In patients with healthier RPE and Müller cells, the response to the drug will be better and the cysts can shrink more rapidly.²¹

VA remained stable in 5 eyes and increased in 3 eyes. Reduction in CLA and CFT were not correlated with change in VA except for patient 3. Previous studies in XLRS and RP reported that reduction of CFT was not correlated with improvement in VA.^{11,23}

The ages of our cases ranged from 4 to 39 years, and this difference should be considered in terms of drug efficacy and safety. In their study, Khandhadia et al.²⁴ examined 4 patients diagnosed with XLRS, 3 of whom were children, and attributed

the fact that the only patient who showed continuous clinical improvement with a topical CAI was the adult patient due to his potential high drug compliance. Topical brinzolamide has been reported to be effective when given twice daily in congenital glaucoma cases under 6 years of age and no serious adverse effects have been reported.²⁵ Yang et al.²⁶ reported that topical brinzolamide used 3 times daily was effective and safe in 4 patients aged 4 to 10 years with the diagnosis of XLRS. However, there is no comparative study between adult and pediatric age group in terms of side effect profile and posology of topical brinzolamide in the literature.

Due to potential requirement for long-term treatment, the use of oral acetazolamide may be limited by potential systemic side effects and a topical drug may be preferred. We used brinzolamide due to its better side effect profile.^{27,28} Karatas et al.²⁹ found partial improvement in VA and relative stabilization in CFT in 8 XLRS patients with brinzolamide treatment. In their XLRS case series, Yang et al.²⁶ achieved a favorable outcome with topical brinzolamide in the reduction of macular cysts, with no reported adverse drug effects. None of our patients reported any unfavorable side effects.

Conclusion

Considering the efficacy of topical brinzolamide in the treatment of macular cysts and schisis in XLRS and RP, we have tried to find a cure with brinzolamide in macular cystoid lesions resembling macular schisis of PM in which no treatment is available so far. We observed that topical brinzolamide 1% treatment caused partial reduction in cystoid lesions' area in PM patients. Prospective studies with longer follow-up period and higher number of patients are needed for evaluating the long-term efficacy.

Ethics

Informed Consent: Informed consent was obtained from all patients

Peer-review: Externally peer-reviewed.

Authorship Contributions

Surgical and Medical Practices: C.D.E., A.O.S., Concept: A.O.S., Design: C.D.E., A.O.S., Data Collection or Processing: C.D.E., Analysis or Interpretation: C.D.E., U.B.E., A.S., Literature Search: C.D.E., Writing: C.D.E.

Conflict of Interest: No conflict of interest was declared by the authors.

Financial Disclosure: The authors declared that this study received no financial support.

References

- Bardakjian T, Schneider A, Weiss A. Microphthalmia/Anophthalmia/Coloboma Spectrum. In: Adam MP, Ardinger HH, Pagon RA, Wallace SE, Bean LJH, Stephens K, Amemiya A, editors. GeneReviews. Seattle: University of Washington; 2007.
- Spitznas M, Gerke E, Bateman VB. Hereditary posterior microphthalmos with papillomacular fold and high hyperopia. *Arch Ophthalmol.* 1983;101:413-417.
- Khairallah M, Messaoud R, Zaouali S, Yahia SB, Ladjimi A, Jenzri S. Posterior segment changes associated with posterior microphthalmos. *Ophthalmology.* 2002;109:569-574.
- Alkin Z, Ozkaya A, Karakucuk Y, Demirok A. Detailed ophthalmologic evaluation of posterior microphthalmos. *Middle East Afr J Ophthalmol.* 2014;21:186-188.
- Nguyen AT, Johnson MA, Hutcheson KA. Good visual function in posterior microphthalmos. *J AAPOS.* 2000;4:240-242.
- Tekin K, Teke MY, Citirik M. Clinical appraisal and retinal imaging in posterior microphthalmos. *Semin Ophthalmol.* 2018;33:412-418.
- Kim JW, Boes DA, Kinyoun JL. Optical coherence tomography of bilateral posterior microphthalmos with papillomacular fold and novel features of retinoschisis and dialysis. *Am J Ophthalmol.* 2004;138:480-481.
- Aras C, Ozdamar A, Ustundag C, Ozkan S. Optical coherence tomographic features of papillomacular fold in posterior microphthalmos. *Retina.* 2005;25:665-667.
- Warburg M. Classification of microphthalmos and coloboma. *J Med Genet.* 1993;30:664-669.
- Wright, Kenneth W, Spiegel PH. *Pediatric Ophthalmology and Strabismus.* 2nd ed. New York: Springer-Verlag. 2013:12-13.
- Park SH, Ahn YJ, Shin SY, Lee YC. Clinical features of posterior microphthalmos associated with papillomacular fold and high hyperopia. *Clin Exp Optom.* 2016;99:590-593.
- Dhrami-Gavazi E, Schiff WM, Barile GR. Nanophthalmos and acquired retinoschisis. *Am J Ophthalmol.* 2009;147:108-110.
- Wolfensberger TJ. The role of carbonic anhydrase inhibitors in the management of macular edema. *Doc Ophthalmol.* 1999;97:387-397.
- Nowilaty SR, Khan AO, Aldahmesh MA, Tabbara KF, Al-Amri A, Alkuraya FS. Biometric and molecular characterization of clinically diagnosed posterior microphthalmos. *Am J Ophthalmol.* 2013;155:361-372.e7.
- Wilkins GR, Houghton OM, Oldenburg AL. Automated segmentation of intraretinal cystoid fluid in optical coherence tomography. *IEEE Trans Biomed Eng.* 2012;59:1109-1114.
- Slokum N, Ghorbel I, Zghal I, Belgacem R, Trabelsi H. Contribution to intra-retinal fluid segmentation in optical coherence tomography by using automatic personalized thresholding. *J Clin Exp Ophthalmol.* 2018;9:738.
- Wistrand PJ, Schenholm M, Lonnerholm G. Carbonic anhydrase isoenzymes CA I and CA II in the human eye. *Invest Ophthalmol Vis Sci.* 1986;27:419-428.
- Wolfensberger TJ, Mahieu I, Jarvis-Evans J, Boulton M, Carter ND, Nogradi A, Hollande E, Bird AC. Membrane-bound carbonic anhydrase in human retinal pigment epithelium. *Invest Ophthalmol Vis Sci.* 1994;35:3401-3407.
- Cox SN, Hay E, Bird AC. Treatment of chronic macular edema with acetazolamide. *Arch Ophthalmol.* 1988;106:1190-1195.
- Grover S, Fishman GA, Fiscella RG, Adelman AE. Efficacy of dorzolamide hydrochloride in the management of chronic cystoid macular edema in patients with retinitis pigmentosa. *Retina.* 1997;17:222-231.
- Apushkin MA, Fishman GA. Use of dorzolamide for patients with X-linked retinoschisis. *Retina.* 2006;26:741-745.
- Molday RS, Kellner U, Weber BHF. X-linked juvenile retinoschisis: clinical diagnosis, genetic analysis, and molecular mechanisms. *Prog Retin Eye Res.* 2012;31:195-212.
- Huang Q, Chen R, Lin X, Xiang Z. Efficacy of carbonic anhydrase inhibitors in management of cystoid macular edema in retinitis pigmentosa: A meta-analysis. *PLoS One.* 2017;12:e0186180.
- Khandhadia S, Trump D, Menon G, Lotery AJ. X-linked retinoschisis maculopathy treated with topical dorzolamide, and relationship to genotype. *Eye (Lond).* 2011;25:922-928.
- Whitson JT, Roarty JD, Vijaya L, Robin AL, Gross RD, Landry TA, Dickerson JE, Scheib SA, Scott H, Hua SY, Woodside AM, Bergamini MV; Brinzolamide Pediatric Study Group. Efficacy of brinzolamide and levobetaxolol in pediatric glaucomas: a randomized clinical trial. *J AAPOS.* 2008;12:239-246.e3.

26. Yang FP, Willyasti K, Leo SW. Topical brinzolamide for foveal schisis in juvenile retinoschisis. *J AAPOS*. 2013;17:225-227.
27. Silver LH. Ocular comfort of brinzolamide 1.0% ophthalmic suspension compared with dorzolamide 2.0% ophthalmic solution: Results from two multicenter comfort studies. Brinzolamide Comfort Study Group. *Surv Ophthalmol*. 2000;44:141-145.
28. Stewart WC, Day DG, Stewart JA, Holmes KT, Jenkins JN. Short-term ocular tolerability of dorzolamide 2% and brinzolamide 1% vs placebo in primary open-angle glaucoma and ocular hypertension subjects. *Eye (Lond)*. 2004;18:905-910.
29. Karataş E, Ayhan Z, Yaman A, Saatci AO. X'e baęlı juvenil retinoskizisde topikal brinzolamid tedavisi sonuçlarımız. *Ret-Vitr*. 2019;28:32-36.



Sarcoid-like Granulomatous Intraocular Inflammation Caused by Vemurafenib Treatment for Metastatic Melanoma

© Hilal Eser Öztürk, © Yüksel Süllü

Ondokuz Mayıs University Faculty of Medicine, Department of Ophthalmology, Samsun, Turkey

Abstract

Vemurafenib is a potent inhibitor of genetically activated BRAF, which is responsible for tumoral proliferation in cutaneous melanoma. A 56-year-old man receiving vemurafenib therapy presented with uveitis. Over the course of the disease, he developed bilateral, granulomatous uveitis with multiple peripheral chorioretinal lesions. Serum angiotensin-converting enzyme levels increased. The patient was diagnosed with probable ocular sarcoidosis related to vemurafenib and was treated with an intravitreal dexamethasone implant. This case is the first report that shows the clinical and angiographic features of a patient with vemurafenib-related sarcoid-like granulomatous uveitis.

Keywords: Melanoma, BRAF, vemurafenib, uveitis, sarcoidosis

Introduction

Vemurafenib is a potent inhibitor of the BRAF-mitogen-activated protein kinase/extracellular signal-regulated kinase pathway. BRAF mutation is present in almost half of melanoma patients and is responsible for tumoral proliferation in the absence of growth factors. Vemurafenib has been used for the treatment of BRAF mutation-positive late stage (Stage III-C and Stage IV) melanoma since 2011.^{1,2} Vemurafenib-related uveitis has been reported in phase I, II, and III clinical trials, case reports, and case series in the literature.³⁻⁷ In addition to this, there is an article in the literature that reported 5 patients with sarcoidosis related to vemurafenib therapy for metastatic melanoma.⁸ Sarcoidosis is a multisystem granulomatous disease of unknown etiology. Genetically susceptible individuals may

develop an exaggerated immune response to unknown antigens including tumor cells or drugs.⁹ Vemurafenib may stimulate the immune system and then induce sarcoidosis in some patients.

We present here the clinical and angiographic features of a patient with sarcoid-like granulomatous intraocular inflammation which was induced by vemurafenib therapy for metastatic melanoma.

Case Report

A 56-year-old man with a history of cutaneous melanoma presented with new-onset conjunctival hyperemia and blurred vision in both eyes. The best-corrected visual acuity was 20/30 and intraocular pressure was 10 mmHg in both eyes. Biomicroscopic evaluation revealed fine keratic precipitates, 4+ cells in the anterior chamber and pupillary membrane

Address for Correspondence: Hilal Eser Öztürk MD, Ondokuz Mayıs University Faculty of Medicine, Department of Ophthalmology, Samsun, Turkey
Phone:+90 532 573 70 25 E-mail: hilaleser@yahoo.com **ORCID-ID:** orcid.org/0000-0002-0050-7894

Received: 25.06.2019 **Accepted:** 03.12.2019

Cite this article as: Eser Öztürk H, Süllü Y. Sarcoid-like Granulomatous Intraocular Inflammation Caused by Vemurafenib Treatment for Metastatic Melanoma. Turk J Ophthalmol. 2020;50:50-52

in both eyes. Fundus examination showed normal findings bilaterally. Staining of the optic disc was detected on fluorescein angiography (FA).

The patient had been under treatment with vemurafenib 960 mg twice a day for 9 months. Laboratory workup including complete blood count, biochemistry, urine test, and chest X-ray was within normal limits. Serologic tests for infectious diseases including syphilis were negative. Vemurafenib was considered the cause of the uveitis. The oncologist was informed of the situation. However, discontinuation of therapy was not considered because of the life-threatening feature of the disease. Topical corticosteroid and cycloplegic treatment were initiated. During the first week of follow-up, fundus examination revealed multiple peripheral yellow-white lesions that mostly disappeared within 3 weeks (Figure 1).

After 2 months, the patient presented to the clinic because of uveitis recurrence, which had a granulomatous appearance. The patient complained about floaters. His visual acuity was 20/25 in both eyes. Vitreous cells and snowballs were accompanied by a few atrophic chorioretinal lesions. Tuberculin skin test and interferon gamma release assay were negative. Chest computerized tomography was unremarkable. However, serum angiotensin converting enzyme (ACE) level was elevated to 90 U/L (reference range=9-67).

FA showed bilateral staining of the optic disc and vascular leakage. Indocyanine green angiography revealed sporadic peripheral hypo fluorescent lesions that appeared mid-phase and disappeared in the late phase (Figure 2). With these clinical, angiographic, and laboratory results, the patient was diagnosed as having probable ocular sarcoidosis and was treated with

intravitreal dexamethasone implant. Intraocular inflammation resolved in a month and has not recurred in 6 months of follow-up. The patient's visual acuity was 20/25 in both eyes at the final visit. Control FA revealed only late staining of the optic disc bilaterally.

Discussion

The introduction of vemurafenib and other BRAF inhibitors has been a great improvement in the treatment of advanced cutaneous melanoma. However, they have adverse effects including cutaneous symptoms, arthralgia, nausea, diarrhea, headache, and neutropenia.¹ Ocular adverse events including uveitis, conjunctivitis, dry eye, episcleritis, and keratitis were also reported with vemurafenib therapy. Uveitis was the most common ocular side effect of vemurafenib in clinical trials.³

Lheure et al.⁸ suggested that vemurafenib may induce sarcoidosis or sarcoid-like reactions by increasing serum levels

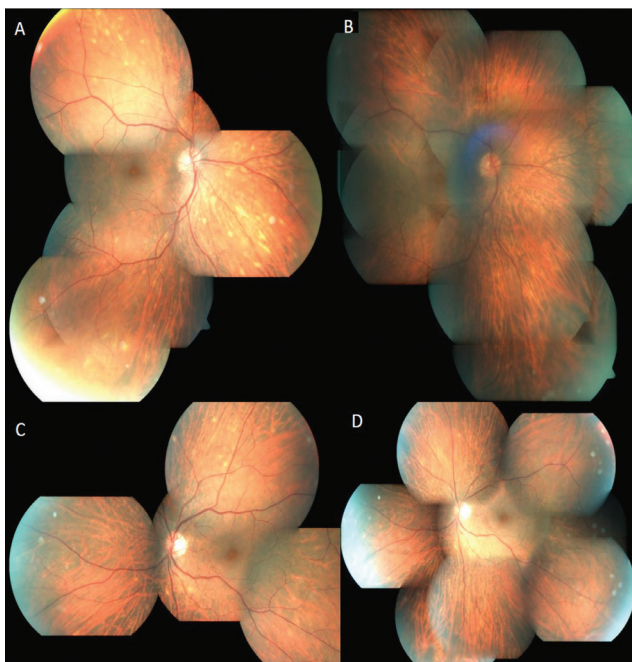


Figure 1. Color fundus photographs show multiple peripheral chorioretinal lesions in the right eye (A, B) and the left eye (C, D), which mostly disappeared within 3 weeks

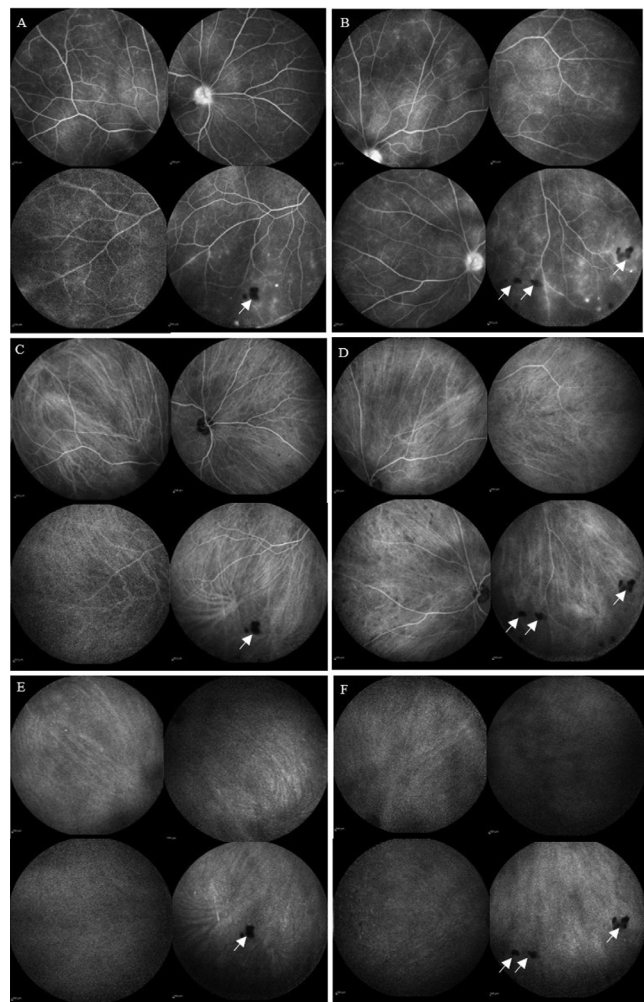


Figure 2. Late-phase fluorescein angiography reveals bilateral staining of the optic disc and vascular leakage in the right eye (A) and left eye (B). Sporadic peripheral hypo fluorescent lesions were seen in mid-phase of indocyanine green angiography in the right eye (C) and left eye (D). These lesions disappeared in the late phase in both eyes (E, F). The arrows indicate snowballs

of tumor necrosis factor- α and interferon- γ , which induce granuloma formation. They reported 5 patients diagnosed with vemurafenib-related sarcoidosis. Two of the patients had intraocular inflammation. One of them met the criteria for systemic sarcoidosis and the other had Heerfordt syndrome that had been in remission for 15 years and presented with a relapse.⁸ Even though sarcoidosis was not a definitive diagnosis in our patient, bilateral involvement, granulomatous appearance, presence of snowballs, multiple peripheral chorioretinal lesions, negative tuberculin test, and increased serum ACE levels supported probable ocular sarcoidosis according to the international criteria for the diagnosis of ocular sarcoidosis.¹⁰

Ocular inflammation can usually be controlled by topical, local, and/or systemic corticosteroid therapy in this group of patients. However, treatment guidelines have not been established and management of these patients demands close cooperation with oncologists. Temporary discontinuation of vemurafenib may be suggested to control uveitis. However, some patients need to continue taking the medicine due to the life-threatening nature of the primary disease.³ In our case, we cooperated with the patient's oncologist and decided to treat the patient with local steroids.

Lheure et al.⁸ argued that patients who develop sarcoidosis have a better prognosis with vemurafenib therapy than others. They explained this situation by saying that the activation of the immune system by cytokines may induce both sarcoidal reaction and antitumor response. In our case, cutaneous melanoma has been controlled successfully for 3 years with vemurafenib therapy.

This case is the first report that shows clinical and angiographic features of a patient with vemurafenib-related sarcoid-like granulomatous uveitis and highlights that ocular sarcoidosis should be considered in patients with vemurafenib-related uveitis.

Ethics

Informed Consent: Informed consent was obtained.

Peer-review: Externally and internally peer reviewed.

Authorship Contributions

Surgical and Medical Practices: H.E.Ö., Y.S.,
Concept: H.E.Ö., Y.S., Design: H.E.Ö., Y.S., Data Collection

or Processing: H.E.Ö., Analysis or Interpretation: H.E.Ö., Y.S.,
Literature Search: H.E.Ö., Writing: H.E.Ö., Y.S.

Conflict of Interest: No conflict of interest was declared by the authors.

Financial Disclosure: The authors declared that this study received no financial support.

References

1. Chapman PB, Hauschild A, Robert C, Haanen JB, Ascierto P, Larkin J, Dummer R, Garbe C, Testori A, Maio M, Hogg D, Lorigan P, Lebbe C, Jouary T, Schadendorf D, Ribas A, O'Day SJ, Sosman JA, Kirkwood JM, Eggermont AM, Dreno B, Nolop K, Li J, Nelson B, Hou J, Lee RJ, Flaherty KT, McArthur GA; BRIM-3 Study Group. Improved survival with vemurafenib in melanoma with BRAF V600E mutation. *N Engl J Med.* 2011;364:2507-2516.
2. Sosman JA, Kim KB, Schuchter L, Gonzalez R, Pavlick AC, Weber JS, McArthur GA, Hutson TE, Moschos SJ, Flaherty KT, Hersey P, Kefford R, Lawrence D, Puzanov I, Lewis KD, Amaravadi RK, Chmielowski B, Lawrence HJ, Shyr Y, Ye F, Li J, Nolop KB, Lee RJ, Joe AK, Ribas A. Survival in BRAF V600-mutant advanced melanoma treated with vemurafenib. *N Engl J Med.* 2012;366:707-714.
3. Choe CH, McArthur GA, Caro I, Kempen JH, Amaravadi RK. Ocular toxicity in BRAF mutant cutaneous melanoma patients treated with vemurafenib. *Am J Ophthalmol.* 2014;158:831-837.
4. Wolf SE, Meenen C, Moll AC, Haanen JB, van der Heijden MS. Severe panuveitis in a patient treated with vemurafenib for metastatic melanoma. *BMC Cancer.* 2013;13:561.
5. Guedj M, Queant A, Funck-Brentano E, Kramkimel N, Lellouch J, Monnet D, Longvert C, Gantzer A and Brezin AP. Uveitis in patients with late-stage cutaneous melanoma treated with vemurafenib. *JAMA ophthalmology.* 2014;132:1421-1425.
6. Agemy SA, Mehta AN, Pachydaki SI, Tewari A. Bilateral panuveitis in a patient on vemurafenib BRAF inhibitor therapy for stage IV melanoma. *Eur J Ophthalmol.* 2014;24:629-632.
7. Sızmaz S, Görkemli N, Esen E, Demircan N. A rare cause of uveitis: Vemurafenib. *Turk J Ophthalmol.* 2018;48:323-325.
8. Lheure C, Kramkimel N, Franck N, Laurent-Roussel S, Carlotti A, Queant A, Goldwasser F, Avril MF, Dupin N. Sarcoidosis in Patients Treated with Vemurafenib for Metastatic Melanoma: A Paradoxical Autoimmune Activation. *Dermatology.* 2015; 231:378-384.
9. Valeyre D, Prasse A, Nunes H, Uzunhan Y, Brillet PY, Müller-Quernheim J. Sarcoidosis. *Lancet.* 2014;383:1155-1167.
10. Herborn CP, Rao NA, Mochizuki M; members of Scientific Committee of First International Workshop on Ocular Sarcoidosis. International criteria for the diagnosis of ocular sarcoidosis: results of the first International Workshop On Ocular Sarcoidosis (IWOS). *Ocul Immunol Inflamm.* 2009;17:160-169.



Extranodal Ocular Adnexal Marginal Zone Lymphoma in a Ten-Year-Old Child

✉ Nazan Çetingül*, ✉ Melis Palamar**, ✉ Şükriye Hacıkara*, ✉ Serra Kamer***, ✉ Hamiyet Hekimci Özdemir*, ✉ Eda Ataseven*, ✉ Özlem Barut Selver**, ✉ Mine Hekimgil****

*Ege University Faculty of Medicine, Department of Child Diseases, İzmir, Turkey

**Ege University Faculty of Medicine, Department of Ophthalmology, İzmir, Turkey

***Ege University Faculty of Medicine, Department of Radiation Oncology, İzmir, Turkey

****Ege University Faculty of Medicine, Department of Pathology, İzmir, Turkey

Abstract

A 10-year-old girl was brought to the clinic with the complaint of a salmon-colored conjunctival lesion for 1 month. With the aid of histopathological evaluation and other tests, extranodal ocular adnexal marginal zone lymphoma was diagnosed. The patient was graded as T1bN0M0 according to AJCC and Stage 1 according to Ann Arbor classification. She was treated with external radiotherapy at 1.8 Gy/day for 17 days for a total dose of 36 Gy. She is in remission for 26 months and still being followed up.

Keywords: Conjunctiva, eye, lymphoma, marginal zone, ocular adnexal lymphoma

Introduction

Lymphomas in the ocular adnexa predominantly result from B-cell proliferation and can arise from the conjunctiva, eyelids, lacrimal glands, and orbit. The most common type of ocular adnexal lymphoma (OAL) is extranodal marginal zone B-cell lymphoma (MZL), which is an extremely rare subtype of non-Hodgkin lymphoma (NHL) in childhood.^{1,2} Although most NHL in children show aggressive behavior, this rare type tends to be indolent. There are few reported cases of primary ocular adnexal MZL in children.³ OALs have recently been classified according to the American Joint Committee on Cancer (AJCC) staging system with variable prognoses.⁴

Some infectious agents, immunodeficiency, autoimmunity, genetic mutations and immunosuppression have been linked

to MZL and appear to be integral to the etiopathology.⁵ Retrospective studies documented the use of various treatment modalities such as local surgery alone, local radiotherapy alone, and several chemotherapy, targeted therapy, immunotherapy, or antimicrobial therapies in adult patients. Although local radiation may provide local control in adults, there is no well-established treatment modality for pediatric patients.⁶

Case Report

A 10-year-old girl presented to the ophthalmology department with a fast-growing salmon-colored mass protruding from the medial aspect of the right lower eyelid for approximately 1 month (Figure 1A). The orbital lesion was also demonstrated on magnetic resonance imaging (MRI) (Figure 1B) and excisional

Address for Correspondence: Melis Palamar MD, Ege University Faculty of Medicine, Department of Ophthalmology, İzmir, Turkey
Phone: +90 232 390 37 88 E-mail: melispalamar@hotmail.com **ORCID-ID:** orcid.org/0000-0002-2494-0131

Received: 04.07.2019 **Accepted:** 03.12.2019

Cite this article as: Çetingül N, Palamar M, Hacıkara Ş, Kamer S, Özdemir HH, Ataseven E, Barut Selver Ö, Hekimgil M. Extranodal Ocular Adnexal Marginal Zone Lymphoma in a Ten-Year-Old Child. Turk J Ophthalmol. 2020;50:53-55

biopsy of the mass was performed. Histopathological examination revealed B-cell MZL (Figure 2 A, B, C, D, E, F).

Upon diagnosis, the patient was referred to the pediatric oncology department. On physical examination, lymphadenopathy and hepatosplenomegaly were not detected. The metastatic workup including hemogram, biochemistry tests, immunoglobulins, brain MRI, cerebrospinal fluid cytology, and bone marrow study were within normal limits. Autoantibody tests were negative. *Helicobacter pylori*, *Chlamydia psittaci*, and *Chlamydia trachomatis* antibodies were negative. Conjunctival smear was unremarkable. The patient did not have any history of conjunctivitis or exposure to birds. Apart from the lesion in the right eye, no other pathological involvement was detected in PET-CT. The patient was graded as T1bN0M0 according to AJCC and as Stage 1 according to Ann Arbor staging.

As repeated ophthalmological examinations revealed bilateral suspicious follicular reaction, *Chlamydia* was assumed and antimicrobial treatment (doxycycline, 200 mg/day) was initiated. After 2 weeks of treatment, progression of the tumor was observed, and external radiotherapy was planned immediately. The prescribed dose was 36 Gy in 17 fractions to the isocenter (1.8 Gy/fraction dose) using 6 MeV electrons. Cerrobend block was created to protect the lens. Radiotherapy resulted in rapid remission. The child is currently in remission

for 26 months. The patient's mother consented to all treatments and publication of this article.

Discussion

Pediatric B-cell MZLs are detected in the marginal zone of secondary lymphoid tissues. These lymphomas can occur in lymph organs/nodes (nodal MZL) (15%), spleen (15%), and in nonlymphoid organs such as conjunctiva, lung, skin, stomach, orbit, and dura (extranodal MZL) (70%).^{1,2,5} Pediatric extranodal MZL is an extremely rare entity, comprising less than 1% of all pediatric lymphomas.^{1,2,5}

Extranodal MZLs that occur in the periocular region are termed as OAL and often involve several tissues such as conjunctiva, orbit, and eyelid. The incidence of OAL is approximately 0.2 per 100,000 individuals. Most OALs are B-cell NHL belonging to 1 of 5 subtypes: extranodal marginal zone/mucosa-associated lymphoid tissue (MALT) lymphoma, follicular lymphoma, diffuse large B-cell lymphoma, mantle cell lymphoma, and lymphoplasmacytic lymphoma.⁷ Extranodal MZL/MALT lymphomas are approximately 80% low grade and typically follow an indolent course.

MZL is a relatively common entity in adults (5-17% of all NHL diagnoses). The median age at MALT/MZL diagnosis is approximately 60 years, and few pediatric cases have been reported.^{2,7} Some chronic infectious agents (*H. pylori* in gastric extranodal MZL, *Chlamydia* spp. in ocular adnexal MZL, etc.), immunodeficiency, autoimmunity (Sjögren's syndrome, Hashimoto's thyroiditis, and other autoimmune diseases), genetic mutations, and immunosuppression have been reported to be linked to MZL.⁷ Chronic inflammation at the affected site certainly plays a major role, with both exogenous and endogenous antigens being potentially responsible for the activation of inflammatory responses in ocular adnexal MZL patients.⁵ In the present 10-year old patient, *H. pylori*, *Ch. psittaci*, and *Ch. trachomatis* antibodies and all autoimmune tests were negative and conjunctival smear was unremarkable.

Morphologically, extranodal MZL resembles the adult counterparts, and the differential diagnosis includes reactive marginal zone hyperplasia and pediatric follicular lymphoma. These blastic cells from the diagnostic lymphoepithelial lesions are helpful in the morphologic distinction of this lymphoma from reactive lymphoid hyperplasia associated with chronic inflammation such as chronic conjunctivitis. The blastic cells express the common B cell markers such as CD20.⁸ The present case presented dense small lymphocytic infiltrate with destruction of normal architecture, forming follicular colonization. Immunophenotypically, the neoplastic cells were positive for CD20, BCL2, CD23, and CD43, but negative for CD5, CD10, CD23, BCL6, and cyclin D1. The diagnosis was confirmed by the BCL2 and CD43 expression of neoplastic small lymphocytes, which may further be confirmed by the demonstration of monotypic expression of light chains on the plasma cell component by immunohistochemistry or in-situ hybridization. Unfortunately, the plasma cells were scarce in

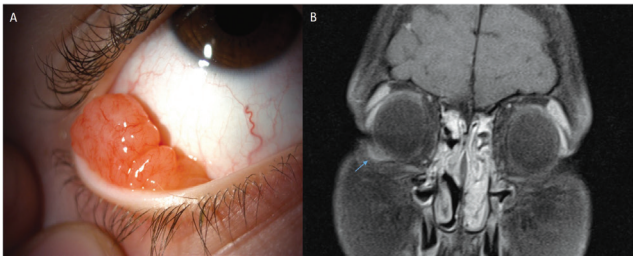


Figure 1. A) The salmon-colored lesion at the inferotemporal conjunctiva. B) The mass lesion on the right inferolateral region on T1 fat-suppressed MRI (arrow)

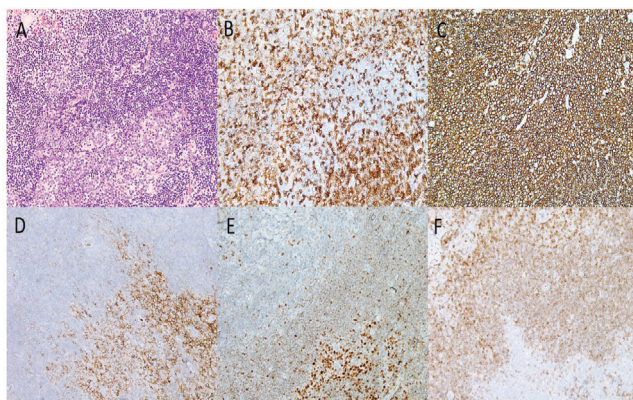


Figure 2. A) Neoplastic small lymphoid cell infiltration and follicular colonization (residual germinal center on the right lower field) (H&E, x20). B) CD3 was expressed on the rare nonneoplastic T lymphocyte population. C) CD20 positivity of neoplastic B lymphocytes. D, E.) CD10 and Bcl-6 positivity of residual germinal center cells. F) Bcl-2 negativity of residual germinal center cells and positivity of neoplastic B lymphocytes (B-F- DAB, x20)

our case, and showed polytypical expression of both the light and heavy chains by immunohistochemistry. Monoclonal IgH rearrangement might be demonstrated by PCR to further confirm the clonal nature of the infiltration, which was not performed in our case due to the small amount of tissue left. Bilateral bone marrow biopsies and aspirates did not reveal any neoplastic infiltration. As no other pathological involvement was detected on PET-CT, the patient was diagnosed as T1bN0M0 according to AJCC and Stage 1 according to Ann Arbor classification.

Primary localized ocular adnexal MZLs are malignancies that show indolent behavior, usually associated with a favorable prognosis. Only a few large prospective studies on the effectiveness of the various treatment options can be found in the literature. For ocular adnexal MZLs of the conjunctiva in adults, treatment is generally planned according to stage of the disease. Surgery or radiotherapy has been used in the management of adult patients with low-grade ocular adnexal MZLs of the conjunctiva. The few reported cases of conjunctival extranodal MZLs in the pediatric population were all stage 1 disease. For the treatment of stage 1 ocular adnexal MZLs, a decision must be made between surgical excision or antimicrobial therapies and/or radiotherapy, or immunotherapy.^{9,10} Currently the role of surgery is limited only to diagnostic biopsy. In a recent study reporting the outcomes of 71 newly diagnosed ocular adnexal MZL patients treated with radiotherapy (median dose of 30 Gy in 15 fractions), local control of the disease was obtained in 100% of the patients.¹¹ Toxicity was acceptable and limited to grade 1 acute conjunctivitis (20%) and acute erythema (20%), with only 4% of patients developing acute dry eye. However, late cataract was observed in 6%. As repeated examinations of the present patient showed follicular reaction in bilateral conjunctival regions, chlamydia was assumed and antimicrobial treatment (doxycycline 200 mg/day) was initiated. In the third week of treatment, the tumor enlarged rapidly. For this reason, external radiotherapy 1.8 Gy/day for 7 days with a total dose of 36 Gy was performed. No complications other than acute erythema were observed due to radiotherapy and the patient is currently in remission for 26 months.

In conclusion, although rare, ocular adnexal MZL may also occur in children. As with adult patients, biopsy is mandatory to achieve prompt diagnosis in suspected cases. Systemic evaluation for additional involvement should also not be neglected.

Ethics

Informed Consent: It was obtained.

Peer-review: Externally and internally peer-reviewed.

Authorship Contributions

Surgical and Medical Practices: M.P., N.Ç., S.K., Concept: M.P., N.Ç., S.K., Ş.H., H.H.Ö., E.A., M.H., Design: M.P., N.Ç., S.K., Ş.H., H.H.Ö., E.A., M.H., Data Collection or Processing: M.P., N.Ç., S.K., Ş.H., H.H.Ö., E.A., M.H., Ö.B.S., Analysis or Interpretation: M.P., N.Ç., S.K., Ş.H., H.H.Ö., E.A., M.H., Literature Search: M.P., N.Ç., S.K., Ş.H., H.H.Ö., E.A., M.H., Writing: M.P., N.Ç., S.K., Ş.H., H.H.Ö., E.A., M.H.

Conflict of Interest: No conflict of interest was declared by the authors.

Financial Disclosure: The authors declared that this study received no financial support.

References

1. Shields CL, Chien JL, Surakiatchanukul T, Sioufi K, Lally SE, Shields JA. Conjunctival Tumors: Review of clinical features, risks, biomarkers, and outcomes- the 2017 Donald M Gass Lecture. *Asia-Pacific J Ophthalmology*. 2017;6:109-120.
2. Kram DE, Brathwaite CD, Khatib ZA. Bilateral Conjunctival Extranodal Marginal Zone B-cell Lymphoma. *Pediatr Blood Cancer*. 2010;55:1414-1416.
3. Incesoy- Ozdemir S, Yuksek N, Bozkurt C, Sahin G, Memis L, Dizman A, Ertem U. A rare type of cancer in children: extranodal marginal zone B-cell (MALT) lymphoma of the ocular adnexa. *Turk J Pediatr*. 2014;56:295-298.
4. Graue GF, Finger PT, Maher E, Della Rocca D, Della Rocca R, Lelli GJ Jr, Milman T. Ocular adnexal lymphoma staging and treatment: American Joint Committee on Cancer versus Ann Arbor. *Eur J Ophthalmol*. 2013;23:344-355.
5. Foster LH, Portell CA. The role of infectious agents, antibiotics, and antiviral therapy in the treatment of extranodal marginal zone lymphoma and other low-grade lymphomas. *Curr Treat Options Oncol*. 2015;16:28.
6. Uno T, Isobe K, Shikama N, Nishikawa A, Oguchi M, Ueno N, Itami J, Ohnishi H, Mikata A, Ito H. Radiotherapy for extranodal, marginal zone, B-cell lymphoma of mucosa-associated lymphoid tissue originating in the ocular adnexa: a multiinstitutional, retrospective review of 50 patients. *Cancer*. 2003;98:865-871.
7. Tiemann M, Häring S, Heidemann M, Reichelt J, Claviez A. Mucosa-associated lymphoid tissue lymphoma in the conjunctiva of a child. *Virchows Arch*. 2004;444:198-201.
8. Taddesse-Heath L, Pittaluga S, Sorbara L, Bussey M, Raffeld M, Jaffe ES. Marginal zone B-cell lymphoma in children and young adults. *Am J Surg Pathol*. 2003;27:522-531.
9. Tuncer S, Tanyıldız B, Basaran M, Buyukbabani N, Dogan O. Systemic Rituximab Immunotherapy in the Management of Primary Ocular Adnexal Lymphoma: Single Institution Experience. *Curr Eye Res*. 2015;40:780-785.
10. Çalış F, Gündüz K, Kuzu I, Erden E. Clinical findings and treatment results in ocular adnexal lymphomas. *Turk J Ophthalmol*. 2014;44:374-378.
11. Dhakal B, Fenske TS, Ramalingam S, Shuff J, Epperla N, Hosking P, Rein L, Banerjee A, Hari P, D'Souza A, Shah N, Siker M, Griepentrog GJ, Harris GJ, Wells TS, Erickson BA, Hamadani M. Local disease control in ocular adnexal lymphoproliferative disorders: comparative outcomes of MALT versus non-MALT histologies. *Clin Lymphoma Myeloma Leuk*. 2017;17:305-311.



An Unusual Case: Self-separation of an Idiopathic Epiretinal Membrane

© Jale Menteş, © Serhad Nalçacı

Ege University Faculty of Medicine, Department of Ophthalmology, İzmir, Turkey

Abstract

Self-separation or peeling of an idiopathic epiretinal membrane (ERM) in an eye with partial posterior vitreous detachment (PVD) is a rare event. A 56-year-old woman presented to our clinic with complaints of floaters in her right eye. Best-corrected visual acuity (BCVA) was 9/10 in this eye. Fundus examination and Spectral domain optical coherence tomography (SD-OCT) revealed an idiopathic ERM and Grade 3 PVD in this eye. Four months later, she had complaints of metamorphopsia in her right eye. BCVA was 7/10, while SD-OCT images of the right macula were similar to previous images. One week after the last visit, she presented again due to the sudden disappearance of her metamorphopsia complaints. BCVA had improved to 10/10. Fundus examination demonstrated that the ERM had spontaneously separated from the retinal surface as a flap floating in the vitreous and the foveal contour had returned to normal. The etiologic mechanism may be explained as the contracting forces within an immature ERM being stronger than its adhesion to the retina.

Keywords: Epiretinal membrane, posterior vitreous detachment, spectral domain optical coherence tomography

Introduction

Idiopathic epiretinal membrane (ERM) is a vitreoretinal interface disorder of unknown etiology characterized by the formation of a layer of avascular fibrocellular tissue over the internal limiting membrane.^{1,2,3,4,5} Idiopathic ERMs generally occur in individuals over the age of 50 in the absence of any other eye disease and are known to be accompanied by partial or complete posterior vitreous detachment (PVD) in 80-95% of cases.^{2,5}

Spontaneous self-separation of an idiopathic ERM from the retinal surface is a rare event. It was reported in the literature that spontaneous separation may occur in eyes with secondary ERM, especially in young patients.^{6,7} However, self-separation of an idiopathic ERM from the retina appearing as a flap in an eye with findings of partial PVD is a very rare phenomenon.

In this article, we present a case of idiopathic ERM that spontaneously separated from the retinal surface in the form of a flap in an eye with partial PVD, which was immediately followed by resolution of the patients' visual complaints and anatomic findings.

Case Report

A 56-year-old woman presented with complaints of floaters in her right eye. She had no history of trauma or eye problems and her best corrected visual acuity (BCVA) was 9/10 and 10/10 in the right and left eye, respectively. Intraocular pressure was 16 mmHg in both eyes and anterior segment and fundus examination findings were normal. Spectral domain optical coherence tomography (SD-OCT) (Topcon 3D-OCT, 2000 Corporation, Tokyo, Japan) revealed idiopathic ERM in the macula of the

Address for Correspondence: Serhad Nalçacı MD, Ege University Faculty of Medicine, Department of Ophthalmology, İzmir, Turkey
Phone:+90 505 311 39 13 E-mail: serhadnalcaci@hotmail.com **ORCID-ID:** orcid.org/0000-0002-0401-9492

Received: 23.04.2019 **Accepted:** 03.12.2019

Cite this article as: Menteş J, Nalçacı S. An Unusual Case: Self-separation of an Idiopathic Epiretinal Membrane. Turk J Ophthalmol. 2020;50:56-58

right eye and stage 3 PVD, in which the vitreous is attached only to the optic nerve head. Loss of foveal contour was noted and central macular thickness (CMT) was measured as 360 μm (Figure 1 A, B, C). SD-OCT scan of the left eye was normal with no signs of PVD. The patient was followed up with a diagnosis of idiopathic ERM. Four months later, the patient presented with complaints of metamorphopsia. BCVA was 7/10 in her right eye and there was no change in ERM findings on SD-OCT. The vitreous had detached from the optic nerve head, progressing to stage 4 PVD, and CMT was 370 μm . One week later, the patient presented again because her metamorphopsia complaints had suddenly disappeared. BCVA was 10/10 in the right eye. Fundus examination revealed that the ERM had spontaneously detached from the retinal surface and was floating freely in the vitreous in the form of a thin, transparent, grayish-white flap attached to the retina along one side just below the macula. Foveal reflex was completely normal. B-scan and 3D SD-OCT examinations also showed this flap floating in the vitreous with one side still adhering to the retina. Findings pertaining to macular Grade 1 ERM had resolved, the foveal contour had returned to normal,

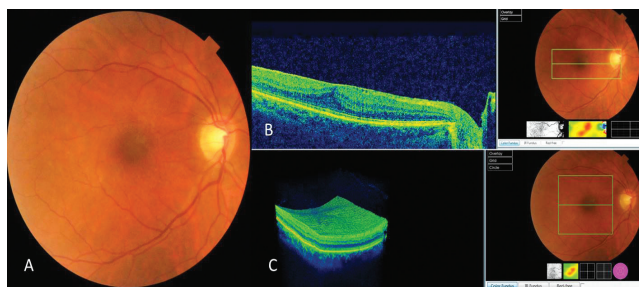


Figure 1. Right eye, idiopathic epiretinal membrane: A) Color fundus photograph, B) B-scan spectral domain optical coherence tomography (SD-OCT) image showing epiretinal membrane and flattening of the foveal contour, C) Three-dimensional SD-OCT image

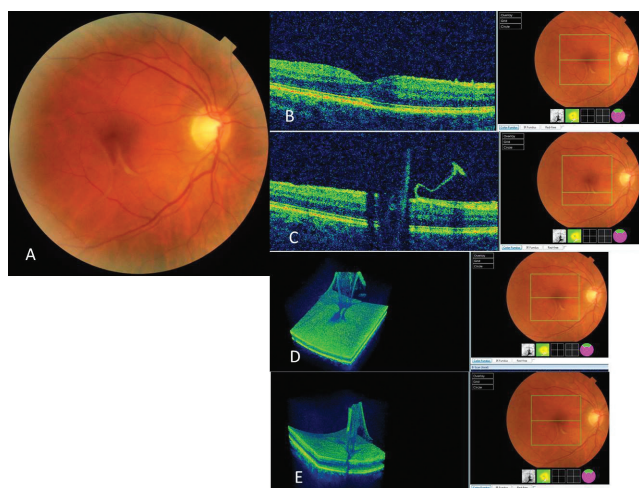


Figure 2. Right eye, idiopathic epiretinal membrane spontaneously detached as a flap: A) Color fundus photograph, B) B-scan spectral domain optical coherence tomography (SD-OCT) image showing recovery of the foveal contour, C) B-scan SD-OCT image showing epiretinal membrane forming a flap with one end freely floating in the vitreous, D, E) Three-dimensional SD-OCT image showing epiretinal membrane floating as a flap in the vitreous

and CMT was 210 μm (Figure 2 A, B, C, D). The case was considered spontaneous separation of an idiopathic Grade 1 ERM. At 4-year follow-up, the patient's BCVA was 10/10. The flap-shaped ERM was slightly contracted and had folded on itself, continuing to float in the vitreous, and CMT was 220 μm .

Discussion

Spontaneous ERM separation is an uncommon clinical phenomenon, reported to occur in 1-3% of all ERM cases.⁴ Spontaneous full-thickness, free, or partial flap separations are known to occur in cases of secondary ERM, especially in adolescents and cases of ERM that develop after inflammatory retinal diseases.^{5,6,7} However, the self-separation of an idiopathic ERM from the retinal surface is rare.^{2,3,4,5} In this article, we present an eye with partial PVD which developed an idiopathic ERM that later spontaneously separated from the retinal surface as a flap. In their series of 1248 idiopathic ERM cases, Yang et al.³ determined with SD-OCT that the prevalence of spontaneous separation in eyes with and without PVD was 1.5% and 13.4%, respectively, during the 33-month follow-up period. Meyer et al.⁶ reported spontaneous separation rates of 0.47 and 2.3% in eyes with and without PVD, respectively, during 2-13 months of follow-up in their series of 210 patients under the age of 30 who had idiopathic ERM. Our patient had stage 3 PVD at initial examination.

An interesting and previously unreported finding in the current case is that the base of the self-separated ERM flap was positioned inferiorly and toward the peripheral retina, as with peripheral retinal tears. In earlier cases of ERM with partial spontaneous separation described in the literature, whether idiopathic or secondary, the base of the flap is usually positioned toward the optic disc or the temporal or superior directions.^{3,6} In a study reporting decreased CMT and increased BCVA following spontaneous idiopathic ERM separation, it was determined that new defects may form at the retinal inner segment/outer segment (IS/OS) line after spontaneous separation and that ERM recurrence is more common in such cases, emphasizing that the IS/OS line is more susceptible to vertical forces.⁶ The absence of any defects in the retinal layers in our patient could be attributed to the retinal traction being weak and of short duration.

Two mechanisms have been proposed in the literature to explain the pathogenesis of spontaneous ERM separation. The first and most common mechanism is a process that occurs due to the induction of PVD. The ERM may spontaneously detach when the contractive forces within an immature ERM are stronger than its adhesion to the retina. The second mechanism is a process resulting from the tangential traction created by the cells in the inner retinal layers that occur in eyes in which PVD has already developed.^{5,6}

We believe that the spontaneous idiopathic ERM detachment in our patient is consistent with the first mechanism. In our opinion, the likely mechanism is that the anteroposterior tractional forces in the concentrated vitreous overcome the tangential tractional forces, and due to this force, the base of the

already thin and immature ERM detaches from the retina in the form of a flap in the periphery.

Ethics

Informed Consent: Obtained.

Peer-review: Externally peer-reviewed.

Authorship Contributions

Surgical and Medical Practices: J.M., Concept: J.M., Design: J.M., Analysis or Interpretation: J.M., Literature Search: J.M., S.N., Writing: J.M., S.N

Conflict of Interest: No conflict of interest was declared by the authors.

Financial Disclosure: The authors declared that this study received no financial support.

References

1. Kolomeyer AM, Schwartz DM. Spontaneous epiretinal membrane separation. *Oman J Ophthalmol.* 2013;6:56-57.
2. Nomoto H, Matsumoto C, Arimura E, Okuyama S, Takada S, Hashimoto S, Shimomura Y. Quantification of changes in metamorphopsia and retinal contraction in eyes with spontaneous separation of idiopathic epiretinal membrane. *Eye (Lond).* 2013;27:924-930.
3. Yang HS, Hong JW, Kim YJ, Kim JG, Joe SG. Characteristics of spontaneous idiopathic epiretinal membrane separation in spectral domain optical coherence tomography. *Retina* 2014;34:2079-2087.
4. Lin J, Chang JS, Fuchs W, Chang S. Spontaneous separation of macular epiretinal membrane without peripheral posterior vitreous detachment. *Journal of Vitreoretinal Disease* 2017;5:341-343.
5. Romano MR, Comune C, Ferrara M, Cennamo G, De Cilla S, Toto L, Cennamo G. Retinal changes induced by epiretinal tangential forces. *J Ophthalmol.* 2015;2015:1-13.
6. Meyer CH, Rodrigues EB, Mennel S, Schmidt JC, Kroll P. Spontaneous separation of epiretinal membrane in young subjects: personal observations and review of the literature. *Graefes Arch Clin Exp Ophthalmol.* 2004;242:977-985.
7. Andrew AN, Bushuev AV, Svetozarskly SN. A case of secondary epiretinal membrane spontaneous release. *Case Reports in Ophthalmological Medicine.* 2016;4925763:3.